HEAT AND MASS TRANSFER PAST A SEMI – INFINITE VERTICAL POROUS PLATE IN MAGNETOHYDRODYNAMICS (MHD) FLOW IN TURBULENT BOUNDARY LAYER.

NGESA JOEL OCHOLA (MSc)

REG NO: I84/21983/2012

A Thesis Submitted in Fulfillment of the Requirements for the Degree of Doctor of Philosophy in Applied Mathematics in the School of Pure and Applied Sciences of Kenyatta University

MAY, 2019

DECLARATION

This thesis is my original work and has not been presented for a degree in any other University or any other award.

Signature:…….…….Date: …….

Ngesa Joel Ochola

I84/21983/2012

We confirm that the work reported in this thesis was carried out by the candidate under our supervision.

Signature:…….Date……

Dr. Kennedy O. Awuor
Department of Mathematics and Actuarial Sciences
Kenyatta University

Signature :……Date……

Prof. Jeconia O. Abonyo
Department of Mathematics
JomoKenyatta University of Agriculture and Technology

DEDICATION

I would like to dedicate this Thesis to my parents Teresa Adhiambo Ochola and Samson Ochola Ochola for their love and encouragement.

ACKNOWLEDGEMENT

I am greatly indebted to my supervisors, Dr. Kennedy Awuor, who has tirelessly inspired me to undertake this thesis. His timely academic advice and encouragement, friendship and support have not only made completion of this research possible but also left an impression which will continue to influence my work. I would like to thank my co-supervisor, Prof. Jeconiah O. Abonyo, his enthusiastic participation and valuable suggestions are greatly appreciated. I have gained greatly from his warm friendship and his continuous encouragement during this research. I wish to thank the Chairperson of Mathematics and Actuarial Sciences Department, Dr. Lydiah Njuguna, for her administrative guidance during this study. Special thanks go to Prof. Kamuti, Prof. Leo Odongo, Prof. David Malonza, Dr. Bernard Kivunge, Dr. Isaac Chepkwony, Dr. Stower all from the department of mathematics and actuarial sciences, Kenyatta university and Dr. Mark Kimathi of Machakos University for their continuous encouragement, academic support and advice throughout this work.

I extend acknowledgement to Professor Francis Gatheri of Technical University of Kenya for his sincere encouragement throughout my academic life and work. Special thanks to my parents, Teresa Adhiambo Ochola and Samson Ochola Ochola for their prayers and support during my studies.

Finally, I wish to thank the Almighty Father God for the wisdom and life He granted to me this far.

TABLE OF CONTENTS

DEDICATION ..... **iii**
ACKNOWLEDGEMENT ..... **iv**
TABLE OF CONTENTS ..... **v**
LIST OF TABLES ..... **viii**
LIST OF FIGURES ..... **ix**
GREEK SYMBOLS ..... **xiv**
ABSTRACT ..... **xvi**

CHAPTER ONE **1**
1.1.3 Boundary layer thickness in turbulent flow 2
Velocity boundary layer 3
Thermal boundary layer 3
Concentration boundary layer 3
Significance of the boundary layer 3
1.1.3 Hall and Ion-Slip Currents 4
1.1.4 Convection heat transfer 4
1.1.5 Mass transfer 6
1.1.6 Turbulent flow over a flat plate 7
1.1.7 Classification of turbulent motion 8
1.1.8 Characteristics of turbulence flow. 8
1.1.9 Shear stress in turbulence flow 9
1.2 Statement of the problem 14
1.3 Justification of the study 14
1.4 Objectives of the study 15
1.4.1 General objective 15
1.4.2 Specific objectives 15
1.5 Significance of the study 16
CHAPTER TWO **19**
LITERATURE REVIEW **19**
2.1 Literature review 19

CHAPTER THREE 27
GENERAL GOVERNING EQUATIONS 27
3.1 General Governing Equations 27
3.1.1 Continuity equation 27
3.1.2 Equation of conservation of momentum of incompressible viscous fluid flow 28
3.1.3 The equation of conservation of energy 29
3.1.4 The concentration equation 32
3.1.5 Maxwell's equations 32
3.1.6 Ohm's law 33
3.1.7 Conservation of electric charge 34
3.2 Approximations and Assumptions 35
3.3 Specific equations governing fluid flow 36
3.3.1 The nature of turbulence and time averaging equations 41
3.3.2 Reynolds Decomposition 41
3.3.3 Boussinesq's Approximation 46
3.4 Simultaneous heat and mass transfer in unsteady turbulent free convection fluid flow with Hall and Ion-Slip currents. 47
3.5 Non-dimensionalization 53
3.5.1 Reynold's Parameter, Re 53
3.5.2 Prandtl Parameter number, Pr 54
3.5.3 Grashof Parameter Number, Gr 54
3.5.4 Eckert Parameter Number, Ec 55
3.5.5 Hartmann number, M 55
3.5.6 Schmidt number, Sc 55
3.5.7 Nusselt number, Nu 55
3.5.8 Sherwood number, Sh 56
CHAPTER FOUR 61
NUMERICAL METHOD OF SOLUTION 61
4.1 Method of Solution 61
4.1.1 Definition of mesh 61
4.1.2 Calculation of rates of heat transfer, mass transfer and skin friction 65

CHAPTER FIVE 67

RESULTS AND DISCUSSION 67

5.1 Discussion of Results 67

5.1.1 Figures and Tables for cooling of the plate by convection currents 68

$\Pr = 0.71, M^2 = 5.0, Gr = +0.4$ 68

5.1.2 Figures and tables for heating of the plate by convection currents 85

$\Pr = 0.71, M^2 = 5.0, Gr = -0.4$ 85

CHAPTER SIX 101

CONCLUSIONS AND RECOMMENDATIONS 101

6.1 Conclusions 101

6.2 Recommendations 107

REFERENCES 108

APPENDIX I 113

THESIS ANALYSIS PROGRAM CODE 113

APPENDIX II 120

Research papers and Publications. 120

LIST OF TABLES

Table 1:Rate of mass transfer Sh values, $M^2 = 5.0$, Pr = 0.71, Gr = +0.4 81

Table 2:Values of skin friction, τ_x and τ_y for $\Pr = 0.71, M^2 = 5.0, Gr = +0.4$ 82

Table 3:Values of convective heat transfer Nu rate, Pr = 0.71, M^2= 5.0, Gr = + 0.4 84

Table 4:Values of skin friction τ_x and τ_y for $\Pr = 0.71, M^2 = 5.0, Gr = -0.4$ 97

Table 5:Rate of convective heat transfer Nu values, for $, M^2 = 5.0, \Pr = 0.71, Gr = -0.4$ 99

LIST OF FIGURES

Figure 1:Random velocity fluctuations at a point in turbulent flow 9
Figure 2:Flow Geometry 36
Figure 3: The Computational Mesh 62
Figure 4: Variation of concentration with Schmidt number Sc 68
Figure 5: Variation of concentration with Suction velocity wo 69
Figure 6: Variation of concentration with time t 69
Figure 7: Variation of Temperature with heat source parameter σ 70
Figure 8: Variation of Temperature with suction velocity wo 70
Figure 9: Variation of Temperature with time 71
Figure 10: Variation of Primary velocity with angle of inclination ϕ 72
Figure 11: Variation of Secondary velocity with angle of inclination ϕ 72
Figure 12: Variation of Primary velocity with Ion-Slip n 73
Figure 13: Variation of Secondary velocity with Ion-Slip n 73
Figure 14:Variation of Primary velocity with Hall parameter m 74
Figure 15:Variation of Secondary velocity with Hall parameter m 74
Figure 16: Variation of Primary velocity with Schmidt number Sc 75
Figure 17: Variation of Secondary velocity with Schmidt number Sc 75
Figure 18: Variation of Primary velocity with heat source parameter σ 76
Figure 19: Variation of Secondary velocity with heat source parameter σ 77
Figure 20: Variation of Primary velocity with suction velocity 77
Figure 21: Variation of Secondary velocity with suction velocity wo 78
Figure 22: Variation of Primary velocity with time 78
Figure 23: Variation of Secondary velocity with time t 79
Figure 24: Variation of Primary velocity with Modified Grashof Gc 79
Figure 25: Variation of Secondary velocity with Modified Grashof Gc 80
Figure 26: Variation of concentration with Schmidt number Sc 85
Figure 27: Variation of concentration with time t 86
Figure 28: Variation of concentration with suction velocity wo 86
Figure 29: Variation of Temperature with heat source parameter σ 87

Figure 30: Variation of Temperature with time t 87
Figure 31: Variation of Temperature with Suction velocity wo 88
Figure 32: Variation of Primary velocity with angle of inclination ϕ 88
Figure 33: Variation of Secondary velocity with angle of inclination ϕ 89
Figure 34: Variation of Primary velocity with Hall parameter m 90
Figure 35: Variation of secondary velocity with Hall parameter m 90
Figure 36: Variation of Primary velocity with Schmidt number Sc 91
Figure 37: Variation of Secondary velocity with Schmidt number Sc 91
Figure 38: Variation of Primary velocity with heat source parameter σ 92
Figure 39: Variation of secondary velocity with heat source parameter σ 92
Figure 40: Variation of Primary velocity with time t 93
Figure 41:Variation of Secondary velocity with time t 94
Figure 42: Variation of Primary velocity with Suction velocity wo 94
Figure 43: Variation of Secondary velocity with Suction velocity wo 95
Figure 44: Variation of Primary velocity with Modified Grashof Gc 95
Figure 45: Variation of Secondary velocity with Modified Grashof Gc 96

NOMENCLATURE

Roman Symbols	Quantity
$\vec{B}$	Magnetic induction vector
C_p	Specific heat capacity at constant pressure, $JKg^{-1}K^{-1}$
C	Dimensionless concentration of the species.
C^*	Dimensional concentration of the species, Kgm^{-3} a
C_w^*	Dimensional concentration of the species at the plate, Kgm^{-3}
C_∞^*	Dimensional concentration of the species at the free stream, Kgm^{-3}
D	Diffusion coefficient, m^2s^{-1}
$\frac{D}{Dt}$	Material or substantive operator.
$\vec{E}$	Electric field, vm^{-1}
Ec	Eckert number.
e	Electric charge, $Coulomb$
F_i	Body forces, N
F_e	Electromagnetic force, N
F_g	Non-electric force per unit volume, N
g	Gravitational acceleration, m/s^2
Gr	Grashof Parameter number
Gc	Modified Grashof Parameter number
h	Specific enthalpy, $KJkg^{-1}$
H	Magnetic field intensity, Wbm^{-2}

H_0	Fixed magnetic field intensity, Wbm^{-2}
$\hat{i}, \hat{j}, \hat{k}$	Unit vectors in the x^*, y^*, z^* directions respectively
$\vec{J}$	Current density, Am^{-2}
J_i	Flow rate per unit area, $Kgs^{-2}m^{-2}$
$J_{x^*}, J_{y^*}, J_{z^*}$	Current density components, A/m^2
K	Heat **(**Thermal) conductivity, w/mk
M	Magnetic field parameter.
m_*	Hall current parameter
n_*	Ion-slip current parameter
Nu	Nusselt number
P	Pressure of fluid, Nm^{-2}
Pr	Prandtl number
Pe	The electron pressure, Nm^{-2}
$\vec{q}$	Velocity vector of the fluid, ms^{-1}
Q_1^*	Internal heat generation, Wm^{-3} g
Q^+	Dissipation function
Q	Heat flux vector, Wm^{-2}
Re	Reynolds number
S	Specific entropy, $KJkg^{-1}$
Sc	Schmidt number
Sh	Sherwood number

t	Dimensionless time.
t^*	Time in seconds (s)
T^*	Fluid temperature in Kelvins(K)
T_∞^*	Free stream fluid temperature in Kelvins
T	Dimensionless fluid temperature.
$\bar{u}$	Time average or temporal mean velocity, and
u'	Velocity fluctuations (fluctuating components)
U	Initial velocity of the plate, ms^{-1}
u^*, v^*, w^*	Velocity components, ms^{-1}
V	Fluid volume, m^3
w_0^*	Dimensional suction velocity, ms^{-1}
w_0	Dimensionless suction velocity.
x^*, y^*, z^*	Cartesian co- ordinates in dimensional form

GREEK SYMBOLS

Symbol	Quantity
β	Volumetric expansion coefficient, $\frac{1}{K}$
$\beta^{\bullet}$	Concentration gradient expansion coefficient, $\frac{1}{K}$
ω_e	Electron cyclotron frequency, Hz
ω_t	Ion- cyclotron frequency, Hz
τ_e	Collision time of electrons, s
τ_i	Collision time of ions, s
σ	Electrical conductivity, $\Omega^{-1}m^{-1}$
μ_e	Magnetic permeability, Hm^{-1}
ρ	Fluid density, Kgm^{-2}
υ	Kinematic viscosity of the fluid, m^2s^{-1}
α	Thermal diffusivity, m^2s^{-1}
θ	Dimensionless temperature of the fluid.
δ	Heat source parameter
η_e	Number density of electrons
τ_x	Primary velocity profiles' skin friction
τ_y	Secondary velocity profiles' skin friction.
δ_{ij}	Stress tensor.
η	Dynamic viscosity, $Kgm^{-1}s^{-1}$

Δt	Time interval.
Δz	Distance interval.
MHD	Magnetohydrodynamics.
Hot	Higher order terms
δ_{ij}	Kronecker delta
ϕ	Magnetic field angle of inclination to the plate
Φ	Viscous dissipation

ABSTRACT

Turbulent flows in electrically conducting media (MHD) remains one of the last unresolved problems in engineering industry and classical physics, but has general importance for the evolution of astro and geophysical plasmas. Turbulence in plasmas, i.e. ionized gases, also offers valuable insights into the not yet fully understood nonlinear dynamics of spectral cascades and structure formation due to the presence or generation of magnetic fields. These allow additional diagnostic access to the underlying nonlinear interaction of turbulent fluctuations. In experimental devices for thermonuclear fusion the magnetically confined hot plasma is basically collisionless and requires kinetic treatment. Exceptions are the thin and comparably cool edge layer near the vessel boundaries and plasmas in reversed-field pinch configurations. Turbulent plasmas in or beyond the earth often allow a fluid description due to the immense size of the dynamical regions and associated time-scales of interest compared to the effective mean-free-path and the frequencies related to the plasma particles. Since plasma turbulence is a fully nonlinear problem comprising the dynamics of many interacting degrees of freedom, the relatively simple single fluid description of magnetohydrodynamics (MHD) represents a sensible starting point for theoretical and numerical investigations. The interesting properties of MHD turbulence lies mainly in its potential universality, that is to say the inherent properties of turbulence might well be important for the dynamics of systems involving gravity, radiation, rotation, or convection. Many authors have studied the theory of magnetohydrdynamics (MHD)flow problems as well as to various methods of solving these problems though mostly addressed heat and mass transfer with Hall and ion-slip currents in laminar boundary layer and rotating turbulent system past a semi-infinite vertical porous plate. In this research work we address the problem of heat and mass transfer of unsteady free convection incompressible fluid flow past a semi-infinite vertical porous plate in (MHD) flow in turbulent boundary layer, in the presence of a strong magnetic field inclined at an angle ϕ to the plate with Hall and Ion-Slip currents. The determination of the concentration, temperature and velocity profiles' distribution for fluid flow, the rate of heat transfer, the skin friction, rate of mass transfer and effects of various flow parameters on the turbulent boundary layer fluid flow field are carried out. An explicit finite difference approximation method is used to analyze the partial differential equations governing the flow for a heat generating fluid with Hall and ion-slip effects. The computation of skin friction, rate of heat and mass transfers at the plate is achieved by Newton's interpolation approximation over the first five points. In both cases when Gr < 0 (in the presence of heating of the plate by free convection currents) and Gr> 0 (in the presence of cooling of the plate by the free convection currents) have been discussed extensively. The effects of various flow parameters on the convectively cooled or convectively heated plate restricted to turbulent boundary layer is considered. The results demonstrate that, Hall current, Schmidt number, Modified Grashof number, Heat source parameter, Suction velocity, Time, Angle of inclination, Ion-Slip current on the convectively cooled or convectively heated plate affect the velocity, temperature and concentration profiles. Increases in Hall current parameter cause a decrease in both primary and secondary velocity profiles while increase in Ion Slip current, decreases primary velocity profiles but increases secondary velocity profiles. As a result, skin friction, rate of heat and mass transfers are altered by their variations.

CHAPTER ONE

INTRODUCTION

1.1 Background

Turbulent flows in electrically conducting media (MHD) remains one of the last unresolved problems in engineering industry and classical physics, but has general importance for the evolution of astro and geophysical plasmas. Turbulence in plasmas, i.e. ionized gases, also offers valuable insights into the not yet fully understood nonlinear dynamics of spectral cascades and structure formation due to the presence or generation of magnetic fields. These allow additional diagnostic access to the underlying nonlinear interaction of turbulent fluctuations. In experimental devices for thermonuclear fusion the magnetically confined hot plasma is basically collisionless and requires kinetic treatment. Exceptions are the thin and comparably cool edge layer near the vessel boundaries and plasmas in reversed-field pinch configurations. Turbulent plasmas in or beyond the earth often allow a fluid description due to the immense size of the dynamical regions and associated time-scales of interest compared to the effective mean-free-path and the frequencies related to the plasma particles. Since plasma turbulence is a fully nonlinear problem comprising the dynamics of many interacting degrees of freedom, the relatively simple single fluid description of magnetohydrodynamics (MHD) represents a sensible starting point for theoretical and numerical investigations. The interesting properties of MHD turbulence lies mainly in its potential universality, that is to say the inherent properties of turbulence might well be important for the dynamics of systems involving gravity, radiation, rotation, or convection.

In this chapter the main terms used in this research are defined, the objectives of this study and applications are also stated.

1.1.1 Magnetohydrodynamics (MHD)

MHD is the study of motion of electrically conducting fluids in the presence of a magnetic field. The magnetic field exerts mechanical forces on the induced electric currents in the fluid particles' motion region, which produces induced magnetic field in turn, affecting the original magnetic field.

1.1.2 Boundary layer

This is the fluids' layer in the adjacent vicinity of the bounding surface, experiencing significant effects of viscosity. Furthermore, in theory of heat transfer, thermal boundary layer develops.

1.1.3 Boundary layer thickness in turbulent flow

Turbulence boundary layer thickness is the distance from the boundary in which the velocity reaches ninety-nine per cent of the free stream velocity. The velocity within the boundary layer increases from zero at the boundary surface to the velocity of the main stream asymptotically. In fact, Prandtl proposed a formula which agrees satisfactorily with the measured velocity profile. His formula doesn't hold for the boundary layer thickness near the plate's wall, and is expressed as;

$$u = u_{\infty}\left(\frac{y}{\delta}\right)^{\frac{1}{7}} \tag{1.00}$$

Velocity gradient;

$$\frac{du}{dy} = \frac{1}{7}\frac{u_{\infty}}{\delta^{\frac{1}{7}} y^{\frac{6}{7}}} \tag{101}$$

At the plate's wall $(y = 0)$, $\frac{du}{dy} = \infty$ (1.02)

making it not possible to experience infinite shear stress value by the plate's wall. Moreover,

turbulence dies off down near the wall where laminar sub layer exists and fluid's velocity linearly increases with the distance y. This is true for large Reynold's numbers and smooth surfaces outside this layer. Some of the aspects of boundary layer include;

i. Velocity boundary layer

It is the distance from the plate's surface where velocity reaches 0.99 that of the free-stream velocity. When fluid particles are in contact with a flat surface, their velocity is retarded. These particles then act to retard the motion of the adjoining fluid layer which in turn act to retard the motion of particles in the next layer, the process continues until the effect becomes negligible, this illustrates the phenomena of the velocity boundary layer.

ii. Thermal boundary layer

Thermal boundary layer is the fluid flow region where Temperature gradients exist. It develops when fluid temperature at the plate's surface differs with that of the free stream. Fluid particles in contact with the plate gains plate's surface temperature. These particles exchange energy in turn with the adjacent particles in the fluid layers, developing fluids' temperature gradient.

iii. Concentration boundary layer

This is the fluid flow region experiencing the concentration gradient. This develops when certain species concentration at the surface differs with that of the free stream, the transfer by convection of species between free stream and the surface gets controlled by boundary conditions.

iv. Significance of the boundary layer

The velocity boundaries are associated with shear stress and gradient presence while temperature gradients and heat transfer with thermal boundary layer whereas concentration gradient and mass

transfer characterize the concentration boundary layer. In our study the three boundary layers are demonstrated to be mainly manifested by surface friction, convective heat and mass transfers respectively.

1.1.3 Hall and Ion-Slip Currents

Hall Effect is the generation of an electric potential perpendicular to both an electric current flowing along a conducting material and an external magnetic field applied at right angles to the current upon application of the magnetic field. The electrical current density $\vec{J}$ represents the relative motion of charged particles in a fluid. The equation of electric current density may be derived from the diffusion velocities of the charged particles. The major forces on charged particles are electromagnetic forces. If we consider only the electromagnetic forces, the generalized Ohm's law become useful. When electric field $\vec{E}$ is applied, there will be an electric current in the $\vec{E}$ direction. If the magnetic field $\vec{H}$ is perpendicular to $\vec{E}$, there will be an electromagnetic force $\vec{J} \times \vec{B}$, which is perpendicular to both $\vec{E}$ and $\vec{H}$, which is known as Hall current. For the same electromagnetic force, the motion of ions is different from that of electrons, when the electromagnetic force is very large (such as in a very strong magnetic field) the diffusion velocity of ions cannot be neglected. If we consider the diffusion velocity of ions as well as that of electrons, we have the phenomenon of ion-slip current.

1.1.4 Convection heat transfer

This involves energy exchange between the surface boundary and the neighboring fluid particles due to temperature variations. In liquids and gases, convection is dominantly the form of heat transfer. Even though discussed distinctly as a method of heat transfer, convective heat transfer

combines processes of conduction (heat diffusion) and advection (heat transfer by bulk fluid flow). The heat transfer process from a solid surface to fluid particles and vice versa, isn't only by bulk motion of fluid, but also heat diffusion and conduction across the still boundary layer to the solid. Thus, this process in the absence of moving fluid calls for both diffusion and advection of heat, a process which is widely known as convection. ''Forced" convection fluid's motion is due to external forces acting on the fluid other than buoyancy forces (case like water pump in automobile engine) and thermal expansion of fluids. Natural convection as a process where fluid motion entirely depends on natural buoyancy forces due to heated fluid also arise as a possible case, around any fire or the chimney draft. An increase in temperature in Natural convection produces a reduction in density, causing the fluid motion due to pressure and forces where fluids of different densities are affected by gravity.

Furthermore, energy transfer as a result of diffusion (specific molecular motion) involves bulk or macroscopic motion of the fluid. Such motion obeys the principle that, at any point, molecules move collectively in large numbers or as aggregates. This type of motion contributes to heat transfer in the presence of temperature gradient. Since molecules retain their random motion in aggregate, the total transfer of heat is thus due to superposition of energy transport by molecular random motion and bulk motion of the fluid. Customarily, the term convection is used to refer to cumulative transport while advection is the transport due to bulk fluid motion. Separating heat transfer problem from that of fluid motion isn't possible, therefore, it's of necessity to study fluid hydrodynamic behavior for the purpose of gaining an understanding of heat transfer phenomena within the fluid flow, whose analysis involves conservation of mass principle (continuity equation), Momentum equation and Thermodynamic laws (Energy equation) alongside

Phenomenological laws such as Fourier's law of heat conduction , Fick's law of diffusion and Newton's law of viscosity. Fluids include both liquids and gases, with liquids being incompressible while gases compressible, and have densities varying immensely with pressure and temperature.

The study of heat transfer by convection is concerned with the calculation of rates of heat exchange between fluids and solid boundaries. Transfer of energy between a solid surface and the surrounding fluid particles involve mass, momentum and heat transfer. Modes of heat transfer are by conduction, convection and radiation.

1.1.5 Mass transfer

Mass transfer is defined as the net flow of particles from a location, usually referred to as phase, stream, component or fraction, to another. It is experienced in processes like evaporation, adsorption, absorption, drying, membrane filtration, precipitation and distillation. The bulk flow of fluid due to pressure gradient occurring at a macroscopic level is a kind of mass transfer usually treated in the subject of fluid mechanics. In this work, our concern is the transfer of mass at a molecular or a microscopic level, which is dealing with the transport of a single constituent of fluid solution or gas mixture from higher concentration to lower concentration regions. Heat gets transferred in a direction which reduces existing temperature gradient while mass gets transferred to the direction which will reduce existing concentration gradient. Drying, evaporation, chemical reaction, absorption, adsorption, solution and so on are all instances of mass transfer.

Convection mass transfer involves the transport of material between boundary surface and moving fluid or between two relatively immiscible moving fluids mainly due to concentration variations. The mechanism of mass transfer in turbulence is similar to that of heat transfer in turbulent flow and plays an important role in many industrial processes; the removal of pollutants from plant discharge streams by absorption and striping of gases from waste water. Considering an air stream

flowing on a pool of water's surface, the distribution of air's velocity is similar to that over a flat plate. Near the surface there is a laminar sub-layer, followed by a buffer layer, and a turbulent stream. Water vapors are the diffusing components. Water vapor moles are transported from the interface first by molecular diffusion through the laminar convection film and then get transported in the air by eddies. The more the mixing of particles in motion, the more the rate of mass transfer.

1.1.6 Turbulent flow over a flat plate.

This is the fluid flow with innumerable number of eddies over a flat plate boundary layer. Fluid flow over a flat solid surface is often more turbulent with increased shear stress to the surface than in laminar flows. The convectional heat transfers in which the fluid viscosity is important can be divided into two types; namely, laminar flow and turbulent flow. Laminar flow is where fluid elements move in continuous paths or a well- defined straight path, without mixing with the fluid in the adjacent paths whereas turbulent flow is where the eddy motion of small fluid elements fluctuates in the direction of fluid flow and perpendicular to it, and so results in mixing of the fluid in natural convection, the driving force for the fluid motion is the gravity field acting on density difference. Buoyant force causes denser parts of the fluid to move downwards and less dense parts to move upwards. The density differences can result from various effects such as differences in concentration of dissolved matter or in temperature.

Typical examples of turbulent flows are flow around, as well as in cars, airplanes and buildings. The boundary layers and the wakes around and after bluff bodies such as cars, airplanes and buildings are all turbulent. The flow and combustion in engines, both in piston engines and gas turbines and combustors, are highly turbulent. Air movement's in rooms are also turbulent, at least along the walls where wall jets are formed. Hence, turbulent fluid flow is characterized by;

i. Velocity distribution more uniform than in laminar flow due to the continuous generation of the innumerable eddies.

ii. Velocity gradients near the boundary are quite large resulting in more shears.

iii. Flatness of velocity distribution curve in the core region away from the wall is because of the mixing of fluid layers and exchange of momentum between them.

iv. Velocity distribution follows power and logarithmic laws than laminar which is parabolic.

v. Random orientation of fluid particles in a turbulent flow gives rise to additional stresses, called the Reynolds stresses.

vi. Formation of eddies, mixing and curving of path lines in turbulent flow results in much greater frictional losses for the same rate of discharge, viscosity and pipe size.

1.1.7 Classification of turbulent motion

Turbulent motion is classified into;

i.) Wall turbulence; occurs in immediate vicinity of solid surfaces and in the boundary layer flows where the fluid has a negligible mean acceleration.

ii.) Free turbulence; occurs in jets, wakes, mixing layers etc

iii.) Convective turbulence; takes place where there is conversion of potential energy to kinetic energy by the process of mixing (for example the turbulent flow in the annular space between the concentric rotating cylinder, conventional flow between parallel horizontal plates)

1.1.8 Characteristics of turbulence flow.

Characterized by random, irregular and haphazard movement of fluid particles; it has been observed during experimentation that at any fixed point in turbulent field, the velocity and

consequently the pressure fluctuates with time about a mean value.

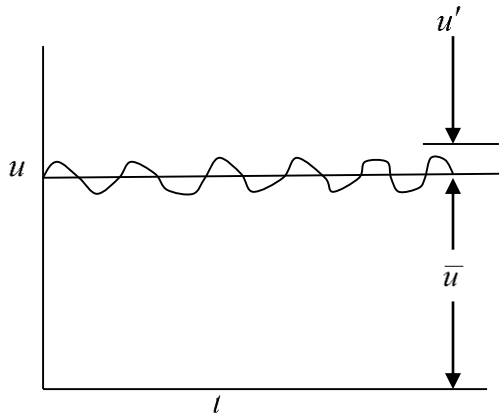

Figure 1:Random velocity fluctuations at a point in turbulent flow

The instantaneous velocity that is, velocity at any time at the given point can be expressed as;

$u = \bar{u} + u'$

Where, u……...Instantaneous velocity

$\bar{u}$..... Time average or temporal mean velocity, and

u' ……Velocity fluctuations (fluctuating components)

Similarly, $v = \bar{v} + v'$, $w = \bar{w} + w'$, $p = \bar{p} + p'$

The mean and fluctuation velocities are determined (Smith 1974) by;

$$\frac{1}{T}\int_{O}^{T} u\,dt = \bar{u}\ ; \qquad \frac{1}{T}\int_{0}^{T} v\,dt = \bar{v}\ ; \qquad \frac{1}{T}\int_{0}^{T} w\,dt = \bar{w}\,; \qquad \frac{1}{T}\int_{0}^{T} P\,dt = \bar{P}$$

and

$$\frac{1}{T}\int_{0}^{T} u'\,dt = \bar{u}' = 0\,; \qquad \frac{1}{T}\int_{0}^{T} v'\,dt = \bar{v}' = 0\,; \qquad \frac{1}{T}\int_{0}^{T} w'\,dt = \bar{w}' = 0\,; \quad \frac{1}{T}\int_{0}^{T} P'\,dt = \bar{P}' = 0 \qquad (1.03)$$

Where T = large interval of time:

1.1.9 Shear stress in turbulence flow

In turbulent flow, as stated earlier, velocity fluctuations cause momentum transport which results

in developing additional shear stresses of high magnitude, between adjacent layers of the fluid. In order to determine the magnitude of the turbulent shear stress a number of semi- empirical theories have been developed some of which are;

i. Boussinesq's theory;

According to this theory (1877), the expression for the shear stress, τ_t for the turbulent flow can be written as;

$$\tau_t = \eta \cdot \frac{d\bar{u}}{dy}; \tag{1.04}$$

where η (eta) is called "eddy" viscosity,

$\bar{u}$ - temporal mean velocity in the direction of flow at a point at distance y from the solid boundary.

Similarly, kinematics viscosity $\upsilon = \frac{\mu}{\rho}$, the "eddy" kinematic viscosity ε is also obtained by dividin eddy viscosity η by the mass density of the fluid ρ, thus;

$$\varepsilon = \frac{\eta}{\rho} \tag{1.05}$$

When viscous action is also included, the total shear stress is expressed as;

$$\tau = \tau_\upsilon + \tau_t \tag{1.06}$$

; where τ_υ = shear stress due to viscosity or

$$\tau_\upsilon = \mu \frac{du}{dy} + \eta \frac{d\bar{u}}{dy} \tag{1.07}$$

The magnitude of η vary from zero (if the flow is laminar) to several thousand times that of μ.

ii. Reynolds theory

According to this theory (1886) the turbulent shear stress between two layers of a liquid at a small distance apart is given as;

$$\tau = \rho u' \upsilon' \qquad (1.08a)$$

u' …fluctuating velocity in direction of x due to turbulence.

υ' ……. fluctuating velocity in direction of y due to turbulence.

Since both u' *and* v' vary and subsequently τ , therefore, to find the shear stress, the time average is taken and equation $\tau = \rho u' \upsilon'$ becomes;

$$\bar{\tau} = \rho \overline{u'v'} = \rho \overline{u'v'} \qquad (1.08b)$$

iii. Prandtl mixing length theory

The Prandtl mixing length l theory (1925), is defined as the average lateral distance through which small mass of fluid particles would move from one layer to the other adjacent layers before acquiring the velocity of the new layer.

Assuming that components u' *and* v' are of the same order and the velocity fluctuations in $x-$ direction is related to the mixing length the;

$$u' = l\frac{du}{dy} \qquad (1.08c)$$

$$\overline{u' \times v'} = \overline{u'v'}$$
$$= \left(l\frac{du}{dy}\right) \times \left(l\frac{du}{dy}\right);$$
$$= l^2\left(\frac{du}{dy}\right)^2$$

and

$$v' = l\frac{du}{dy} \tag{1.08d}$$

Substituting the value of $u'v'$ in $\bar{\tau} = \overline{\rho u'v'} = \rho\,\overline{u'v'}$

We get;

$$\bar{\tau} = \rho l^2\left(\frac{du}{dy}\right)^2 \tag{1.08e}$$

When the viscous action is also included the total shear stress may be expressed as;

$$\bar{\tau} = \mu\frac{du}{dy} + \rho l^2\left(\frac{du}{dy}\right)^2 \tag{1.08f}$$

This equation is used for most turbulent flow problem in determining the shear stress (viscous shear stress negligible except near the boundary).

iv. Universal velocity distribution equation

Assuming the viscous shear stress to be negligible near the boundary the shear stress in turbulent flow is given by;

$$\bar{\tau} = \rho l^2\left(\frac{du}{dy}\right)^2 \tag{1.08g}$$

From this equation we can obtain velocity distribution if the relation between l , the mixing length and y is known. Also $l \;\alpha\; y$ (from the pipe wall) ……Prandtl's hypothesis or $l = \lambda y$, where $\lambda =$ constant of proportionality, known as Karman's universal constant (=0.4). Substituting the values of l in $\bar{\tau} = \rho l^2\left(\frac{du}{dy}\right)^2$ we get;

$$\bar{\tau} \;\; or \;\; \tau = \rho\times(\lambda y)^2\times\left(\frac{du}{dy}\right)^2 = \rho\lambda^2 y^2\left(\frac{du}{dy}\right)^2 \;\ldots\ldots\ldots\ldots\ldots\ldots\ldots\ldots\ldots\ldots\ldots\ldots\ldots\ldots \tag{1.08h}$$

Assuming that the turbulent shear stress remains constant in the vicinity of wall, we have $\tau = \tau_0$

where ($\tau_0 = the\ \ boundary\ \ shear\ \ \ stress$)

The equation (1.08g) becomes;

$$\tau_0 = \rho\lambda^2 y^2 \left(\frac{du}{dy}\right)^2 \text{ or } \frac{du}{dy} = \frac{1}{\lambda y}\sqrt{\frac{\tau_0}{\rho}} = u_f\left(\frac{1}{\lambda y}\right) \tag{1.08i}$$

Where u_f =shear friction velocity or shear velocity = $\sqrt{\frac{\tau_0}{\rho}}$ or $du = u_f\left(\frac{1}{\lambda y}\right)dy$

(u_f is constant for a given case of turbulent flow). Integrating the other equation, we get

$$u = \frac{u_f}{\lambda}\log y + c \quad \ldots\ldots\ldots\ldots\ldots\ldots\ldots\ldots\ldots\ldots\ldots\ldots\ldots\ldots (1.09)$$

where;

c- constant of integration and equation (1.2) shows that velocity distribution in turbulent flow is logarithmic in nature. The constant of integration c, is determined by the boundary condition. The shear in momentum flow is mainly due to momentum transfer. The contribution of fluid viscosity to total shear is small and is usually neglected.

In this study, only turbulent natural convection flows past semi- infinite vertical porous plate will be considered. It enjoys noticeable interest from the thermal sciences communities. The importance of this case is due to the fact that natural convection can be found in many industrial or civil engineering applications like energy transfer in rooms and buildings, nuclear reactor cooling, solar collectors and electric component cooling. For these cases, detailed information on temperature and velocity distribution is important.

Natural convection problems require the solution of the complete Navier- Stokes equations together with the coupled energy equation. Due to complexity of the equations describing this

motion, analytical solutions have not been found. Various natural convective flow investigations such as the rate of heat transfer, temperature distribution profiles, velocities profiles and turbulence intensities are obtained by either numerical or experimental methods. Experimental approach is normally expensive and time consuming whereas numerical analysis methods have comparative flexibility in geometry and boundary conditions. Numerical modeling has shown to be a powerful tool for predicting Low- Rayleigh number natural convection problems; this is why numerical method is used in this study.

1.2 Statement of the problem

Most flows encountered in engineering practice and in nature are turbulent. The averaging process in turbulence results in unknown turbulent correlations in the momentum and energy equations. The unknown turbulent correlation terms are nonlinear and therefore to determine these terms, modeling is required, that is to model correlation terms using known term to close the equations. Most researchers have developed different models to try to complete turbulent modeling for different flow problems but no specific model has been proposed to be the best approximation to these nonlinear terms in heat and mass transfer past a semi-infinite vertical porous plate in MHD flows in turbulent boundary layer. Therefore, in this work, MHD flow of unsteady free convection incompressible fluid in turbulent boundary layer in the presence of a strong magnetic field inclined at an angle ϕ to the plate is modeled to assist in better approximation of results in MHD turbulent fluid flow.

1.3 Justification of the study

It is difficult to fully explain many physical phenomena. Even when an explanation exists, the mathematical prediction may not be exact since there are many assumptions. In most MHD studies,

the assumption is that the flow is streamlined and laminar. In the current problem a deviation from this is sought as turbulence is taken into account. We also take into account the porosity of the plate as well as the effect of a strong magnetic field. Further, the Hall and ion-slip currents are factored in to give a model which is closer to the physical phenomenon of MHD. The fact that MHD borrows from the same principle as the electrical generators, there is hope that by further study of MHD problems a future source of electricity may be found. This is so because the world we live in is surrounded by fluids (air) that can be tapped to generate electricity. Other applications of MHD are plasma studies, nuclear reactors, oil exploration, geothermal extraction and boundary layer control in the field of aerodynamics. Due to these applications the field of MHD is an active area of study. Reduction of the number of assumptions yields closer predictions to the physical phenomenon of MHD theory and practice.

In the next chapter, relevant literature is reviewed and the current MHD fluid flow problem placed in context.

1.4 Objectives of the study

1.4.1 General objective

To investigate the dynamics of heat and mass transfer past a semi-infinite vertical porous plate in MHD flows in turbulent boundary layer.

1.4.2 Specific objectives

i.) To determine the concentration, temperature and velocity profiles' distribution for fluid flow in turbulent boundary layer.

ii.) To determine the rate of mass transfer, the skin friction and rate of mass transfer for unsteady free convection fluid flow in turbulent boundary layer.

iii) To investigate the effects of heat source parameter, mass diffusion, Grashof number, Hall current, time, ion-slip current, magnetic field, angle of inclination and suction velocity on the turbulent boundary layer fluid flow field.

1.5 Significance of the study

In industry, issues like productivity and competitiveness require engineering solutions, which heavily rely on mathematical model. Therefore, it is a major goal for the industry to understand the fluid behavior and accurately predict the flow regime of fluids. Turbulent convection is used in engineering and industrial systems.

Turbulent flow causes more complete mixture of the fluid with greater average velocity flow. These characteristics can help us determine the type of flow we want. For instance, engineers designing sewage systems would typically desire turbulent flow for its mixing property to avoid waste build up and blockage. To avoid erosion caused by secondary flow in pipe bends and elbows, engineers would desire a lower maximum flow velocity inherent in turbulent flow, otherwise, laminar flow is desirable in that it saves energy to flow fluid down a pipe. In turbulence, although there is an increase in velocity, a portion of the energy goes into not only translation, but rotation as well. A water utility would like to channel this energy into pure translation of the fluid in delivering water to customers to cut down on its operating costs. Turbulence manifests in other areas, with varying causes, during an air plane flight, for example, the turbulence experienced is due to the mixing of warm and cold air in the atmosphere, causing the airplane to shake.

The phenomenon of turbulent air flow must be accounted for in many applications. For example, race cars are unable to follow each other around fast corners because the leading car creates turbulent air flow in its wake (this can lead to under-steering). Industrial equipment, such as pipes,

ducts, and heat exchangers are often designed to induce the flow regime of interest (laminar or turbulent). When flow is turbulent, particles exhibit additional transverse motion. This enhances the rate of energy and momentum exchange between them, increasing the heat transfer. Turbulent flow is thus desirable in application where a relatively cool fluid is mixed with a warmer fluid to reduce the temperature of the warmer fluid. It's also very important to take into account turbulent flow when designing certain structures, such as a bridge support, in the late summer and fall, when river flow is slow, water flows smoothly around the support legs. In the spring when the flow is faster, the flow may start off as laminar but it is quickly separated from the leg and becomes turbulent. The bridge supports must be designed such that they can withstand the turbulent flow of the water in the spring.

The heat and mass transfer flow arise in the field of power industry, metrology and cosmic fluid dynamics. The radiation heat transfer is also important in field of nuclear power plants, thermal power plants, gas turbines, missiles, satellites and in the various pertinent devices used in aircraft. Here, various properties associated with the interplay of magnetic fields and thermal perturbation in porous medium past a vertical plate find useful applications in astrophysics, geophysical fluid dynamics and engineering. In chemical engineering processes, the chemical reaction occurs between a foreign mass and the fluid in which the plate is moving. In these processes heat and mass transfer through radiation and convection, can be controlled by fixing or taking the values of various flow dynamic numbers such as Prandtl number, Reynolds number, Solutal Grashof number, Grashof number, Schmidt number and Eckert number as per geometry of the problem or the requirement under applications. In a nut shell, our work has a theoretical motivation in the areas such as cooling of nuclear reactors and thermal power plants, flight aerodynamics, chemical

engineering processes, soil physics, space technology, furnace design, plasma physics and in many industrial areas such as manufacturing of ceramics or glassware, polymer production and food processing. Moreover, Interactions between magnetic fields, velocity fields and electric fields are utilized in the operating principles of most MHD devices, which are designed to perform the functions of various Engineering machines.

CHAPTER TWO

LITERATURE REVIEW

2.1 Literature review

The first research in magnetohydrodynamics was done by Faraday (1839), performing an experiment with mercury flowing in a glass tube between the poles of a magnet, he proposed that for power generation, tidal currents in the terrestrial magnetic field should be used. Job *et al*. (2018) investigated magnetohydrodynamics turbulent fluid flow past an infinite vertical porous plate in a rotating system coupled with Hall currents, mass transfer and Joule's heating. They used finite difference approximation method to solve the problem's modeled equations and reported that, mass transfer, rotation, Hall currents and Joule's heating had profound effect on the primary velocities, secondary velocities, temperature and concentration profiles. The rotational parameter and Hall parameter were found to inhibit the primary velocities while enhanced the secondary velocities. Injection enhanced all the flow variables while suction inhibited all flow variables.

Kennedy and Dickson (2017), in their study entitled, Hydrodynamic turbulent flow between two parallel infinite plates, considered an incompressible electrically conducting fluid and used a finite difference method to solve the coupled non-linear dimensionless partial differential equations, the results show that, Eckert number has a fundamental influence in the dynamics of fluid's temperature and velocity. Rajput and Neetu (2016) researched on MHD flow past a vertical plate with constant temperature and mass diffusion in the presence of Hall current. They considered an electrically conducting, radiation absorbing and emitting but a non-scattering medium in the laminar boundary layer and used Laplace transforms technique to solve their equations for velocity

profiles and skin friction. The results show that primary velocity and τ_x (skin friction due to primary velocity) increases with Hall parameter but secondary velocity and τ_z (skin friction due Secondary velocity) decreases when Hall parameter is increased. Abhay *et al*. (2016), carried out research about convective effects on MHD flow and heat transfer between vertical plates moving in opposite direction and partially filled with a porous medium. They analytically solved the momentum and energy equations by applying the homotopic perturbation technique combined with ordinary differential equation. Observations from their work demonstrate that, magnetic parameter(M)had a retarding effect on the main flow velocity and enhances the temperature distribution, while the reversal phenomenon occurs for the Darcy dissipation (Da). The magnetic parameter(M)reduces the skin friction coefficient for clear fluid region whereas, it increases the skin friction coefficient for the porous region.

Alim *et al*. (2016) studied MHD boundary layer flow of heat and mass transfer over a stretching sheet in a rotating system with Hall Current. They transformed the governing equations to a system of non-linear ordinary differential equations and solved them numerically by the shooting method. The results presented graphically illustrated that primary velocity field decreased due to increase of rotational and magnetic parameter but reverse results arose in case of Hall and heat generation parameter while secondary velocity decreased for stretching parameter and increased for Hall, rotational and magnetic parameter. The thermal boundary layer decreased for the increased values of mentioned parameter. Also, concentration profiles decreased for increased values of magnetic parameter, rotational parameter, reaction parameter and Schmidt number but increased for heat generation and Dufour number. They also showed the numerical values of the skin friction, wall temperature gradient and concentration gradient in tabular form.

Maswai *et al*. (2015) studied MHD turbulent flow in presence of inclined magnetic field past a rotating semi-infinite plate. In their work they determined the effect of various non-dimensional parameters and angle of inclination of the magnetic field on the flow variables and employed the numerical finite difference approximation method to solve the modelled equations for the flow. Their results demonstrate that parameters in the governing equations affected the velocity and temperature profiles followed, they presented results in graphs and tables.

Situma *et al*. (2015) researched on the effect of Hall Current and rotation on MHD free convection flow past a vertical infinite plate under a variable transverse magnetic field. The fluid was considered conducting, turbulent due to the plate roughness and flowing under a strong variable transverse magnetic field. Their equations describing the flow are a combination of the generalized Ohm's law, Maxwell's, Momentum and Energy equations which they solved using the Numerical finite difference approximation method. Their results demonstrate that both Hall and Rotation affected velocity profile and Temperature distribution of the fluid.

Hawa *et al*. (2014) studied turbulent unsteady MHD free convective heat and mass transfer flow past a vertical porous plate with suction. Their research investigated the behavior of two-dimensional magnetohydrodynamics (MHD) free convection flow of an electrically conducting fluid past a moving vertical porous plate with heat and mass transfer considering the effects of radiation, chemical reaction, heat generation/ absorption, viscous dissipation, frequency of excitation and suction through different research formulations. They reduced governing partial differential equations of the flow into a system of ordinary differential equations by applying

suitable similarity transformations. Perturbation theory of first/ second order was employed to solve the equations involved in the various research problems. Rossel approximation and Boussinesq's approximation have been taken and, they considered the geometry of the problem, that x -axis along the plate in the vertical direction and y-axis normal to the plate so that all characteristics of the fluid were independent of variable, x. They discovered that velocity, temperature and concentration profiles are utilized to compute the skin-friction coefficient, rate of heat transfer coefficient (Nusselt number) and rate of mass transfer coefficient (Sherwood number).

Bo Lu and Ziaonzhang (2013) did a study on three dimensional MHD simulation of the electromagnetic flow meter for laminar and turbulent flows. Their numerical results showed that induced electric potential difference at the electrodes agreed with the theoretical values, and that simulations also rendered the detailed distributions of induced electric field, current density, electric potential and induced magnetic field. Mohammad and Nicolas (2012) carried out study on turbulence characteristics and vertical structures in combined convection boundary layers along a heated vertical flat plate, they performed Time-developing direct numerical simulations for the combined-convection boundary layers created by imposing aiding and opposing free streams to the pure natural-convection boundary layer in air along a heated vertical flat plate to clarify their structural characteristics. Their numerical results revealed that with a slight increase in free stream velocity, the transition region moved downstream for aiding flow and upstream for opposing flow. Kinyanjui *et al*. (2012) investigated a turbulent flow of a rotating system past a semi-infinite vertical porous plate. They considered the flow in the presence of a variable magnetic field. They noted that the Hall current, rotation, Eckert number, injection and Schmidt number affected the

velocity, temperature and concentration profiles proportionally. Chaudhary and Shin (2011) on direct numerical simulations of transverse and span wise magnetic field effects on turbulent flow in a 2:1 aspect ratio rectangular duct, used magnetic fields extensively to direct liquid metal flows in material processing. Their work aimed at understanding the effect of a magnetic field on the turbulent metal flow at a nominal bulk Reynolds number. They examined instantaneous and time-averaged natures of the flow through distribution of velocities, various turbulence parameters and budget terms. Their findings show that, span wise (horizontal) magnetic field reorganizes and suppresses secondary flows more strongly. More so, turbulence suppression and velocity flattening effects are stronger with transverse (vertical) magnetic field. Rodriquez-Sevillano (2011) experimentally researched on the problem of determining the turbulence onset in natural convection on heated inclined plates in an air environment. The onset of turbulence has been considered to take place where velocity fluctuations (measured through turbulence intensity) start to grow. Their experimental results show that, the onset depends not only on the Grashof number defined in terms of the temperature difference between the heated plate and the surrounding air but also a correlation between dimensionless Grashof and Reynolds numbers.

Shin-ichi *et al*. (2010) studied direct numerical simulation of unstable stratified turbulent flow under a magnetic field. In this research; liquid-metal as coolant material in a fusion reactor has a significant role in the design of advanced reactors. Using the simulation, they observed that with an increase in heat transfer, thermal plume by the effect of buoyancy filled the entire region of the channel. In case of an applied magnetic field, they found out that, the turbulence became weak with the magnetic field, although the thermal transport was also increased by the buoyancy effect of the thermal plume. Xenos *et al*. (2009), researched on methods of optimizing separation of

compressible turbulent boundary- layer flow over a wedge with heat and mass transfer. The steady, compressible, turbulent boundary-layer flow, with heat and mass transfer, over a wedge, were considered. The obtained results show that, the flow field can be controlled by the suction/injection velocity and it is influenced by the dimensionless pressure parameter m. Yamamoto *et al*. (2008) studied DNS and $k-\varepsilon$ model Simulation of MHD turbulent channel flows with heat transfer. The magneto-hydro-dynamic (MHD) pressure loss and heat-transfer characteristics of the low-magnetic Reynolds number and higher Prandtl number *(*Pr*)* fluid such as the FLiBe, were investigated by means of direct numerical simulation (DNS) and the evaluation of MHD turbulence model carried out in higher Reynolds number (*Re*) condition. As the results, the similarity-law between the velocity and the temperature profiles was not satisfied with increase of Hartman number (*Ha*) and was noticeable at the near critical *Ha* condition to maintain turbulent flow.

Nakaharai and Yokomine (2007) investigated the influence of a transverse magnetic field on the local and average heat transfer of an electrically conducting, turbulent fluid flow with high Prandtl number experimentally. The mechanism of heat transfer modification due to magnetic field was considered with the aid of available numerical simulation data for turbulent flow field. They discovered that, the influence of the transverse magnetic field on the heat transfer was to suppress the temperature fluctuation and to steepen the mean temperature gradient in near-wall region in the direction parallel to the magnetic field. The mean temperature gradient is not influenced compared to the temperature fluctuation in the direction vertical to the magnetic field. Hattori *et al*. (2006) investigated turbulence characteristics of a natural-convection boundary layer in air along a vertical plate heated at high temperatures experimentally. In their study two-dimensional

velocity vectors and instantaneous temperature in the boundary layer at a wall temperature up to 300 °C were measured using a particle image velocimetry and a cold wire, they found that heat transfer rates even for a wall temperature of 300 °C were well expressed by an empirical formula obtained for low wall temperature and the region of transition from laminar to turbulence didn't change much with increase in wall temperature. In addition, the profiles of turbulent quantities measured at a wall temperature of 300 °C resembled those observed at low wall temperatures, and thus the effects of high heat on the turbulent behavior in the boundary layer were quite small. The measured velocity vectors and the higher-order statistics, such as skewness and flatness factors of fluctuating velocities and temperature, also suggested that the structure of large-scale fluid motions in the outer layer of the natural-convection boundary layer, closely connected with turbulence generation, were maintained even under high wall temperature conditions.

Zikanova and Thess (2004) did research on Direct Numerical Simulation as a tool for understanding MHD liquid metal turbulence; they applied direct numerical simulation (DNS) to investigate the most general properties of turbulent flows of liquid metals in the presence of a constant magnetic field. The evolution is found to depend strongly on the magnetic interaction parameter (Stuart number). In the case of small Stuart number, the flow remains three-dimensional, turbulent and approximately isotropic. At large Stuart number (strong magnetic field) the turbulence is suppressed rapidly and the flow becomes two-dimensional and laminar. The influence of a constant magnetic field on scalar transport properties of liquid metal turbulence is investigated using the simplified formulation of a homogeneous flow driven by an imposed mean temperature gradient. The flow structure is dominated by two turbulent antiparallel jets providing an effective mechanism of heat transfer. They discovered that, the magnetic field parallel to the

mean temperature gradient stabilizes the jets and, thus, enhances heat transfer considerably. In the third part, freely decaying MHD turbulence is considered. Numerical simulations are applied to verify the theoretical model proposed in [J. Fluid Mech. 336 (1997) 123] and confirmed that the structure of viscous dissipation and evolution of perpendicular length scale are affected slightly by the magnetic field.

The review work thus, hasn't focused much on the unsteady incompressible free convective heat and mass transfers in presence of a strong magnetic field with hall and ion-slip currents, hence the motivation of our title of study. In this study we consider heat and mass transfer for unsteady MHD free convection fluid flow past a porous semi – infinite vertical plate in the turbulent boundary layer subjected to a strong magnetic field with an angle of inclination ϕ to the plate, which has received less attention.

CHAPTER THREE

GENERAL GOVERNING EQUATIONS

3.1 General Governing Equations

The general equations governing flow of electrically conducting fluid in the presence of a strong magnetic field are continuity, momentum, energy and concentration equations, together with Maxwell's equations and Ohm's law. This chapter outlines these equations. The non-dimensionalization process of the governing equations and the method of solution in our research are also discussed. The classical thermodynamics postulates that the thermodynamic state of a fluid is determined by only two independent thermodynamics properties which are pressure and temperature. A third thermodynamic property is related to the two independent properties by the equation of state of the fluid $\rho = \rho(P,T)$ where ρ is density, P and T are the thermodynamic pressure and temperature respectively. A fluid with velocity component u_j in the time t and space with Cartesian coordinates x_j is considered in the following sections for easier presentation.

3.1.1 Continuity equation

The principle of conservation of mass, states that, in any closed system subject to no external force, the mass is constant irrespective of its changes in form; the principle that matter cannot be created or destroyed. The continuity equation can be expressed in tensor form as (Currie 1974);

$$\frac{\partial \rho}{\partial t} + \frac{\partial (\rho U_j)}{\partial x_j} = 0 \quad \ldots\ldots\ldots\ldots\ldots\ldots\ldots\ldots\ldots\ldots\ldots\ldots\ldots\ldots\ldots\ldots\ldots\ldots\ldots\ldots \quad (3.1)$$

For an incompressible (steady) fluid equation (3.1) becomes,

$$\frac{\partial(\rho U_j)}{\partial x_j} = 0 \tag{3.2}$$

where j =1,2,3 along the x, y and z axes respectively.

3.1.2 Equation of conservation of momentum of incompressible viscous fluid flow

The momentum conservation principle is an application of Newton's second law of motion to an element of fluid particles in motion. It states that, the sum of surface and body forces on a system equals the rate of change of momentum with time.

A balance between body and surface forces with the rate of momentum change yields a general equation of momentum conservation, expressed in tensor form by;

$$\rho\left(\frac{\partial U_j}{\partial t} + U_j \frac{\partial U_j}{\partial x_j}\right) = \rho Fi + \frac{\partial \sigma_{ji}}{\partial x_j} - \frac{\partial p}{\partial x} \tag{3.3}$$

In which $\rho \frac{\partial U_j}{\partial t}$ represents temporal acceleration, $\rho U_j \frac{\partial U_j}{\partial t}$ represents convective acceleration, $\frac{\partial p}{\partial x}$ represents pressure gradient term which is assumed to be zero in this case, ρF_i represents the body force per unit volume and σ_{ji} is the stress tensor or viscous force. For Newtonian fluid, the stress tensor may be decomposed as;

$$\sigma_{ji} = -P\delta_{ij} + \tau_{ij} \tag{3.4}$$

In which δ_{ji} is the Kronecker delta and τ_{ji} is the viscous stress tensor, given by

$$\tau_{ji} = \mu\left(\frac{\partial u_i}{\partial x_i} + \frac{\partial u_j}{\partial x_j}\right) + \mu_s \delta_{ji} \frac{\partial u_k}{\partial x_k} \tag{3.5}$$

where μ and μ_s are the first and second coefficient of viscosity respectively, u_k *and* x_k are velocity and space axis in the k unit vector respectively. It follows that

$$\sigma_{ji} = -P\delta_{ij} + \mu\left(\frac{\partial u_i}{\partial x_i} + \frac{\partial u_j}{\partial x_j}\right) + \mu_s \delta_{ji} \frac{\partial u_k}{\partial x_k} \tag{3.6}$$

Considering the gravitational force g and electromagnetic force so that the volume density of the external forces is given by (Moreau 1990) as;

$$F_i = \rho g + J \times B \tag{3.7}$$

$$\rho\left(\frac{\partial U_j}{\partial t} + U_j \frac{\partial U_j}{\partial x_j}\right) = -\frac{\partial p}{\partial x_i} + \rho\{\rho g + J \times B\} + \frac{\partial}{\partial x_j}\left[\mu\left(\frac{\partial u_i}{\partial x_i} + \frac{\partial u_j}{\partial x_j}\right) + \mu_s \delta_{ji} \frac{\partial u_k}{\partial x_k} - P\delta_{ij}\right] \tag{3.8}$$

or

$$\rho\left(\frac{\partial U_j}{\partial t} + U_j \frac{\partial U_j}{\partial x_j}\right) = -\frac{\partial p}{\partial x_i} + \rho\nu\nabla^2 U_i + \rho\{\rho g + J \times B\} \tag{3.9}$$

3.1.3 The equation of conservation of energy

It states that the rate of energy increase in a system equals the heat added to the system and work done on the system. It is derived from the first law of thermodynamics in the form $dE = dQ - dW$ where E is the energy, Q heat added to system and dW work done by system.

If heat produced by external forces is ignored then, it's written in tensor form as (Currie 1974)

$$\rho\left(\frac{\partial h}{\partial t}\right) + \frac{\partial(\rho U_j h)}{\partial x_j} = \frac{\partial P}{\partial t} + \frac{\partial(U_j p)}{\partial x_j} - \frac{\partial q_j}{\partial x_j} + \Phi \tag{3.10}$$

Where Φ is the viscous dissipation in 3-dimension and given as;

$$\Phi = \mu\left[\left(\frac{\partial u}{\partial x}\right)^2 + \left(\frac{\partial v}{\partial y}\right)^2 + \left(\frac{\partial w}{\partial z}\right)^2\right] + \left(\frac{\partial u}{\partial y} + \frac{\partial v}{\partial x}\right)^2 + \left(\frac{\partial v}{\partial z} + \frac{\partial w}{\partial y}\right)^2 + \left(\frac{\partial w}{\partial x} + \frac{\partial u}{\partial z}\right)^2$$

Or $$\Phi = \tau_{ji} \frac{\partial u_i}{\partial x_j} \tag{3.11}$$

To simplify equation (3.10), we use the thermodynamic definition of h,

$$h = e + \frac{p}{\rho} \tag{3.12}$$

Where e is the specific internal energy. Equation (3.12), in differential form;

$$dh = de + \frac{dp}{\rho} + pd\left(\frac{1}{\rho}\right) \tag{3.13}$$

Since it is possible to express change in specific energy, de, using first and second laws of thermodynamic (Hatsopolous and Keenan 1965), it is possible to express change in specific energy as;

$$de = Tds - pd\left(\frac{1}{\rho}\right) \tag{3.14}$$

In (3.13), we obtain;

$$dh = Tds + \frac{1}{\rho}dp \tag{3.15}$$

Where s is the entropy.

Since the entropy depends on temperature and pressure, it can be written as

$s = s(T, P)$, so that

$$ds = \left(\frac{\partial s}{\partial T}\right)_p dT + \left(\frac{\partial s}{\partial p}\right)_T dp \tag{3.16}$$

By using the generalized thermodynamics relations (Hatsopolous and Keenan 1965);

$$\left(\frac{\partial s}{\partial p}\right)_T = \frac{-\beta}{\rho}; \qquad \left(\frac{\partial s}{\partial T}\right)_p = \frac{c_p}{T}\ ; \left(\frac{\partial\left(\frac{1}{\rho}\right)}{\partial T}\right)_P = \frac{-\beta}{\rho} \tag{3.17}$$

Where β is the coefficient of volumetric expansion and c_p is the specific heat at constant

pressure. Equation (3.17) in (3.16) gives;

$$ds = \frac{c_p}{T} dT - \frac{\beta}{\rho} dp \tag{3.18}$$

substituting equation (3.18) into equation (3.15) leads to;

$$dh = c_p dT + \frac{1}{\rho}(1 - \beta T) dp \tag{3.19}$$

Using Fourier's law of heat conduction given by;

$$q_j = -k \frac{\partial T}{\partial x_j} \tag{3.20}$$

Where k is thermal conductivity, c_p is the specific heat capacity at constant pressure. Substituting in equation (3.10), the energy equation reduces to;

$$\rho c_p \frac{DT}{Dt} = k\nabla^2 T + Q^+ + \beta T \frac{Dp}{Dt} + \Phi \tag{3.21}$$

Where Q^o is the dissipation function which is as result of electromagnetic interaction. By considering electrical dissipation, which is the least energy produced by the work done by the electrical currents and is given by $\frac{J^2}{\sigma}$,equation (3.21) becomes;

$$\rho c_p \frac{DT}{Dt} = k\nabla^2 T + \mu\left(\frac{\partial u_i}{\partial x_j} + \frac{\partial u_j}{\partial x_i}\right)^2 + \frac{J^2}{\sigma} + \Phi \qquad \text{or}$$

$$\frac{\partial}{\partial t}(\rho c_p T) + \frac{\partial}{\partial x_j}\left(\rho c_p u_j T\right) = \frac{\partial}{\partial x_j}\left(k \frac{\partial T}{\partial x_j}\right) + \beta T\left(\frac{\partial p}{\partial t} + \frac{\partial u_j p}{\partial x_j}\right) + \frac{J^2}{\sigma} + \Phi \tag{3.22}$$

neglecting the electrical dissipation function and electromagnetic dissipation terms we obtain

$$\rho c_p \frac{DT}{Dt} = k\nabla^2 T + \Phi \tag{3.23}$$

3.1.4 The concentration equation

It is based on the principle of mass concentration for each species in a fluid mixture, for the fluid flow in consideration the tensor form of the diffusion equation is

$$\frac{DC_j}{Dt} = \frac{\partial J_j}{\partial x_j} \tag{3.24}$$

3.1.5 Maxwell's equations

They provide a link between the electric and magnetic fields independent of the properties of matter. The basic laws of electricity and magnetism can be summarized by four differential equations called Maxwell's electromagnetic equations. The set of Maxwell's electromagnetic equations that consider the fact that most hydromagnetic flows are unsteady is given by; Pai (1962), Moreau (1990);

$$\begin{aligned}
&\vec{\nabla}\times\vec{H} = \vec{J} + \frac{\partial \vec{D}}{\partial t} \text{.....} Ampere's\ law \\
&\vec{\nabla}.\vec{B} = 0 \text{.....} Absence\ of\ \ free\ magnetic\ poles \\
&\vec{\nabla}\times\vec{E} = -\frac{\partial \vec{B}}{\partial t} \text{.....} Faraday's\ law \\
&\vec{\nabla}.\vec{D} = \rho_e \text{.....} Coulomb's\ law(equation)
\end{aligned} \tag{3.25}$$

Where $\vec{H}$ represents magnetizing field, $\vec{D}$ represents Displacement field, $\vec{E}$ represents electric field, $\vec{B}$ represents Magnetic field and $\vec{J}$ represents Current density.

By the assumptions given in section (3.2) the displacement current $\vec{D}$ is negligible with respect to $\vec{J}$, $\frac{\partial \vec{D}}{\partial t}$ is negligible with respect to $\vec{J}$ *and* $\vec{\nabla}\times\vec{H}$. Since ρ_e is usually not known the last equation of (3.25) will not be utilized Moreau (1990)

$$\vec{\nabla} \times H = \vec{J}$$
$$\vec{\nabla} . \vec{B} = 0$$
$$\vec{\nabla} \times \vec{E} = -\frac{\partial \vec{B}}{\partial t} \tag{3.26}$$

3.1.6 Ohm's law

Ohm's law relates the magnetic effect to the flow. If an extra magnetic field $\vec{B}$ is present and the conductor is not at rest but moving at velocity v , then, an extra term must be added to account for the current induced by the Lorenz force on the charge carriers. $\vec{J} = \sigma\left[\vec{E} + v \times \vec{B}\right]$. In the rest frame of the moving conductor, this term drops out because $v = 0$. There is no contradiction because the electric field in the rest frame differs from the $\vec{E} - field$ in the lab frame: $\vec{E}' = \vec{E} + v \times \vec{B}$; electric and magnetic fields are relative.

This law characterizes the ability of material to transport electric charge under the influence of an applied electric field. For electrically conducting material at rest the current density is given by;

$$\vec{J} = \sigma \vec{E} \tag{3.27}$$

In moving electrically conducting fluids the magnetic field induces a voltage in the conductor of magnitude $\vec{q} \times \vec{B}$.The generalized Ohm's law is given by;

$$\vec{J} = \sigma\left(\vec{E} + \vec{q} \times \vec{B}\right)\rho eq \tag{3.28}$$

Where ρeq represents the displacement current usually neglected at fluid velocity q, the law reduces to $\vec{J} = 0$ meaning that no current density in the system. $\vec{J}$ represents current density at a given location in a resistive material, $\vec{E}$ represents electric field at the location and σ represents material dependent parameter called conductivity.

3.1.7 Conservation of electric charge

Conservation laws of electric charge and equations of electric current density are required in order to describe some phenomenon in MHD problems. Since charge is conserved and thus, can't be created or destroyed, all charges in motion or stationary must be accounted for at all times. The relationship derived from the principle of conservation of electric charge with density λ is given as;

$$\vec{\nabla} \cdot \vec{J} = -\frac{\partial \lambda}{\partial t} \tag{3.29}$$

Equation (3.29) is known as the continuity equation for electric charges. For steady current the charge density does not vary with time, hence, $\frac{\partial \lambda}{\partial t} = 0$,equation (3.29) becomes;

$$\vec{\nabla} \cdot \vec{J} = 0 \tag{3.30}$$

Together with the approximations and assumptions stated in section (3.2) the fundamental equations governing magnetohydrodynamics flows result from a combination of electromagnetic theory and fluid mechanics.

3.2 Approximations and Assumptions

Every mathematical description of natural phenomenon is based on certain approximations and assumptions, in this study, the following will be utilized:

i. Liquid metals and ionized gases have permeability μ_e, so that we write $\vec{B} = \mu_e \vec{H}$ in any frame of reference.

ii. All velocities are small compared with that of light $q^2 / c^2 << 1$

iii. The fluid flow is turbulent.

iv. The fluid is incompressible (density is assumed constant).

v. There is no external applied electric field, $E' = 0$

vi. The internal heat generation is given by $Q^* = -\left(T^* - T_\infty^*\right)Q$

vii. The electric displacement current is negligible since the flow velocity is small relative to the speed of light.

viii. Viscosity μ is assumed constant.

ix. Thermal conductivity k is assumed constant.

x. The induced magnetic field is negligible.

xi. The fluid is assumed to be electrically neutral that is no surplus electrical charge distribution in the fluid.

3.3 Specific equations governing fluid flow

The equations governing incompressible unsteady free convection fluid flow in the presence of heat and mass transfers are considered. We study unsteady magnetohydrodynamic natural convection fluid flow in a turbulent boundary layer, past a vertical semi-infinite vertically placed porous plate in a strong magnetic field with an inclination ϕ to the plate and constant suction. The $x^* - axis$ is taken parallel to the plate vertically in the upward direction, which is also the flow's direction, while z^* - axis is normal to the plate. Since the plate is semi- infinite in length and the flow is two-dimensional free convective, the physical variables are functions of $x^{\bullet}, z^{\bullet}$ *and* t^*. The fluid is permeated by a strong magnetic field $\vec{H} = \left(H_0\sqrt{1-\psi^2}\ ,0, H_0\psi\right)$ where $H_0 = |H|$ is the magnitude of the magnetic field and $\psi = \cos\phi$.

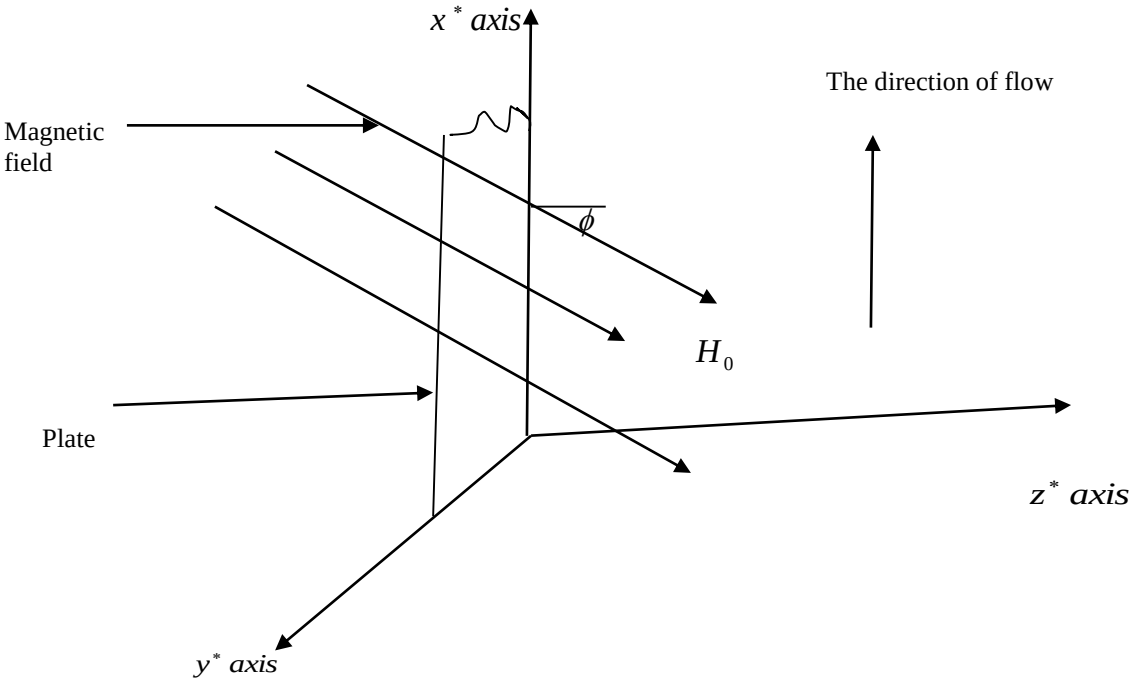

Figure 2:Flow Geometry

The continuity equation for the fluid flow under consideration is given by;

$$\frac{\partial w^*}{\partial z^\bullet} = 0 \tag{3.31}$$

Since the fluids particle velocity equal to zero because of no-slip condition. On integration equation (3.31) gives the constant suction velocity

$$w^* = -w_0^* \tag{3.32}$$

Determining pressure gradient term for the equation (3.9), at the boundary layer edge, where $\rho \to \rho_\infty$ and $U \to 0$. The x^* direction pressure term, $-\frac{\partial p}{\partial x^*} = -\rho_\infty g$ results from change in elevation. Along negative x^* direction, equation (3.9) body force term is $-\rho g$. Thus, the combination of the pressure and body force terms give;

$$-\rho g - \frac{\partial p}{\partial x*} = g(\rho_\infty - \rho) \tag{3.33}$$

Defining the thermal expansion volumetric coefficient as;

$$\beta = -\frac{1}{\rho}\left(\frac{\Delta\rho}{\Delta T}\right)_p = -\frac{1}{\rho}\left(\frac{\rho_\infty^* - \rho^*}{T_\infty^* - T^*}\right) = \frac{1}{\rho}\left(\frac{\rho_\infty^* - \rho^*}{T^* - T_\infty^*}\right) \tag{3.34}$$

and the concentration volumetric coefficient as;

$$\beta' = -\frac{1}{\rho}\left(\frac{\Delta\rho}{\Delta C}\right)_p = -\frac{1}{\rho}\left(\frac{\rho_\infty^* - \rho^*}{C_\infty^* - C^*}\right) = \frac{1}{\rho}\left(\frac{\rho_\infty^* - \rho^*}{C^* - C_\infty^*}\right) \tag{3.35}$$

From equation (3.34) and equation (3.35) we have,

$$\begin{aligned} \beta\rho(T^* - T_\infty^*) &= p_\infty^* - p^* \\ \beta'\rho(C^* - C_\infty^*) &= p_\infty^* - p^* \end{aligned} \tag{3.36}$$

The total change in density as a result of temperature and concentration is given by;

$$\Delta\rho = \beta\rho(T^* - T_\infty) + \beta'\rho(C^* - C_\infty^*) \tag{3.37}$$

From Ohm's law $\vec{J} = \sigma(\vec{q} \times \vec{B})$, where $\vec{J}$ is the electric current density, $\vec{J} = (J_{x^*,} J_{y^*,} J_{z^*})$ and $\vec{B}$ is the magnetic induction, $\vec{B} = (\mu_e H)$ which in component form is given as,

$$B_{x^*} = \mu_e H_0 \sin\phi$$
$$B_{y^*} = 0$$
$$B_{z^*} = \mu_e H_0 \cos\phi$$

$$\vec{J} = \sigma \begin{vmatrix} i & j & k \\ u^* & v^* & 0 \\ B_{x^*} & 0 & B_{z^*} \end{vmatrix} = \sigma\left(v^* B_{z^*} i - u^* B_{z^*} j\right) = \sigma\mu_e H_0 \psi (v^* i - u^* j) \tag{3.38}$$

Where the term in equation (2.7) is simplified as,

$$\vec{J} \times \vec{B} = \begin{vmatrix} i & j & k \\ J_{x^*} & J_{y^*} & 0 \\ \mu_e H_0 \sqrt{1-\psi^2} & 0 & \mu_e H_0 \psi \end{vmatrix} = iJ_{y*}\mu_e H_0 \psi - jJ_{x^*}\mu_e H_0 \psi \tag{3.39}$$

Considering electric charges conservation equation $\vec{\nabla} \cdot \vec{J} = 0$, yields, $J_{z^*} = \mathrm{C}$ (constant), with the constant being zero, because, $J_{z^*} = 0$ at the electrically non- conducting plate, thus, $J_{z^*} = 0$ elsewhere within the flow region, and because of the geometrical nature of the flow, $B_{y^*} = 0$.

Equations (3.37) and (3.39) substituted in equation (3.9) yields;

$$\rho\left(\frac{\partial u^*}{\partial t^*} + u^* \frac{\partial u^*}{\partial x^*} - w_0^* \frac{\partial u^*}{\partial z^*}\right) = \mu\left(\frac{\partial^2 u^*}{\partial x^{*2}} + \frac{\partial^2 u^*}{\partial z^{*2}}\right) + \beta\rho\left(T^* - T_\infty^*\right) + \beta'\rho\left(C^* - C_\infty^*\right) + \mu_e \psi H_0 J_{y^*} \tag{3.40}$$

$$\rho\left(\frac{\partial v^*}{\partial t^*} + u^* \frac{\partial v^*}{\partial x^*} - w_0^* \frac{\partial v^*}{\partial z^*}\right) = \mu\left(\frac{\partial^2 v^*}{\partial x^{*2}} + \frac{\partial^2 v^*}{\partial z^{*2}}\right) - \mu_e \psi H_0 J_{x^*} \tag{3.41}$$

Considering Ohm's law with the Hall current effects (Cowling 1957);

$$\vec{J} + \frac{we\tau e}{H}\left(\vec{J} \times \vec{H}\right) = \delta\left[\vec{E} + \mu_e\left(\vec{q} \times \vec{H}\right) + \frac{1}{e\eta_e}\nabla p_e\right] \tag{3.42}$$

According to Meyer (1958), there being no external electric field (whose applied electron field being zero $\vec{E} = 0$)and neglecting electron pressure gradient for partially ionized fluids, equation (3.42) reduces to;

$$\vec{J} + \frac{we\tau e}{H}\left(\vec{J} \times \vec{H}\right) = \delta\mu_e\left(\vec{q} \times \vec{H}\right) \tag{3.43}$$

Expanding the x and y components become;

$$\begin{gathered}\left(J_x\ , J_y\right) + \frac{we\tau e}{H}\left(j_x H_0\ , -j_y H_0\right) = \delta\mu_e\left(vH_0 - w_0 H_0\right) \\ or \\ \begin{pmatrix} j_x \\ j_y \\ 0 \end{pmatrix} + \frac{\omega_e\tau_e}{H}\begin{pmatrix} j_y H_0 \\ -j_x H_0 \\ 0 \end{pmatrix} = \delta\mu_e\begin{pmatrix} vH_0 \\ -uH_0 \\ 0 \end{pmatrix}\end{gathered} \tag{3.44}$$

Equating the x and y components in the equation (3.44) yields;

$$\begin{aligned} j_x + \omega_e\tau_e j_y &= \delta\mu_e vH_0 \\ j_y - \omega_e\tau_e j_x &= -\delta\mu_e uH_0 \end{aligned}$$

Let $m = we\tau e$, solving these equations simultaneously for current density components j_x *and* j_y;

$$m\left[j_x + mj_y\right] = m\delta\mu_e vH_0$$

$$\begin{aligned} mj_x + j_y &= -\delta\mu_e uH_0 \\ j_y\left(m^2 - 1\right) &= \delta\mu_e H_0\left(mv - u\right) \end{aligned}$$

$$j_y = \frac{\delta\mu_e H_0\left(mv - u\right)}{m^2 + 1} \text{ and } j_x = \frac{\delta\mu_e H_0\left(um + v\right)}{m^2 + 1}$$

Hence;

$$J_x = \frac{\delta \mu_e H_0 (v + um)}{1 + m^2} \tag{3.45}$$

$$J_y = \frac{\delta \mu_e H_0 (vm - u)}{1 + m^2} \tag{3.46}$$

where $m = we\tau e$ (Hall parameter)

Substituting (3.45) and (3.46) in momentum equations with shear stress terms $\frac{\partial uv}{\partial x}$ and $\frac{\partial uw}{\partial x}$ introduced yields;

$$\rho\left(\frac{\partial u^*}{\partial t^*} + u^* \frac{\partial u^*}{\partial x^*} - w_0^* \frac{\partial u^*}{\partial z^*}\right) = \mu\left(\frac{\partial^2 u^*}{\partial x^{*2}} + \frac{\partial^2 u^*}{\partial z^{*2}}\right) + \beta\rho\left(T^* - T_\infty^*\right) + \beta'\rho\left(C^* - C_\infty^*\right) - \frac{\partial uv}{\partial x} + \frac{\delta\psi\mu_e^2 H_0^2 (vm - u)}{1 + m^2} \tag{3.47}$$

$$\rho\left(\frac{\partial v^*}{\partial t^*} + u^* \frac{\partial v^*}{\partial x^*} - w_0^* \frac{\partial v^*}{\partial z^*}\right) = \mu\left(\frac{\partial^2 v^*}{\partial x^{*2}} + \frac{\partial^2 v^*}{\partial z^{*2}}\right) - \frac{\partial uw}{\partial x} - \frac{\delta\psi\mu_e^2 H_0^2 (um + v)}{1 + m^2} \tag{3.48}$$

If electrical dissipation function and electromagnetic dissipation terms are neglected the energy equation (3.23) becomes,

$$\frac{\partial T^*}{\partial t^*} + u^* \frac{\partial T^*}{\partial x^*} - w_0^* \frac{\partial T^*}{\partial z^*} = \frac{k}{\rho c_p}\left(\frac{\partial^2 T^*}{\partial x^{*2}} + \frac{\partial^2 T^*}{\partial z^{*2}}\right) + \Phi + \frac{Q^+}{\rho c_p} \tag{3.49}$$

Finally, the concentration equation (3.24) is given by,

$$\frac{\partial C^*}{\partial t^*} + u^* \frac{\partial C^*}{\partial x^*} - w_0^* \frac{\partial C^*}{\partial z^*} = D\left(\frac{\partial^2 C^*}{\partial x^{*2}} + \frac{\partial^2 C^*}{\partial z^{*2}}\right) \tag{3.50}$$

3.3.1 The nature of turbulence and time averaging equations

Turbulent flow is defined as an eddying motion in which the various quantities show random variation with time and space coordinates, so that statistically distinct average values can be discerned (Hinze 1974, Reynolds 1976). The basic nature of turbulence can be described as a wide spectrum of various sized vortex elements which interact with each other in a highly random and unsteady fashion. The largest eddies fluctuate at relatively low frequency while smallest eddies are associated with high frequency fluctuation. The width of the spectrum and thus the difference between the smallest and lowest eddies increases with the Reynolds number, large scale turbulent motion is mainly responsible in transporting the momentum and heat (Rodi 1980 and Hinze 1974). The larger eddies interact with the mean flow by extracting energy from it and feeding that energy into the large scale turbulent motion. This energy is passed on to smaller and smaller eddies until a scale is reached where the viscous forces are predominant and dissipate the energy. The process is referred to as energy Cascades (Cebeci and Smith 1974, Rodi 1980). When buoyant forces are present there is also an exchange between potential energy of the mean energy which can go in both directions but is also affected through the large-scale motion.

3.3.2 Reynolds Decomposition

This is a mathematical technique for separating the averaging and fluctuating terms of a quantity of turbulent nature. Reynolds decomposition of the governing equations simply separates the instantaneous value of a variable ϕ, in the case of the velocity components u_i,the pressure P, density ρ and temperature T, into mean (time-average) value $\bar{\phi}$ and the fluctuating part ϕ',such that;

$$\bar{\phi}(x_i,t) = \bar{\phi}(x_i) + \phi'(x_i,t) \tag{3.51}$$

The time average value is given by;

$$\bar{\phi} = \frac{1}{\Delta t}\int_{t_0}^{t_0+\Delta t} \phi(x_i, t)\, dt \tag{3.52}$$

where averaging time Δt is large compared with the time scale of turbulence motion and in transient state, Δt has to be small compared to the time scale of the mean flow. Δt is sometimes indicated to approach infinity as a limit but is interpreted as being relative to the characteristic fluctuating period of the turbulence. For practical measurements Δt must be finite. Since, by equation (3.52)

$$\bar{\phi}(x_i, t) = \bar{\phi}(x_i) \tag{3.53}$$

According to this decomposition, time averaging value for fluctuations equals to zero ($\bar{\phi}' = 0$). Other fluid properties such as viscosity, thermal conductivity and specific heat are thus neglected (Rodi 1980 and Anderson *et al* 1984). This procedure allows us to simplify the Navier-Stokes equations by substituting in, the sum of the steady component and fluctuation to the velocity and taking the mean value. The resulting equation contains a nonlinear term known as the Reynolds stress. Applying the Reynolds decomposition equation to the continuity equation (3.1), momentum (3.47 and 3.48) and energy equation (3.22), the resulting equations are obtained as below. From equation (3.1), we decompose the variable u_j and ρ into time average variables plus fluctuating components by equation (3.51). That is;

$$\rho = \bar{\rho} + \rho', \qquad u_j = \bar{u}_j + u_j' \qquad , \; p = \bar{p} + p'$$

The continuity equation (3.1) then becomes;

$$\frac{\partial}{\partial t}(\bar{\rho} + \rho') + \frac{\partial}{\partial x_j}(\bar{\rho} + \rho')(\bar{u}_j + u_j') = 0 \tag{3.54}$$

$$\frac{\partial}{\partial t}(\overline{\bar{\rho}+\rho'})+\frac{\partial}{\partial x_j}(\overline{\bar{\rho}+\rho'})(\overline{\bar{u}_j+u_j'})=0 \qquad \text{where;}$$

$$\frac{\partial}{\partial t}(\overline{\bar{\rho}+\rho'})=\frac{\partial}{\partial t}(\bar{\rho}+\overline{\rho'})=\frac{\partial\bar{\rho}}{\partial t}+\frac{\partial\overline{\rho}'}{\partial t}=\frac{\partial\bar{\rho}}{\partial t} \qquad \text{since} \quad \frac{\partial\overline{\rho}'}{\partial t}=0$$

$$(\bar{\rho}+\rho')(\bar{u}_j+u_j')=\bar{\rho}\,\bar{u}_j+\bar{\rho}\,\bar{u}_j'+\rho'\,\bar{u}_j+\rho'\,u_j'$$

$$\frac{\partial}{\partial x_j}\left(\overline{(\bar{\rho}+\rho')(\bar{u}_j+u_j')}\right)=\frac{\partial}{\partial x_j}\left(\overline{\bar{\rho}\,\bar{u}_j+\bar{\rho}\,u_j'+\rho'\,\bar{u}_j+\rho'\,u_j'}\right)$$

$$=\frac{\partial}{\partial x_j}(\overline{\rho u_j})+\frac{\partial}{\partial x_j}(\rho\overline{u}')+\frac{\partial}{\partial x_j}(\overline{\rho' u_j})+\frac{\partial}{\partial x_j}(\overline{\rho' u_j'})$$

$$=\frac{\partial}{\partial x_j}\left(\overline{\rho u_j}\right)+\frac{\partial}{\partial x_j}\left(\overline{\rho' u_j'}\right)$$

Thus, the continuity equation reduces to;

$$\frac{\partial\bar{\rho}}{\partial t}+\frac{\partial}{\partial x_j}\left(\overline{\rho u_j}\right)+\frac{\partial}{\partial x_j}\left(\overline{\rho' u_j'}\right)=0 \tag{3.55}$$

Averaging the momentum equations;

$$\rho\left(\frac{\partial u^*}{\partial t^*}+u^*\frac{\partial u^*}{\partial x^*}-w_0^*\frac{\partial u^*}{\partial z^*}\right)=\mu\left(\frac{\partial^2 u^*}{\partial x^{*2}}+\frac{\partial^2 u^*}{\partial z^{*2}}\right)+\beta\rho\left(T^*-T_\infty^*\right)$$
$$+\beta'\rho\left(C^*-C_\infty^*\right)-\frac{\partial uv}{\partial x}+\frac{\delta\psi\mu_e^2 H_0^2\left(vm-u\right)}{1+m^2}$$

$$\frac{\partial u^*}{\partial t^*}+u^*\frac{\partial u^*}{\partial x^*}-w_0\frac{\partial u^*}{\partial z^*}=\frac{\mu}{\rho}\left(\frac{\partial^2 u^*}{\partial x^{*2}}+\frac{\partial^2 u^*}{\partial z^{*2}}\right)+\beta\left(T^*-T_\infty^*\right)$$
$$+\beta'\left(C^*-C_\infty^*\right)-\frac{\partial\left(u^*v^*\right)}{\partial x^*}-\frac{\delta\psi\mu_e^2 H_0^2\left(v+um\right)}{\rho\left(1+m\right)^2}$$

become;

$$\frac{\partial(\bar{u}^* + u'^*)}{\partial t^*} = \frac{\partial\overline{(\bar{u}^* + u')}}{\partial t^*} = \frac{\partial\bar{u}^*}{\partial t^*} + \frac{\partial\bar{u}'^*}{\partial t^*} = \frac{\partial\bar{u}^*}{\partial t^*} \qquad \text{since} \quad \frac{\partial\bar{u}'^*}{\partial t^*} = 0$$

$$\left(\bar{u}^* + u'^*\right)\frac{\partial}{\partial x^*}\left(\bar{u}^* + u'^*\right) = \left(\overline{\bar{u}^* + u'^*}\right)\frac{\partial}{\partial x^*}\left(\overline{u^* + u'^*}\right) = \bar{u}^*\frac{\partial\bar{u}^*}{\partial x^*} \qquad \text{since} \quad \frac{\partial\bar{u}'^*}{\partial x^*} = 0$$

$$\left(\bar{w}_0^* + w_0'^*\right)\frac{\partial}{\partial z^*}\left(\bar{u}^* + u'^*\right) = \left(\overline{\bar{w}_0^* + w_0'^*}\right)\frac{\partial}{\partial z^*}\left(\overline{u^* + u'^*}\right) = \bar{w}_0^*\frac{\partial\bar{u}^*}{\partial z^*} \qquad \text{since} \quad \frac{\partial\bar{u}'^*}{\partial z^*} = 0$$

$$\frac{\partial^2}{\partial x^{*2}}\left(\bar{u}^* + u'^*\right) = \frac{\partial^2}{\partial x^{*2}}\left(\overline{\bar{u}^* + u'^*}\right) = \frac{\partial^2\bar{u}^*}{\partial x^{*2}} + \frac{\partial^2\bar{u}'^*}{\partial x^{*2}} = \frac{\partial^2\bar{u}^*}{\partial x^{*2}} \qquad \text{since} \quad \frac{\partial^2\bar{u}'^*}{\partial x^{*2}} = 0$$

$$\frac{\partial^2}{\partial z^{*2}}\left(\bar{u}^* + u'^*\right) = \frac{\partial^2}{\partial z^{*2}}\left(\overline{\bar{u}^* + u'^*}\right) = \frac{\partial^2\bar{u}^*}{\partial z^{*2}} + \frac{\partial^2\bar{u}'^*}{\partial z^{*2}} = \frac{\partial^2\bar{u}^*}{\partial z^{*2}} \qquad \text{since} \quad \frac{\partial^2\bar{u}'^*}{\partial z^{*2}} = 0$$

$$\frac{\partial}{\partial x^*}\left(u^*v^*\right) = \frac{\partial}{\partial x^*}\left(\bar{u}^* + u'^*\right)\left(\bar{v}^* + v'^*\right) = \frac{\partial}{\partial x^*}\left(\overline{\bar{u}^*\bar{v}^* + \bar{u}^*v'^* + u'^*\bar{v}^* + u'^*v'^*}\right) = \frac{\partial}{\partial x^*}\left(\bar{u}^*\bar{v}^*\right)$$

$$\frac{\partial(\bar{v}^* + v'^*)}{\partial t^*} = \frac{\partial\overline{(\bar{v}^* + v'^*)}}{\partial t^*} = \frac{\partial\bar{v}^*}{\partial t^*} + \frac{\partial\bar{v}'^*}{\partial t^*} = \frac{\partial\bar{v}^*}{\partial t^*} \qquad \text{since} \quad \frac{\partial\bar{v}'^*}{\partial t^*} = 0$$

$$\left(\bar{u}^* + u'^*\right)\frac{\partial}{\partial x^*}\left(\bar{v}^* + v'^*\right) = \left(\overline{\bar{u}^* + u'^*}\right)\frac{\partial}{\partial x^*}\left(\overline{\bar{v}^* + v'^*}\right) = \bar{u}^*\frac{\partial\bar{v}^*}{\partial x^*} \qquad \text{since} \quad \frac{\partial\bar{v}'^*}{\partial x^*} = 0$$

$$\left(\bar{w}_0^* + w_0'^*\right)\frac{\partial}{\partial z^*}\left(\bar{v}^* + v'^*\right) = \left(\overline{\bar{w}_0^* + w_0'^*}\right)\frac{\partial}{\partial z^*}\left(\overline{\bar{v}^* + v'^*}\right) = \bar{w}_0^*\frac{\partial\bar{v}^*}{\partial z^*} \qquad \text{since} \quad \frac{\partial\bar{v}'^*}{\partial z^*} = 0$$

$$\frac{\partial^2}{\partial x^{*2}}\left(\bar{v}^* + v'^*\right) = \frac{\partial^2}{\partial x^{*2}}\left(\overline{\bar{v}^* + v'^*}\right) = \frac{\partial^2\bar{v}^*}{\partial x^{*2}} + \frac{\partial^2\bar{v}'^*}{\partial x^{*2}} = \frac{\partial^2\bar{v}^*}{\partial x^{*2}} \qquad \text{since} \quad \frac{\partial^2\bar{v}'^*}{\partial x^{*2}} = 0$$

$$\frac{\partial^2}{\partial z^{*2}}\left(\bar{v}^* + v'^*\right) = \frac{\partial^2}{\partial z^{*2}}\left(\overline{\bar{v}^* + v'^*}\right) = \frac{\partial^2\bar{v}^*}{\partial z^{*2}} + \frac{\partial^2\bar{v}'^*}{\partial z^{*2}} = \frac{\partial^2\bar{v}^*}{\partial z^{*2}} \qquad \text{since} \quad \frac{\partial^2\bar{v}'^*}{\partial z^{*2}} = 0$$

$$\frac{\partial}{\partial x^*}\left(u^*w^*\right) = \frac{\partial}{\partial x^*}\left(\bar{u}^* + u'^*\right)\left(\bar{w}^* + w'^*\right) = \frac{\partial}{\partial x^*}\left(\overline{\bar{u}^*\bar{w}^* + \bar{u}^*w'^* + u'^*\bar{w}^* + u'^*w'^*}\right) = \frac{\partial}{\partial x^*}\left(\bar{u}^*\bar{w}^*\right)$$

Considering that all the terms with fluctuations equal to zero, the momentum equations therefore become;

$$\frac{\partial \bar{u}^*}{\partial t^*}+\bar{u}^*\frac{\partial \bar{u}^*}{\partial x^*}-\bar{w}_0^*\frac{\partial \bar{u}^*}{\partial z^*}=\frac{\mu}{\rho}\left(\frac{\partial^2 \bar{u}^*}{\partial x^{*2}}+\frac{\partial^2 \bar{u}^*}{\partial z^{*2}}\right)+\beta\left(T^*-T_\infty^*\right)+\beta'\left(C^*-C_\infty^*\right)-\frac{\partial}{\partial x^*}\left(\bar{u}^*\bar{v}^*\right)+\frac{\delta\psi\mu_e^2H_0^2\left(m_*\bar{v}^*-\bar{u}^*\right)}{\rho\left(1+m_*\right)^2} \tag{3.56}$$

$$\frac{\partial \bar{v}^*}{\partial t^*}+\bar{u}^*\frac{\partial \bar{v}^*}{\partial x^*}-\bar{w}_0^*\frac{\partial \bar{v}^*}{\partial z^*}=\frac{\mu}{\rho}\left(\frac{\partial^2 \bar{v}^*}{\partial x^{*2}}+\frac{\partial^2 \bar{u}^*}{\partial z^{*2}}\right)-\frac{\partial}{\partial x^*}\left(\bar{u}^*\bar{w}^*\right)-\frac{\delta\psi\mu_e^2H_0^2\left(\bar{v}^*+m_*\bar{u}^*\right)}{\rho\left(1+m_*\right)^2}$$

(3.57)

Applying the same process to the energy and concentration equations respectively yield;

$$\frac{\partial}{\partial t^*}\left(\bar{T}^*+T'^*\right)=\frac{\partial}{\partial t^*}\left(\overline{\bar{T}^*+T'^*}\right)=\frac{\partial \bar{T}^*}{\partial t^*}+\frac{\partial \bar{T}'^*}{\partial t^*}=\frac{\partial \bar{T}^*}{\partial t^*} \quad \text{since} \quad \frac{\partial \bar{T}'^*}{\partial t^*}=0$$

$$\left(\bar{u}^*+u'^*\right)\frac{\partial}{\partial x^*}\left(\bar{T}^*+T'^*\right)=\left(\overline{\bar{u}^*+u'^*}\right)\frac{\partial}{\partial x^*}\left(\overline{\bar{T}^*+T'^*}\right)=\bar{u}^*\frac{\partial \bar{T}^*}{\partial x^*} \quad \text{since} \quad \frac{\partial \bar{T}'^*}{\partial x^*}=0$$

$$\left(\bar{w}_0^*+w_0'^*\right)\frac{\partial}{\partial z^*}\left(\bar{T}^*+T'^*\right)=\left(\overline{\bar{w}_0^*+w_0'^*}\right)\frac{\partial}{\partial z^*}\left(\overline{\bar{T}^*+T'^*}\right)=\bar{w}_0^*\frac{\partial \bar{T}^*}{\partial z^*} \quad \text{since} \quad \frac{\partial \bar{T}'^*}{\partial z^*}=0$$

$$\frac{\partial^2}{\partial x^{*2}}\left(\bar{T}^*+T'^*\right)=\frac{\partial^2}{\partial x^{*2}}\left(\overline{\bar{T}^*+T'^*}\right)=\frac{\partial^2 \bar{T}^*}{\partial x^{*2}}+\frac{\partial^2 \bar{T}'^*}{\partial x^{*2}}=\frac{\partial^2 \bar{T}^*}{\partial x^{*2}} \quad \text{since} \quad \frac{\partial^2 \bar{T}'^*}{\partial x^{*2}}=0$$

$$\frac{\partial^2}{\partial z^{*2}}\left(\bar{T}^*+T'^*\right)=\frac{\partial^2}{\partial z^{*2}}\left(\overline{\bar{T}^*+T'^*}\right)=\frac{\partial^2 \bar{T}^*}{\partial z^{*2}}+\frac{\partial^2 \bar{T}'^*}{\partial z^{*2}}=\frac{\partial^2 \bar{T}^*}{\partial z^{*2}} \quad \text{since} \quad \frac{\partial^2 \bar{T}'^*}{\partial z^{*2}}=0$$

$$\frac{\partial}{\partial t^*}\left(\bar{C}^*+C'^*\right)=\frac{\partial}{\partial t^*}\left(\overline{\bar{C}^*+C'^*}\right)=\frac{\partial \bar{C}^*}{\partial t^*}+\frac{\partial \bar{C}'^*}{\partial t^*}=\frac{\partial \bar{C}^*}{\partial t^*} \quad \text{since} \quad \frac{\partial \bar{C}'^*}{\partial t^*}=0$$

$$\left(\bar{u}^*+u'^*\right)\frac{\partial}{\partial x^*}\left(\bar{C}^*+C'^*\right)=\left(\overline{\bar{u}^*+u'^*}\right)\frac{\partial}{\partial x^*}\left(\overline{\bar{C}^*+C'^*}\right)=\bar{u}^*\frac{\partial \bar{C}^*}{\partial x^*} \quad \text{since} \quad \frac{\partial \bar{C}'^*}{\partial x^*}=0$$

$$\left(\bar{w}_0^*+w_0'^*\right)\frac{\partial}{\partial z^*}\left(\bar{C}^*+C'^*\right)=\left(\overline{\bar{w}_0^*+w_0'^*}\right)\frac{\partial}{\partial z^*}\left(\overline{\bar{C}^*+C'^*}\right)=\bar{w}_0^*\frac{\partial \bar{C}^*}{\partial z^*} \quad \text{since} \quad \frac{\partial \bar{C}'^*}{\partial z^*}=0$$

$$\frac{\partial^2}{\partial x^{*2}}\left(\overline{C}^* + C'^*\right) = \frac{\partial^2}{\partial x^{*2}}\left(\overline{\overline{C}^* + C'^*}\right) = \frac{\partial^2 \overline{C}^*}{\partial x^{*2}} + \frac{\partial^2 \overline{C}'^*}{\partial x^{*2}} = \frac{\partial^2 \overline{C}^*}{\partial x^{*2}} \qquad \text{since} \qquad \frac{\partial^2 \overline{C}'^*}{\partial x^{*2}} = 0$$

$$\frac{\partial^2}{\partial z^{*2}}\left(\overline{C}^* + C'^*\right) = \frac{\partial^2}{\partial z^{*2}}\left(\overline{\overline{C}^* + C'^*}\right) = \frac{\partial^2 \overline{C}^*}{\partial z^{*2}} + \frac{\partial^2 \overline{C}'^*}{\partial z^{*2}} = \frac{\partial^2 \overline{C}^*}{\partial z^{*2}} \qquad \text{since} \qquad \frac{\partial^2 \overline{C}'^*}{\partial z^{*2}} = 0$$

Considering that all the terms with fluctuations equal to zero, the energy and concentration equations respectively become;

$$\frac{\partial \overline{T}^*}{\partial t^*} + \overline{u}^* \frac{\partial \overline{T}^*}{\partial x^*} - \overline{w}_0^* \frac{\partial \overline{T}^*}{\partial z^*} = \frac{k}{\rho c_p}\left(\frac{\partial^2 \overline{T}^*}{\partial x^{*2}} + \frac{\partial^2 \overline{T}^*}{\partial z^{*2}}\right) + \phi + \frac{Q^+}{\rho c_p} \tag{3.58}$$

$$\frac{\partial C^*}{\partial t^*} + \overline{u}^* \frac{\partial C^*}{\partial x^*} - \overline{w}_0^* \frac{\partial C^*}{\partial z^*} = D\left(\frac{\partial^2 C^*}{\partial x^{*2}} + \frac{\partial^2 C^*}{\partial z^{*2}}\right) \tag{3.59}$$

We then adopt the Boussinesq's approximation on the shear stress terms $\frac{\partial\left(\overline{u}^*\overline{v}^*\right)}{\partial x^*}$ and $\frac{\partial\left(\overline{u}^*\overline{w}^*\right)}{\partial x^*}$ appearing in the momentum equations;

3.3.3 Boussinesq's Approximation

The Boussinesq's approximation is used in the field of buoyancy-driven flows (natural convection) in turbulence boundary flows. The approximation advantage arises because when considering a flow of, say warm and cold air of density ρ_1 and ρ_2 the difference $\Delta\rho = \rho_1 - \rho_2$ is negligible.

The Boussinesq's approximation assumptions are;

i. All the fluid motion transport properties are treated constant except for the density.

ii. The density differences are sufficiently small to be neglected.

iii. The density varies linearly with temperature and the deviation from a reference value is small.

iv. The effects due to viscous dissipation are negligible.

v. The characteristic temperature difference ΔT_* be sufficiently small that it tends to zero.

Hence utilizing the Boussinesq's approximation involves;

$$\tau = -\rho\overline{v}\overline{w} = A\frac{\partial \overline{v}}{\partial z} \tag{3.60}$$

From experiment Prandtl deduced that;

$$\rho\overline{v}\overline{w} = -\rho l^2\left(\frac{\partial \overline{v}}{\partial z}\right)^2 \tag{3.61}$$

Let $l = kx$, k the Von Karman constant yields;

$$\overline{u}^*\overline{v}^* = -k^2x^2\left(\frac{\partial \overline{v}^*}{\partial x^*}\right)^2 \tag{3.62}$$

$$\overline{u}^*\overline{w}^* = -k^2x^2\left(\frac{\partial \overline{w}^*}{\partial x^*}\right)^2 \tag{3.63}$$

Equations (3.56) and (3.57) hence become;

$$\begin{aligned}\frac{\partial \overline{u}^*}{\partial t^*} + \overline{u}^*\frac{\partial \overline{u}^*}{\partial x^*} - \overline{w}_0^*\frac{\partial \overline{u}^*}{\partial z^*} &= \frac{\mu}{\rho}\left(\frac{\partial^2 \overline{u}^*}{\partial x^{*2}} + \frac{\partial^2 \overline{u}^*}{\partial z^{*2}}\right) + \beta\left(T^* - T_\infty^*\right) \\ &+ \beta'\left(C^* - C_\infty^*\right) + \frac{\partial}{\partial x^*}\left[k^2x^2\left(\frac{\partial v^*}{\partial x^*}\right)^2\right] + \frac{\delta\psi\mu_e^2H_0^2\left(m_*v^* - u^*\right)}{\rho\left(1+m_*\right)^2}\end{aligned} \tag{3.64}$$

$$\begin{aligned}\frac{\partial \overline{v}^*}{\partial t^*} + \overline{u}^*\frac{\partial \overline{v}^*}{\partial x^*} - \overline{w}_0^*\frac{\partial \overline{v}^*}{\partial z^*} &= \frac{\mu}{\rho}\left(\frac{\partial^2 \overline{v}^*}{\partial x^{*2}} + \frac{\partial^2 \overline{u}^*}{\partial z^{*2}}\right) \\ &+ \frac{\partial}{\partial x^*}\left[k^2x^2\left(\frac{\partial \overline{w}^*}{\partial x^*}\right)^2\right] - \frac{\delta\psi\mu_e^2H_0^2\left(v^* + m_*u^*\right)}{\rho\left(1+m_*\right)^2}\end{aligned} \tag{3.65}$$

3.4 Simultaneous heat and mass transfer in unsteady turbulent free convection fluid flow with Hall and Ion-Slip currents.

In this section, simultaneous heat and mass transfer for unsteady free convection fluid flow past a porous semi-infinite vertical plate subjected to a strong magnetic field inclined at an angle ϕ to the plate in a turbulent boundary layer is discussed. In particular, we consider the effects of Suction

velocity wo, Modified Grashof number Gc, Time t, Angle of inclination ϕ, Mass Diffusion Sc, Hall current m, Ion-Slip current n, Heat source parameter (σ) and Viscous dissipative heat on the flow field. The effects of the above parameter numbers on convective cooling or heating of the plate, limited to a turbulent boundary are investigated. Analysis of these parameters to the concentration, temperature and Velocity profiles are in graphs while the skin friction, rates of heat transfer and mass transfer are presented in tables.

The fluid flow is prompted by the temperature difference between the plate surface and the fluid particles. The hot and cold fluid particles of the flow were isothermal at 323K and 283K respectively giving a Rayleigh number of 1.58×10^{9}. The fluid is heated on the plate and cooled by convection by the cold particles in the neighborhood. All the boundaries of the flow are stationary, no-slip, rigid and impermeable. Further, the Boussinesq's approximation (1903) is assumed and applied in the turbulent flow equations. The major forces acting on charged particles are electromagnetic forces. Usually, the generalized Ohm's law due to electromagnetic forces is derived by considering only the current due to the flow of electrons while neglecting the current due to ions, but the magnetic field is very strong and the electromagnetic force is therefore very large and the diffusion velocity may not be neglected. Consequently, the electric current density must now include the contribution of the ions. The phenomenon in which the electric current density includes the Ion-current as well as the electron current is called the Ion-Slip effect. The temperature of the fluid and the plate are assumed to be the same initially. At time $t^{*}>0$ the porous plate starts moving impulsively in its own plane with a constant velocity U and its temperature is instantaneously raised or lowered to T_{w}^{*} which is maintained constant thereafter. The $x^{*}-axis$ is taken along the plate in vertically upward direction, which is the direction of flow.

The $z^* - axis$ is taken normal to the plate; since the plate is semi-infinite in length and the flow is unsteady; the flow variables are functions of x^* , z^* *and* t^*. The continuity equation (3.31) gives $w^* = -w_0^*$ everywhere in the flow where w_0 is the suction velocity at the plate. It is assumed that the induced magnetic field is negligible so that the fluid is permeated by a strong magnetic field intensity $\vec{H} = \left(H_0\sqrt{1-\psi^2}\ ,0, H_0\psi\right)$ where $H_0 = \left|\vec{H}\right|$(magnitude) of the magnetic field and $\psi = \cos\phi$(assumption for small magnetic Reynold's number). Taking into consideration the Hall current (due to electrons), ion-slip current (due to ions) and collisions between electrons and neutral particles, we obtain a modified Ohm's law of the form,

$$\vec{J} = \sigma\left[\vec{E} + \vec{q}\times\vec{B}\right] - \frac{\omega_e\tau_e}{B_0}\left[\vec{J}\times\vec{B}\right] + \frac{\omega_e\tau_e\omega_i\tau_i}{B_0^2}(\vec{J}\times\vec{B})\times\vec{B} \qquad (3.66)$$

We shall assume that the magnetic Reynolds number for the flow is small so that the induced magnetic field can be neglected. This assumption is justified since the magnetic Reynolds number is usually generally very small for partially ionized gases. The solenoidal relation $\nabla\cdot\vec{B} = 0$ for the magnetic field gives $B_{y^*} = B_0 = $constant everywhere in the flow where $\vec{B} \equiv \left(B_{x^*}, B_{y^*}, B_{z^*}\right)$. The equation of conservation of charge $\nabla\cdot\vec{J} = 0$ gives $J_{y^*} = $constant. This constant is zero since $J_{y^*} = 0$ at the plate which is electrically non-conducting. Thus $J_{y^*} = 0$ everywhere in the flow. Since the induced magnetic fields are neglected, the Maxwell's equation $\nabla\times\vec{E} = -\frac{\partial B}{\partial t}$ becomes $\nabla\times\vec{E} = 0$ which gives $\frac{\partial E_x}{\partial y} = 0$ and $\frac{\partial E_y}{\partial y} = 0$. This implies that $E_x = $constant and $E_y = $constant everywhere in the flow.

In view of the above assumptions, equation (3.66) with an applied electric field $\vec{E} = 0$ (short circuit

problem) gives;

$$\vec{J} = \sigma\left[\vec{q} \times \vec{B}\right] - \frac{\omega_e \tau_e}{B_0}\left[\vec{J} \times \vec{B}\right] + \frac{\omega_e \tau_e \omega_i \tau_i}{B_0^2}(\vec{J} \times \vec{B}) \times \vec{B}$$

Which on using the expansion technique in equation (3.44) and equating the x and y components yield;

$$\begin{aligned} (1 + m_* n_*) J_{x^*} - m_* J_{y^*} &= E_x - \sigma B_0 v^* \\ (1 + m_* n_*) J_{y^*} + m_* J_{x^*} &= E_{y^*} + \sigma B_0 u^* \end{aligned} \qquad (3.67)$$

where $m_* = \omega_e \tau_e$ is the Hall parameter and $n_* = \omega_i \tau_i$ is the ion-slip current. Solving (3.67) simultaneously for J_{x^*} *and* J_{y^*} yields,

$$\vec{J}_{x^*} = \frac{\sigma \times \left[(1 + m_* n_*)\left(E_x - B_0 v^*\right) + m_*\left(E_y + B_0 u^*\right)\right]}{(1 + m_* n_*)^2 + m_*^2} \quad \text{and}$$

$$\vec{J}_{y^*} = \frac{\sigma \times \left[(1 + m_* n_*)\left(E_y + B_0 u^*\right) - m_*\left(E_x - B_0 v^*\right)\right]}{\left[1 + m_* n_*\right]^2 + m_*^2}$$

That is;

$$\vec{J} = \sigma\left[\vec{q} \times \vec{B}\right] - \frac{\omega_e \tau_e}{B_0}\left[\vec{J} \times \vec{B}\right] + \frac{\omega_e \tau_e \omega_i \tau_i}{B_0^2}(\vec{J} \times \vec{B}) \times \vec{B}$$

$$\vec{J} + \frac{\omega_e \tau_e}{B_0}\left(\vec{J} \times \vec{B}\right) = \sigma\left[\vec{q} \times \vec{B}\right] + \frac{\omega_e \tau_e \omega_i \tau_i}{B_0^2}(\vec{J} \times \vec{B}) \times \vec{B}$$

$$\left(\vec{J}_x\ , \vec{J}_y, 0\right) + \frac{m_*}{B_0}\left(\vec{J}_x B_0\ , -\vec{J}_y B_0, 0\right) = \delta\left(vB_0, -uB_0, 0\right) + \frac{m_* n_*}{B_0^2}\left[\vec{J} \times \vec{B}\right] \times \vec{B}$$

or

$$\begin{pmatrix} \vec{J}_x \\ \vec{J}_y \\ 0 \end{pmatrix} + \frac{m_*}{B_0}\begin{pmatrix} \vec{J}_y B_0 \\ -\vec{J}_x B_0 \\ 0 \end{pmatrix} = \delta\begin{pmatrix} vB_0 \\ -uB_0 \\ 0 \end{pmatrix} + \frac{m_* n_*}{B_0}\left[\vec{J} \times \vec{B}\right] \times \vec{B}$$

$$\vec{J}\times\vec{B}=\begin{bmatrix}\vec{J}_{y^*}B_0\\ -\vec{J}_{x^*}B_0\\ 0\end{bmatrix} \quad ; \; \vec{B}=\left[\mu_e H_0\sqrt{1-\psi^2},\ 0,\ \mu_e H_0\psi\right]$$

$$\left[\vec{J}\times\vec{B}\right]\times\vec{B}=\begin{vmatrix} i & j & k\\ J_{y^*}B_0 & -J_{x^*}B_0 & 0\\ \mu_e H_0\sqrt{1-\psi^2} & 0 & \mu_e H_0\psi \end{vmatrix}$$

$$=-B_0\mu_e H_0\psi J_{x^*}i-B_0\mu_e H_0\psi J_{y^*}j+0k$$

flow is two dimensional, hence k component zero

$$\therefore \begin{bmatrix}J_{x^*}\\ J_{y^*}\\ 0\end{bmatrix}+\frac{m_*}{B_0}\begin{bmatrix}J_{y^*}B_0\\ -J_{x^*}B_0\\ 0\end{bmatrix}=\sigma\begin{bmatrix}\bar{v}^*B_0\\ -\bar{u}^*B_0\\ 0\end{bmatrix}+\frac{m_*n_*}{B_0^2}\begin{bmatrix}-B_0\mu_e H_0\psi J_{x^*}\\ -B_0\mu_e H_0\psi J_{y^*}\\ 0\end{bmatrix}$$

$$\left[B_0^2+m_*n_*\mu_e H_0\psi B_0\right]J_{x^*}+\qquad m_*B_0^2J_{y^*}=\sigma B_0^3\bar{v}^* \quad \ldots\ldots\ldots\ldots\ldots\ldots\ldots\ldots\ldots\ldots\ldots\ldots\ldots \text{(i)}$$

$$-m_*B_0^2\ J_{x^*}+\left[B_0^2+m_*n_*B_0\mu_e H_0\psi\right]J_{y^*}=-\sigma B_0^3\,\bar{u}^* \quad \ldots\ldots\ldots\ldots\ldots\ldots\ldots\ldots\ldots \text{(ii)}$$

Solving (i) and (ii)simultaneously;

$$m_*B_0^2\left[B_0^2+m_*n_*\mu_e H_0\psi B_0\right]J_{x^*}\quad+\qquad m_*^2B_0^4J_{y^*}=\ \sigma B_0^5\,\bar{v}^* \qquad +$$

$$-m_*B_0^2\left[B_0^2+m_*n_*\mu_e H_0\psi B_0\right]J_{x^*}+\left[B_0^2+m_*n_*\mu_e H_0\psi B_0\right]^2J_{y^*}=-\sigma B_0^3\bar{u}^*\left[B_0^2+m_*n_*\mu_e H_0\psi B_0\right]$$

$$0\ +\left[m_*^2\ B_0^4+\left(B_0^2+m_*n_*\mu_e H_0\psi B_0\right)^2\right]J_{y^*}=\sigma\, m_*B_0^5\bar{v}^*-\sigma B_0^3\bar{u}^*\left[B_0^2+mn\mu_e H_0\psi B_0\right]$$

$$\left[m_*^2B_0^4+\left(B_0^2+m_*n_*\mu_e H_0\psi B_0\right)^2\right]J_{y^*}=\sigma\, m_*B_0^5\bar{v}^*-\sigma B_0^3\bar{u}^*\left[B_0^2+mn\mu_e H_0\psi B_0\right]$$

With $B_0=\mu_e H_0\psi$;

$$\left[m_*^2B_0^4+\left(B_0^2+m_*n_*B_0^2\right)^2\right]J_{y^*}=\sigma\, m_*B_0^5\bar{v}^*-\sigma B_0^3\bar{u}^*\left[B_0^2+m_*n_*B_0^2\right]$$

$$J_{y^*} = \frac{B_0^5 \sigma\left[m_* \bar{v}^* - \bar{u}^*\left(1+m_* n_*\right)\right]}{B_0^4\left[m_*^2 + \left(1+m_* n_*\right)^2\right]}$$

$$J_{y^*} = \frac{B_0 \sigma\left[m_* \bar{v}^* - \bar{u}^*\left(1+m_* n_*\right)\right]}{\left[m_*^2 + \left(1+m_* n_*\right)^2\right]}$$

Which on further simplification using the above assumptions give;

$$\vec{J}_{x^*} = \frac{\sigma \mu_e H_0 \psi\left[\bar{v}^*\left(1+m_* n_* \psi^2\right) + \bar{u}^* m_* \psi\right]}{\left[1+m_* n_* \psi^2\right]^2 + m_*^2 \psi^2} \tag{3.68}$$

$$\vec{J}_{y^*} = \frac{\sigma \mu_e H_0 \psi\left[\bar{v}^* m_* \psi - \bar{u}^*\left(1+m_* n_* \psi^2\right)\right]}{\left[1+m_* n_* \psi^2\right]^2 + m_*^2 \psi^2} \tag{3.69}$$

Substituting equation (3.68) and (3.69) in the momentum equations (3.64) and (3.65) from equations (3.40) and (3.41) respectively we obtain;

$$\rho\left(\frac{\partial \bar{u}^*}{\partial t^*} + \bar{u}^* \frac{\partial \bar{u}^*}{\partial x^*} - \bar{w}_0^* \frac{\partial \bar{u}^*}{\partial z^*}\right) = \mu\left(\frac{\partial^2 \bar{u}^*}{\partial x^{*2}} + \frac{\partial^2 \bar{u}^*}{\partial z^{*2}}\right) + \beta\rho\left(\bar{T}^* - T_\infty^*\right)$$

$$+ \beta'\rho\left(\bar{C}^* - C_\infty^*\right) + \frac{\partial}{\partial x^*}\left[k^2 x^2 \left(\frac{\partial \bar{v}^\bullet}{\partial x^\bullet}\right)^2\right] + \frac{\sigma \mu_e^2 H_0^2 \psi^2\left[\bar{v}^* m_* \psi - \bar{u}^*\left(1+m_* n_* \psi^2\right)\right]}{\left[1+m_* n_* \psi^2\right]^2 + m_*^2 \psi^2} \tag{3.70}$$

$$\rho\left(\frac{\partial \bar{v}^*}{\partial t^*} + \bar{u}^* \frac{\partial v^*}{\partial x^*} - \bar{w}_0^* \frac{\partial \bar{v}^*}{\partial z^*}\right) = \mu\left(\frac{\partial^2 \bar{v}^*}{\partial x^{*2}} + \frac{\partial^2 \bar{v}^*}{\partial z^{*2}}\right) + \frac{\partial}{\partial x^*}\left[k^2 x^2 \left(\frac{\partial \bar{w}^*}{\partial x^*}\right)^2\right]$$

$$- \frac{\sigma \mu_e^2 H_0^2 \psi^2\left[\bar{u}^* m_* \psi + \bar{v}^*\left(1+m_* n_* \psi^2\right)\right]}{\left[1+m_* n_* \psi^2\right]^2 + m_*^2 \psi^2} \tag{3.71}$$

$$\frac{\partial \bar{T}^*}{\partial t^*} + \bar{u}^* \frac{\partial \bar{T}^*}{\partial x^*} - \bar{w}_0^* \frac{\partial \bar{T}^*}{\partial z^*} = \frac{k}{\rho c_p}\left(\frac{\partial^2 \bar{T}^*}{\partial x^{*2}} + \frac{\partial^2 \bar{T}^*}{\partial z^{*2}}\right) + \frac{Q^+}{\rho c_p}$$

$$+ \frac{\nu}{\rho c_p}\left[\left(\frac{\partial \bar{u}^*}{\partial x^*}\right)^2 + \left(\frac{\partial \bar{v}^*}{\partial x^*}\right)^2 + \left(\frac{\partial \bar{u}^*}{\partial z^*}\right)^2 + \left(\frac{\partial \bar{v}^*}{\partial z^*}\right)^2\right] \tag{3.72}$$

and

$$\frac{\partial \overline{C}^*}{\partial t^*} + \overline{u}^* \frac{\partial \overline{C}^*}{\partial x^*} - \overline{w}_0^* \frac{\partial \overline{C}^*}{\partial z^*} = D\left(\frac{\partial^2 \overline{C}^*}{\partial x^{*2}} + \frac{\partial^2 \overline{C}^*}{\partial z^{*2}} \right) \tag{3.73}$$

3.5 Non-dimensionalization

In the study of fluid mechanics, the adoption of a suitable non-dimensional scheme is of great significance. An appropriate scheme not only expresses experimental and analytic results in the most efficient form but may also make the solution bounded. The process enables the results obtained for a surface experiencing a set of conditions applicable to a geometrically similar surface with entirely different conditions. The surface conditions may vary with nature, velocity or surface size of the flow field. This technique also normalizes the boundary layer equations. For example, non-dimensionalizing velocity such that it varies from 0 to 1. The essential features of the flow problems in MHD are brought out more clearly using some of the important non-dimensionalizing parameters, characterizing these flow problems. Some of the desirable non-dimensional parameters include;

3.5.1 Reynold's Parameter, Re

This is the ratio of inertia to viscous forces acting on the fluid. A flow with this parameter number less than one has inertia force negligible and for the converse (large Reynold's parameter number) viscous force negligible, hence, the fluid is assumed to be inviscid. It is expressed as;

$$\mathrm{Re} = \frac{\rho UL}{\mu} = \frac{UL}{\nu}$$

Its role in forced convection compares to that of Grashof number in natural/free convection which is to govern the transition of flow from laminar to turbulent. The value of Reynold's parameter

number which changes flow pattern from laminar to turbulent motion is called Critical Reynold's Parameter Number. Flow past a flat plate has $\mathrm{Re} \geq 5 \times 10^5$ governing the transition from laminar to turbulent in forced convection.

3.5.2 Prandtl Parameter number, Pr

This is the ratio of viscous to thermal forces acting on fluid particles. This number relates the velocity field with temperature field and is the ratio of the transport properties $\nu \, and \alpha$, which governs the transport of momentum and energy respectively. It plays a role in heat transfer. It has large value when thermal conductivity(denominator) is less than one and viscosity is large, and vice-versa. Expressed as;

$$\mathrm{Pr} = \frac{v}{\alpha}; \quad \alpha = \frac{k}{cp} \quad ;$$

or

$$\mathrm{Pr} = \frac{\mu c_p}{k}$$

3.5.3 Grashof Parameter Number, Gr

This is the ratio of buoyancy forces to viscous forces acting on the fluid particles in the flow field. It usually occurs in natural convection problems due to density differences resulting from concentration differences. It's not as a result of Temperature differences. Its critical value $Gr > 10^9$ governs the transition from laminar to turbulent flow in natural/free convection. A strong convective current is due its large value.

$$Gr = \frac{\nu g \beta \left(T_w^* - T_\infty^* \right)}{U^3}$$

3.5.4 Eckert Parameter Number, Ec

It's the ratio of flow's kinetic energy to thermal energy (boundary layer enthalpy difference). It characterizes heat dissipation and expressed as;

$$Ec = \frac{U^2}{c_p\left(T_w^* - T_\infty^*\right)}$$

3.5.5 Hartmann number, M

The ratio of flow's magnetic force to viscous force, it's expressed as;

$$M^2 = \frac{\sigma\mu_e^2 H_0^2 \nu}{U\rho}$$

3.5.6 Schmidt number, Sc

It relates the velocity field with the concentration field and is the ratio of the transport properties ν *and* D, which govern the transport of momentum and mass respectively. Its role in mass transfer is the same as that of Prandtl number in heat transfer.

$$Sc = \frac{\nu}{D}$$

3.5.7 Nusselt number, Nu

This parameter is equal to the dimensionless temperature gradient at the surface. It provides a measure of the convection heat transfer occurring at the surface.

$$Nu = \frac{\delta\theta}{\delta x}\Big|_{x=0}$$

3.5.8 Sherwood number, Sh

Is the dimensionless concentration gradient at the surface. It provides a measure of the convection mass transfer occurring at the surface and expressed as;

$$Sh = \frac{\delta C}{\delta x}\Big|_{x=0}$$

This study represents dimensional variables with the superscript (*) star basing non-dimensionalization on the set of scaling variables below.

$$t = \frac{t^* U^2}{\nu},\ x = \frac{x^* U}{\nu},\ z = \frac{z^* U}{\nu},\ u = \frac{\bar{u}^*}{U},\ v = \frac{\bar{v}^*}{U},\ w_0 = \frac{\bar{w}_0^*}{U},\ \tau = \frac{\tau^*}{\rho U},\ \theta = \frac{\bar{T}^* - T_\infty^*}{T_w^* - T_\infty^*},$$

$$C = \frac{\bar{C}^* - C_\infty^*}{C_w^* - C_\infty^*},\ Sc = \frac{D}{v},\ \delta = \frac{Qv}{kU^2},\ Gr = \frac{vg\beta(T_w^* - T_\infty^*)}{U^3},\ Gc = \frac{vg\beta'(C_w^* - C_\infty^*)}{U^3}$$

where $T_w^* - T_\infty^*$ is the temperature difference between the surface and free stream temperature and $C_w^* - C_\infty^*$ is the concentration difference between the concentration at the surface and free stream concentration. Writing equations 3.70 and 3.71, in non-dimensional form;

$$\frac{\partial \bar{u}^*}{\partial t^*} = \frac{\partial \bar{u}^*}{\partial t}\frac{\partial t}{\partial t^*} = \frac{U^2}{\nu}\frac{\partial (uU)}{\partial t} = \frac{U^2}{\nu}\{\, U\frac{\partial u}{\partial t} + u\frac{\partial U}{\partial t}\,\} = \frac{U^3}{\nu}\frac{\partial u}{\partial t}$$

$$\bar{u}^*\frac{\partial \bar{u}^*}{\partial x^*} = \bar{u}^*\frac{\partial \bar{u}^*}{\partial x}\frac{\partial x}{\partial x^*} = uU\frac{\partial}{\partial x}(uU)\frac{\partial x}{\partial x^*} = (uU)\frac{\partial}{\partial x}(uU)\frac{U}{\nu} = \frac{(uU^3)}{\nu}\frac{\partial u}{\partial x}$$

$$\bar{w}_0{}^*\frac{\partial \bar{u}^*}{\partial z^*} = w_0 U\frac{\partial \bar{u}^*}{\partial z}\frac{\partial z}{\partial z^*} = w_0 U\frac{\partial}{\partial z}(uU)\frac{\partial z}{\partial z^*} = \left(w_0 U^2\frac{U}{\nu}\right)\frac{\partial u}{\partial z} = \frac{(w_0 U^3)}{\nu}\frac{\partial u}{\partial z}$$

$$\frac{\partial^2 \bar{u}^*}{\partial x^{*2}} = \frac{\partial}{\partial x^*}\left[\frac{\partial \bar{u}^*}{\partial x^*}\right] = \frac{\partial}{\partial x}\left(\frac{U^2}{\nu}\frac{\partial u}{\partial x}\right)\frac{\partial x}{\partial x^*} = \frac{\partial}{\partial x}\left(\frac{U^2}{\nu}\frac{\partial u}{\partial x}\right)\frac{U}{\nu} = \frac{U^3}{\nu^2}\frac{\partial^2 u}{\partial x^2}$$

$$\frac{\partial^2 \bar{u}^*}{\partial z^{*2}} = \frac{\partial}{\partial z^*}\left[\frac{\partial \bar{u}^*}{\partial z^*}\right] = \frac{\partial}{\partial z}\left(\frac{U^2}{\nu}\frac{\partial u}{\partial z}\right)\frac{\partial z}{\partial z^*} = \frac{\partial}{\partial z}\left(\frac{U^2}{\nu}\frac{\partial u}{\partial z}\right)\frac{U}{\nu} = \frac{U^3}{\nu^2}\frac{\partial^2 u}{\partial z^2}$$

$$\frac{\partial}{\partial x^*}\left[k^2x^2\left(\frac{\partial \bar{v}^*}{\partial x^*}\right)^2\right]=k^2x^2\,\frac{\partial}{\partial x^*}\left(\frac{\partial \bar{v}^*}{\partial x^*}\right)^2=k^2x^2\,\frac{\partial}{\partial x^*}\left(\frac{\partial \bar{v}^*}{\partial x}\,\frac{\partial x}{\partial x^*}\right)^2=k^2x^2\,\frac{\partial}{\partial x^*}\left(\frac{\partial}{\partial x}\nu U\frac{U}{\nu}\right)^2$$

$$=\frac{\partial}{\partial x}\left[k^2x^2\frac{U^4}{\nu^2}\frac{\partial^2 v}{\partial x^2}\right]\frac{\partial x}{\partial x^*}=\frac{\partial}{\partial x}\left[k^2x^2\frac{U^5}{\nu^3}\left(\frac{\partial v}{\partial x}\right)^2\right]=\frac{U^5}{\nu^3}\left[2k^2x\left(\frac{\partial v}{\partial x}\right)^2+2k^2x^2\left(\frac{\partial^2 v}{\partial x^2}\right)\left(\frac{\partial v}{\partial x}\right)\right]$$

Since $T^*-T_\infty^*=(T_w^*-T_\infty^*)\theta$ and $C^*-C_\infty^*=(C_w^*-C_\infty^*)C$

Hence;

$$\frac{U^3}{\nu}\frac{\partial u}{\partial t}+\frac{uU^3}{\nu}\frac{\partial u}{\partial x}-\frac{w_0U^3}{\nu}\frac{\partial u}{\partial z}=\frac{\mu}{\rho}\left(\frac{U^3}{\nu^2}\frac{\partial^2 u}{\partial x}+\frac{U^3}{\nu^2}\frac{\partial^2 u}{\partial z^2}\right)+\beta g\left(T_w^*-T_\infty^*\right)\theta$$
$$+g\beta' C\left(C_w^*-C_\infty^*\right)+\frac{U^5}{\nu^3}\left[2k^2x\left(\frac{\partial v}{\partial x}\right)^2+2k^2x^2\left(\frac{\partial^2 v}{\partial x^2}\right)\left(\frac{\partial v}{\partial x}\right)\right]+\frac{\delta\psi^2\mu_e^2H_0^2\left[\nu m_*\psi-u\left(1+m_*n_*\psi^2\right)\right]}{\left[1+m_*n_*\psi^2\right]^2+m_*^2\psi^2}$$

(3.74)

$$\frac{U^3}{\nu}\frac{\partial v}{\partial t}+\frac{uU}{\nu}\frac{\partial v}{\partial x}-\frac{w_0U^3}{\nu}\frac{\partial v}{\partial z}=\frac{\mu}{\rho}\left(\frac{U^3}{\nu^2}\frac{\partial^2 v}{\partial x}+\frac{U^3}{\nu^2}\frac{\partial^2 v}{\partial z^2}\right)+\beta g\left(T_w{}^*-T_\infty^*\right)\theta$$
$$+g\beta' C\left(C_w{}^*-C_\infty^*\right)+\frac{U^5}{\nu^3}\left[2k^2x\left(\frac{\partial w}{\partial x}\right)^2+2k^2x^2\left(\frac{\partial^2 w}{\partial x^2}\right)\left(\frac{\partial w}{\partial x}\right)\right]-\frac{\delta\psi^2\mu_e^2H_0^2\left[um_*\psi+v\left(1+m_*n_*\psi^2\right)\right]}{\left[1+m_*n_*\psi^2\right]^2+m_*^2\psi^2}$$

(3.75)

Dividing equations (3.74) and (3.75) by $\frac{U^3}{\nu}$ obtain;

$$\frac{\partial u}{\partial t}+u\frac{\partial u}{\partial x}-w_0\frac{\partial u}{\partial z}=\left(\frac{\partial^2 u}{\partial x^2}+\frac{\partial^2 u}{\partial z^2}\right)+\frac{\beta g\nu}{U^3}\left(T_w{}^*-T_\infty^*\right)\theta+\frac{\beta' C\nu g}{U^3}\left(C_w{}^*-C_\infty^*\right)$$
$$+\left[2k^2x\left(\frac{\partial v}{\partial x}\right)^2+2k^2x^2\left(\frac{\partial^2 v}{\partial x^2}\right)\left(\frac{\partial v}{\partial x}\right)\right]+\frac{\delta\psi^2\mu_e^2H_0^2\nu\left[\nu m_*\psi-u\left(1+m_*n_*\psi^2\right)\right]}{\rho U^2\left[1+m_*n_*\psi^2\right]^2+m_*^2\psi^2}$$

(3.76)

$$\frac{\partial v}{\partial t}+u\frac{\partial v}{\partial x}-w_0\frac{\partial v}{\partial z}=\left(\frac{\partial^2 v}{\partial x^2}+\frac{\partial^2 v}{\partial z^2}\right)+\left[2k^2x\left(\frac{\partial w}{\partial x}\right)^2+2k^2x^2\left(\frac{\partial^2 w}{\partial x^2}\right)\left(\frac{\partial w}{\partial x}\right)\right]$$
$$-\frac{\delta\psi^2\mu_e^2H_0^2\nu\left[um_*\psi+\nu\left(1+m_*n_*\psi^2\right)\right]}{\rho U^2\left[1+m_*n_*\psi^2\right]^2+m_*^2\psi^2} \qquad (3.77)$$

Since $\nu=\frac{\mu}{\rho}$, non-dimensionalizing equation (3.58) yields;

$$\frac{\partial\overline{T}^*}{\partial t^*}=\frac{\partial\overline{T}^*}{\partial\theta}\cdot\frac{\partial\theta}{\partial t}\cdot\frac{\partial t}{\partial t^*}=\frac{U^2}{\nu}\left(T_w^*-T_\infty^*\right)\frac{\partial\theta}{\partial t}$$

$$\overline{u}^*\frac{\partial\overline{T}^*}{\partial x^*}=\left(uU\right)\frac{\partial\overline{T}^*}{\partial\theta}\frac{\partial\theta}{\partial x}\frac{\partial x}{\partial x^*}=uU\frac{U}{\nu}\left(T_w^*-T_\infty^*\right)\frac{\partial\theta}{\partial x}$$

$$\overline{w}^*{}_0\frac{\partial\overline{T}^*}{\partial z^*}=\left(w_0U\right)\frac{\partial\overline{T}^*}{\partial\theta}\frac{\partial\theta}{\partial z}\frac{\partial z}{\partial z^*}=\frac{w_0U^2}{\nu}\left(T_w^*-T_\infty^*\right)\frac{\partial\theta}{\partial z}$$

$$\frac{\partial^2\overline{T}^*}{\partial x^{*2}}=\frac{\partial}{\partial x^*}\frac{\partial\overline{T}^*}{\partial x^*}=\frac{\partial}{\partial x^*}\frac{\partial\overline{T}^*}{\partial\theta}\frac{\partial\theta}{\partial x}\frac{\partial x}{\partial x^*}=\frac{U^2}{\nu^2}\left(T_w^*-T_\infty^*\right)\frac{\partial^2\theta}{\partial x^2}$$

$$\frac{\partial^2\overline{T}^*}{\partial z^{*2}}=\frac{\partial}{\partial z^*}\frac{\partial\overline{T}^*}{\partial z^*}=\frac{\partial}{\partial z}\frac{\partial\overline{T}^*}{\partial\theta}\frac{\partial\theta}{\partial z}\frac{\partial z}{\partial z^*}\frac{\partial z}{\partial z^*}=\frac{U^2}{\nu^2}\left(T_w^*-T_\infty^*\right)\frac{\partial^2\theta}{\partial z^2}$$

Substituting in (3.58) we obtain;

$$\left(T_w^*-T_\infty^*\right)\frac{U^2}{\nu}\frac{\partial\theta}{\partial t}+\frac{uU^2}{\nu}\left(T_w^*-T_\infty^*\right)\frac{\partial\theta}{\partial x}-\frac{w_0U^2}{\nu}\left(T_w^*-T_\infty^*\right)\frac{\partial\theta}{\partial z}$$
$$=\frac{k}{\rho Cp}\left[\frac{U^2}{\nu^2}\left(T_w^*-T_\infty^*\right)\frac{\partial^2\theta}{\partial x^2}+\frac{U^2}{\nu^2}\left(T_w^*-T_\infty^*\right)\frac{\partial^2\theta}{\partial z^2}\right]+\phi+\frac{Q^+}{\rho Cp} \qquad (3.78)$$

Multiplying by $\frac{\nu}{U^2\left(T_w^*-T_\infty^*\right)}$ we obtain;

$$\frac{\partial\theta}{\partial t}+u\frac{\partial\theta}{\partial x}-w_0\frac{\partial\theta}{\partial z}=\frac{k}{\mu Cp}\left[\frac{\partial^2\theta}{\partial x^2}+\frac{\partial^2\theta}{\partial z^2}\right]+\frac{U^2}{Cp\left(T_w^*-T_\infty^*\right)}\left[\left(\frac{\partial u}{\partial z}\right)^2+\left(\frac{\partial v}{\partial z}\right)^2\right] \qquad (3.79)$$

Non-dimensionalizing equation (3.59);

$$\frac{\partial \overline{C}^*}{\partial t^*} = \frac{\partial \overline{C}^*}{\partial C} \cdot \frac{\partial C}{\partial t} \cdot \frac{\partial t}{\partial t^*} = \frac{U^2}{\nu}\left(C_w^* - C_\infty^*\right)\frac{\partial C}{\partial t}$$

$$\overline{u}^* \frac{\partial \overline{C}^*}{\partial x^*} = \left(uU^2\right)\frac{\partial \overline{C}^*}{\partial C}\frac{\partial C}{\partial x}\frac{\partial x}{\partial x^*} = uU\frac{U}{\nu}\left(C_w^* - C_\infty^*\right)\frac{\partial C}{\partial x}$$

$$\overline{w}_0{}^* \frac{\partial \overline{C}^*}{\partial z^*} = \left(w_0 U^2\right)\frac{\partial \overline{C}^*}{\partial C}\frac{\partial C}{\partial z}\frac{\partial z}{\partial z^*} = w_0\frac{U^2}{\nu}\left(C_w^* - C_\infty^*\right)\frac{\partial C}{\partial z}$$

$$\frac{\partial^2 \overline{C}^*}{\partial x^{*2}} = \frac{\partial}{\partial x^*}\frac{\partial \overline{C}^*}{\partial x^*} = \frac{\partial}{\partial x}\left[\frac{U}{\nu}\left(C_w^* - C_\infty^*\right)\frac{\partial C}{\partial x}\right]\frac{\partial x}{\partial x^*} = \frac{U^2}{\nu^2}\left(C_w^* - C_\infty^*\right)\frac{\partial^2 C}{\partial x^2}$$

$$\frac{\partial^2 \overline{C}^*}{\partial z^{*2}} = \frac{\partial}{\partial z^*}\frac{\partial \overline{C}^*}{\partial z^*} = \frac{\partial}{\partial z}\left[\frac{U}{\nu}\left(C_w^* - C_\infty^*\right)\frac{\partial C}{\partial z}\right]\frac{\partial z}{\partial z^*} = \frac{U^2}{\nu^2}\left(C_w^* - C_\infty^*\right)\frac{\partial^2 C}{\partial z^2}$$

Substituting and multiplying by $\frac{\nu}{U^2\left(C_w^* - C_\infty^*\right)}$ equation (3.73) becomes;

$$\frac{\partial C}{\partial t} + u\frac{\partial C}{\partial x} - w_0\frac{\partial C}{\partial z} = \frac{D}{\nu}\left(\frac{\partial^2 C}{\partial x^2} + \frac{\partial^2 C}{\partial z^2}\right) \tag{3.80}$$

Equations (3.76), (3.77), (3.79) and (3.80) reduced further by dimensionless parameters we obtain;

$$\begin{aligned}\frac{\partial u}{\partial t} + u\frac{\partial u}{\partial x} - w_0\frac{\partial u}{\partial z} &= \left(\frac{\partial^2 u}{\partial x^2} + \frac{\partial^2 u}{\partial z^2}\right) + Gr\theta + GcC \\ &+ \left[2k^2 x\left(\frac{\partial v}{\partial x}\right)^2 + 2k^2 x^2\left(\frac{\partial^2 v}{\partial x^2}\right)\left(\frac{\partial v}{\partial x}\right)\right] + \frac{M^2\psi^2\left[vm_*\psi - u\left(1 + m_* n_* \psi^2\right)\right]}{\left[1 + m_* n_* \psi^2\right]^2 + m_*^2\psi^2}\end{aligned} \tag{3.81}$$

$$\begin{aligned}\frac{\partial v}{\partial t} + u\frac{\partial v}{\partial x} - w_0\frac{\partial v}{\partial z} &= \left(\frac{\partial^2 v}{\partial x^2} + \frac{\partial^2 v}{\partial z^2}\right) + \left[2k^2 x\left(\frac{\partial w}{\partial x}\right)^2 + 2k^2 x^2\left(\frac{\partial^2 w}{\partial x^2}\right)\left(\frac{\partial w}{\partial x}\right)\right] \\ &- \frac{M^2\psi^2\left[um_*\psi + v\left(1 + m_* n_* \psi^2\right)\right]}{\left[1 + m_* n_* \psi^2\right]^2 + m_*^2\psi^2}\end{aligned} \tag{3.82}$$

$$\frac{\partial \theta}{\partial t} + u\frac{\partial \theta}{\partial x} - w_0\frac{\partial \theta}{\partial z} = \frac{1}{\mathrm{Pr}}\left[\frac{\partial^2 \theta}{\partial x^2} + \frac{\partial^2 \theta}{\partial z^2}\right] - \frac{\sigma}{\mathrm{Pr}}\theta + Ec\left[\left(\frac{\partial u}{\partial x}\right)^2 + \left(\frac{\partial v}{\partial x}\right)^2 + \left(\frac{\partial u}{\partial z}\right)^2 + \left(\frac{\partial v}{\partial z}\right)^2\right] \tag{3.83}$$

and

$$\frac{\partial C}{\partial t}+u\frac{\partial C}{\partial x}-w_0\frac{\partial C}{\partial z}=\frac{1}{Sc}\left(\frac{\partial^2 C}{\partial x^2}+\frac{\partial^2 C}{\partial z^2}\right) \tag{3.84}$$

Initial and boundary conditions in non-dimensional form are;

For

$$\left.\begin{aligned} t\le 0; \qquad u(z,x,0) &= 0, v(z,x,0) = 0 \\ \theta(z,\ x,\ 0) &= 0,\ C(z\ ,x,\ 0) = 0 \end{aligned}\right\} \tag{3.85}$$

For

$$\left.\begin{aligned} t>0; \qquad u(0,x,t) &= 1, v(0,x,t) = 0 \\ \theta(0,\ x,\ t) &= 1,\ C(0\ ,x,\ t) = 1 \end{aligned}\right\} \tag{3.86a}$$

$$\left.\begin{aligned} u(\infty,x,t) &= 0, v(\infty,x,t) = 0 \\ \theta(\infty,\ x,\ t) &= 0,\ C(\infty\ ,x,\ t) = 0 \end{aligned}\right\} \tag{3.86b}$$

CHAPTER FOUR

NUMERICAL METHOD OF SOLUTION

4.1 Method of Solution

Equations governing free convection fluid flow considered in our study are non-linear thus, their exact solution is not possible. We generate numerical solutions of the equations by using the finite difference method. This method is preferred because it's stable and flexible to use with the initial and boundary conditions, the method is also fast and convergent for the solution of our problem equations. Newton's interpolation formula is used to determine the skin friction, rate of heat and mass transfers at the plate surface. The Numerical finite difference method used to solve our equations proved to be consistent, stable and convergent. Convergence of a method narrows down to an exact numerical solution whether more grid points are taken or step size decreased. Stability has the effect of boundedness of any single fixed round off error, while consistency means tending to zero of the truncation error as the step size decreases. The numerical error in computations is due to our inability to get exact values, since calculations contain truncation or round off errors. Furthermore, certain cases have exact solutions considerably different from the difference solution. Approximation of equations (3.81) to (3.84) by a set of finite difference equations involves the definition of a suitable mesh.

4.1.1 Definition of mesh

Expressing relationship between the partial derivatives in the differential equation and the function values at the adjacent nodal points, entails the use of a uniform mesh. Taking *x*-*z* plane and dividing into a network of uniform rectangular cells of width Δz and height Δx , with *k* and *i* referring to *z* and *x* respectively as below. Δz representing increment in *z* and Δx representing

increment in x then $z = k\Delta z$ and $x = i\Delta x$. The finite difference approximations of the partial derivatives appearing in equations (3.81), (3.82), (3.83) and (3.84) are then obtained, by Taylor series expansion of the dependent variable about a grid (k,i) as;

$$\phi(k-1,i) = \phi(k,i) - \phi'(k,i)\Delta z + \frac{1}{2}\phi''(k,i)(\Delta z)^2 - \frac{1}{6}\phi'''(k,i)(\Delta z)^3 + ... \quad \ldots\ldots\ldots\ldots \quad (3.88)$$

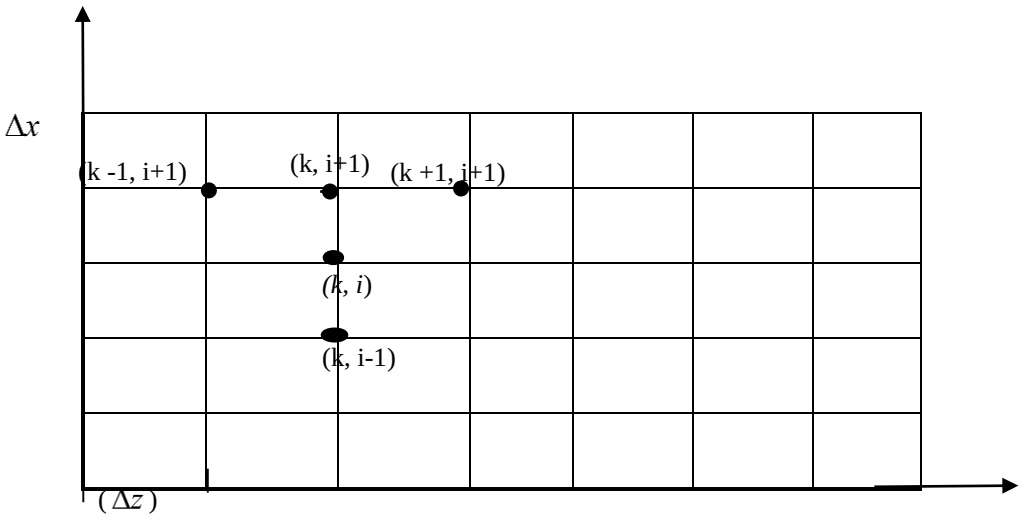

Figure 3: The Computational Mesh

$$\phi(k+1,i) = \phi(k,i) + \phi'(k,i)\Delta z + \frac{1}{2}\phi''(k,i)(\Delta z)^2 + \frac{1}{6}\phi'''(k,i)(\Delta z)^3 + ... \quad (3.89)$$

Subtracting (3.88) from (3.89) and eliminating ϕ'' we obtain;

$$\phi' = \frac{\phi(k+1,i) - \phi(k-1,i)}{2\Delta z} + Hot \quad (3.90)$$

Adding (3.88) to (3.89) and eliminating ϕ' we obtain;

$$\phi'' = \frac{\phi(k+1,i) - 2\phi(k,i) + (k-1,i)}{(\Delta z)^2} + Hot \quad (3.91)$$

Central difference formulae for the first and the second derivatives with respect to x are;

$$\phi' = \frac{\phi(k,i+1) - \phi(k,i-1)}{2\Delta x} + Hot \quad (3.92)$$

$$\phi'' = \frac{\phi(k,i+1) - 2\phi(k,i) + \phi(k,i-1)}{(\Delta x)^2} + Hot \tag{3.93}$$

In forward difference form;

$$\phi' = \frac{\phi(k+1,i) - \phi(k,i)}{\Delta z} + Hot \tag{3.94}$$

$$\phi'' = \frac{\phi(k+1,i) - 2\phi(k,i) + \phi(k-1,i)}{(\Delta z)^2} + Hot \tag{3.95}$$

$$\phi' = \frac{\phi(k,i+1) - \phi(k,i)}{\Delta x} + Hot \tag{3.96}$$

In this study we use subscripts to indicate spatial and superscript to indicate time $T_{(k,i)}^{n+1} = (z_k, x_i, t_{n+1})$. Let the mesh point variable at time t_n be denoted by $\phi_{(k,i)}^n$. The forward difference for the first order derivatives with respect to time is given by;

$$\phi'^{n}_{(k,i)} = \frac{\phi_{(k,i)}^{n+1} - \phi_{(k,i)}^n}{\Delta t} + Hot \tag{3.97}$$

Computing the first order time derivative using forward difference approximation whereas, first and second order spatial derivatives by the central finite difference approximation. The governing equations (3.81) to (3.84) for $u_{(k,i)}^{n+1}$, $v_{(k,i)}^{n+1}$, $\theta_{(k,i)}^{n+1}$ *and* $C_{(k,i)}^{n+1}$ yield;

$$u_{(k,i)}^{n+1} = \Delta t \left\{ \begin{array}{l} -u_{(k,i)}^n \left[\dfrac{u_{(k,i+1)}^n - u_{(k,i-1)}^n}{2\Delta x} \right] + w_0 \left[\dfrac{u_{(k+1,i)}^n - u_{(k-1.i)}^n}{2\Delta z} \right] + \dfrac{u_{(k+1,i)}^n - 2u_{(k,i)}^n + u_{(k-1,i)}^n}{(\Delta z)^2} \\ + \dfrac{u_{(k,i+1)}^n - 2u_{(k,i)}^n + u_{(k,i-1)}^n}{(\Delta x)^2} + Gr\theta_{(k,i)}^n + GcC_{(k,i)}^n + 2k^2 i\Delta x \left(\dfrac{v_{(k,i+1)}^n - v_{(k,i-1)}^n}{2\Delta x} \right)^2 \\ + 2k^2 (i\Delta x)^2 \left(\dfrac{v_{(k,i+1)}^n - 2v_{(k,i)}^n + v_{(k,i-1)}^n}{(\Delta x)^2} \right) \left(\dfrac{v_{(k,i+1)}^n - v_{(k,i-1)}^n}{2\Delta x} \right) \\ + \dfrac{M^2 \psi^2 \left[v_{(k,i)}^n m_* \psi - u_{(k,i)}^n (1 + m_* n_* \psi^2) \right]}{\left[1 + m_* n_* \psi^2 \right]^2 + m_*^2 \psi^2} \end{array} \right\} + u_{(k,i)}^n$$

(3.98)

$$v_{(k,i)}^{n+1}=\Delta t\left\{\begin{array}{l}-u_{(k,i)}^{n}\left[\dfrac{v_{(k,i+1)}^{n}-v_{(k,i-1)}^{n}}{2\Delta x}\right]+w_0\left[\dfrac{v_{(k+1,i)}^{n}-v_{(k-1.i)}^{n}}{2\Delta z}\right]+\dfrac{v_{(k+1,i)}^{n}-2v_{(k,i)}^{n}+v_{(k-1,i)}^{n}}{(\Delta z)^2}\\ +\dfrac{v_{(k,i+1)}^{n}-2v_{(k,i)}^{n}+v_{(k,i-1)}^{n}}{(\Delta x)^2}+2k^2i\Delta x\left(\dfrac{w_{(k,i+1)}^{n}-w_{(k,i-1)}^{n}}{2\Delta x}\right)^2\\ +2k^2(i\Delta x)^2\left(\dfrac{w_{(k,i+1)}^{n}-2w_{(k,i)}^{n}+w_{(k,i-1)}^{n}}{(\Delta x)^2}\right)\left(\dfrac{w_{(k,i+1)}^{n}-w_{(k,i-1)}^{n}}{2\Delta x}\right)\\ -\dfrac{M^2\psi^2\left[u_{(k,i)}^{n}m_*\psi+v_{(k,i)}^{n}(1+m_*n_*\psi^2)\right]}{\left[1+m_*n_*\psi^2\right]^2+m_*^2\psi^2}\end{array}\right\}+u_{(k,i)}^{n}$$

(3.99)

$$\frac{\theta_{(k,i)}^{n+1}-\theta_{(k,i)}^{n}}{\Delta t}+u_{(k,i)}^{n}\left[\frac{\theta_{(k,i+1)}^{n}-\theta_{(k,i-1)}^{n}}{2\Delta x}\right]-w_0\frac{\theta_{(k+1,i)}^{n}-\theta_{(k-1,i)}^{n}}{2\Delta z}=\frac{1}{\mathrm{Pr}}\left[\frac{\theta_{(k,i+1)}^{n}-2\theta_{(k,i)}^{n}+\theta_{(k,i-1)}^{n}}{(\Delta x)^2}\right]$$

$$+\frac{1}{\mathrm{Pr}}\left[\frac{\theta_{(k+1,i)}^{n}-2\theta_{(k,i)}^{n}+\theta_{(k-1,i)}^{n}}{(\Delta z)^2}\right]-\frac{\sigma}{\mathrm{Pr}}\theta_{(k,i)}^{n}+Ec\left[\begin{array}{l}\left(\dfrac{u_{(k,i+1)}^{n}-u_{(k,i-1)}^{n}}{2\Delta x}\right)^2+\left(\dfrac{v_{(k,i+1)}^{n}-v_{(k,i-1)}^{n}}{2\Delta x}\right)^2\\ +\left(\dfrac{u_{(k+1,i)}^{n}-u_{(k-1,i)}^{n}}{2\Delta z}\right)^2+\left(\dfrac{v_{(k+1,i)}^{n}-v_{(k-1,i)}^{n}}{2\Delta z}\right)^2\end{array}\right]+\theta_{(k,i)}^{n}$$

(4.00)

$$\theta_{(k,i)}^{n+1}=\Delta t\left\{\begin{array}{l}-u_{(k,i)}^{n}\left[\dfrac{\theta_{(k,i+1)}^{n}-\theta_{(k,i-1)}^{n}}{2\Delta x}\right]+w_0\left[\dfrac{\theta_{(k+1,i)}^{n}-\theta_{(k-1.i)}^{n}}{2\Delta z}\right]+\dfrac{1}{\mathrm{Pr}}\dfrac{\theta_{(k+1,i)}^{n}-2\theta_{(k,i)}^{n}+\theta_{(k-1,i)}^{n}}{(\Delta z)^2}\\ +\dfrac{1}{\mathrm{Pr}}\dfrac{\theta_{(k,i+1)}^{n}-2\theta_{(k,i)}^{n}+\theta_{(k,i-1)}^{n}}{(\Delta x)^2}-\dfrac{\sigma}{\mathrm{Pr}}\theta_{(k,i)}^{n}+Ec\left[\begin{array}{l}\left(\dfrac{u_{(k,i+1)}^{n}-u_{(k,i-1)}^{n}}{2\Delta x}\right)^2+\left(\dfrac{v_{(k,i+1)}^{n}-v_{(k,i-1)}^{n}}{2\Delta x}\right)^2\\ +\left(\dfrac{u_{(k+1,i)}^{n}-u_{(k-1,i)}^{n}}{2\Delta z}\right)^2+\left(\dfrac{v_{(k+1,i)}^{n}-v_{(k-1,i)}^{n}}{2\Delta z}\right)^2\end{array}\right]\end{array}\right\}+\theta_{(k,i)}^{n}$$

(4.01)

and

$$C_{(k,i)}^{n+1} = \Delta t \left\{ -u_{(k,i)}^{n} \left[\frac{C_{(k,i+1)}^{n} - C_{(k,i-1)}^{n}}{2\Delta x} \right] + w_0 \left[\frac{C_{(k+1,i)}^{n} - C_{(k-1.i)}^{n}}{2\Delta z} \right] + \frac{1}{Sc} \left[\left(\frac{C_{(k,i+1)}^{n} - 2C_{(k,i)}^{n} + C_{(k,i-1)}^{n}}{(\Delta x)^2} \right) + \left(\frac{C_{(k+1,i)}^{n} - 2C_{(k,i)}^{n} + C_{(k-1,i)}^{n}}{(\Delta z)^2} \right)^2 \right] \right\} + C_{(k,i)}^{n} \tag{4.02}$$

Utilizing the initial and boundary conditions (equations 3.85 to 3.86b) and computing using small values of Δt ,by setting $\Delta t = 0.00125$, $\Delta z = \Delta x = 0.1$ and fixing $z = 4.1 \text{or} k = 41$, corresponding to $z = \infty$. Therefore, setting $u_{(41,i)}^{n} = v_{(41,i)}^{n} = C_{(41,i)}^{n} = \theta_{(41,i)}^{n} = 0$ because u, v, C and θ tend to zero around $x = 4.1$. We compute velocities $u_{(k,i)}^{n+1}$ *and* $v_{(k,i)}^{n+1}$, from equations (3.98) and (3.99) while $\theta_{(k,i)}^{n+1}$ *and* $C_{(k,i)}^{n+1}$, computed from equations (4.01) and (4.02) respectively. The procedure is repeatedly carried out up to $n = 400$ implying that

$t = 0.5$ *for* $i = 1$, $x = 0.1$ and the Prandtl number corresponds to air at the value of 0.71,

$M^2 = 5.0$ is the magnetic parameter for a strong magnetic field. We consider two cases;

1. When the Grashof parameter number, $Gr > 0 (+0.4)$ for convective plate cooling.
2. When the Grashof parameter number, $Gr < 0 (-0.4)$ for convective plate heating.

Stability, convergence and consistency of finite difference method of solution is ensured by running this program using small efficient values like, Δt ; $\Delta t = 0.0005,\ 0.0007,\ 0.0015$. In fact, we observed no significant changes in the results, ascertaining that the method used converges, stable and consistent.

4.1.2 Calculation of rates of heat transfer, mass transfer and skin friction

To calculate skin friction from the velocity profiles, we used the equations

$$\left\{ \tau_x = -\left.\frac{\partial u}{\partial z}\right|_{z=0} \quad and \quad \tau_y = -\left.\frac{\partial v}{\partial z}\right|_{z=0} \quad where \quad \tau = \frac{\tau^*}{\rho\mu^2} \right\} \tag{4.06}$$

Rate of mass transfer is calculated from the concentration profile using the equation,

$$Sh = -\left.\frac{\partial C}{\partial z}\right|_{z=0} \tag{4.07}$$

The skin friction and rate of mass transfer are obtained by numerical differentiation using Newton's interpolation formulae below over the first five points,

$$\tau_x = \frac{5}{6}\left[25u(0,i) - 48u(1,i) + 36u(2,i) - 16u(3,i) + 3u(4,i)\right] \tag{4.08}$$

$$\tau_y = \frac{5}{6}\left[25v(0,i) - 48v(1,i) + 36v(2,i) - 16v(3,i) + 3v(4,i)\right] \tag{4.09}$$

$$Sh = \frac{5}{6}\left[25C(0,i) - 48C(1,i) + 36C(2,i) - 16C(3,i) + 3C(4,i)\right] \tag{4.10}$$

The rate of heat transfer is calculated from temperature profiles in Nusselt parameter number

using the expression; $Nu = -\left.\frac{1}{\theta_{(0,0)}^{n+1}}\frac{\partial\theta}{\partial z}\right|_{z=0}$ (4.11)

But $\frac{\partial\theta}{\partial z} = -1$. Hence; $Nu = \frac{1}{\theta_{(0,0)}^{n+1}}$ (4.12)

CHAPTER FIVE

RESULTS AND DISCUSSION

5.1 Discussion of Results

Matlab program was run for different values of the parameters $Sc, m, n, \sigma, wo, t, Gc, Ec \text{ and } \phi$ to generate results for concentration, temperature and velocity profiles from the finite difference equations (3.98) to (4.02) coupled with the initial and boundary condition equations (3.85 to 3.86b). The primary and secondary velocities are (u) and (v) along the x and y axes respectively. The concentration, temperature and velocity profiles are presented graphically in figures (4 to 45). Skin frictions due to primary velocity profiles $\tau_x \text{ and } \tau_y$ due to secondary velocity profiles, rate of mass transfer Sh and rate of heat transfer Nu are presented in tables (1 to 5). The tables and figures are grouped accordingly for Grashof number $Gr > 0, (+0.4)$ corresponding to cooling of the plate by free convection currents and Grashof number $Gr < 0, (-0.4)$ corresponding to heating of the plate by free convection currents respectively. The magnetic parameter $M^2 = 5.0$ and Prandtl parameter nb umber $\Pr = 0.71$ signifies a strong magnetic field and correspondence to air respectively.

5.1.1 Figures and Tables for cooling of the plate by convection currents

$$\Pr = 0.71, M^2 = 5.0, Gr = +0.4$$

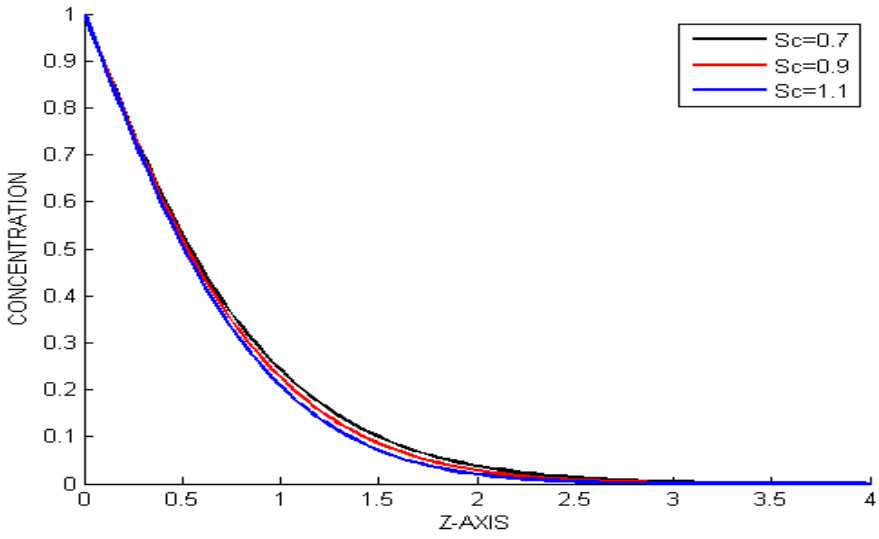

Figure 4: Variation of concentration with Schmidt number Sc

From figure 4, we note that, increasing Mass Diffusion Sc minimally decreases concentration profiles from $Sc = 1.1$ *to* $Sc = 0.7$, this is because under a strong magnetic field, increasing Sc decreases particles' molecular diffusivity resulting to decreased concentration boundary layer, leading to lower concentration species for larger values of Sc.

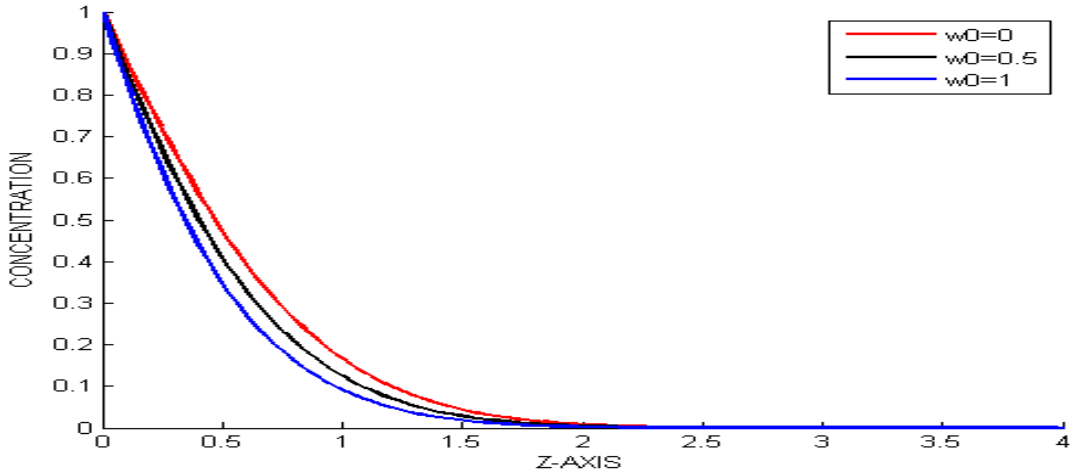

Figure 5: Variation of concentration with Suction velocity wo

From figure 5, we note that, increasing suction velocity *wo* leads to decrease in concentration profiles, reason being that it increases the growth of the boundary layers leading to decrease in concentration profiles.

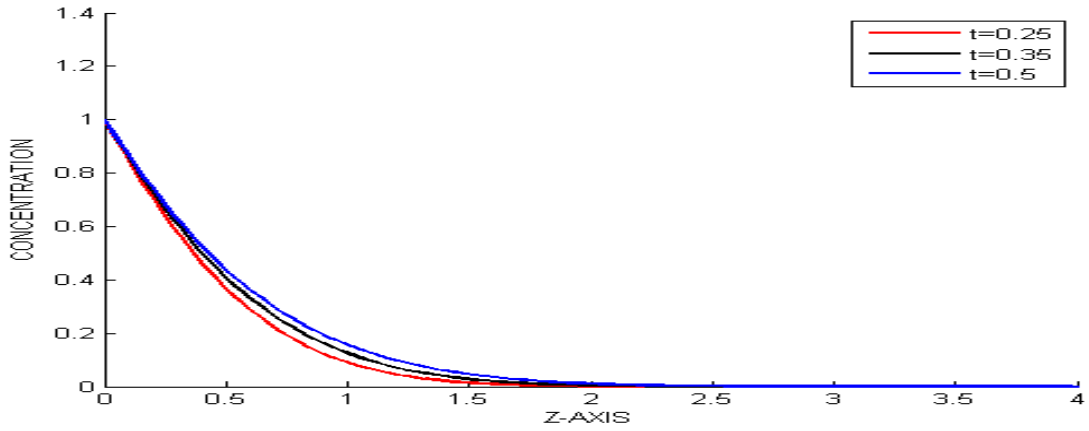

Figure 6: Variation of concentration with time t

From figure 6, we note that, increase in time leads to an increase in concentration profiles, because flow gets to the free stream with time, impacting on its concentration profiles increase.

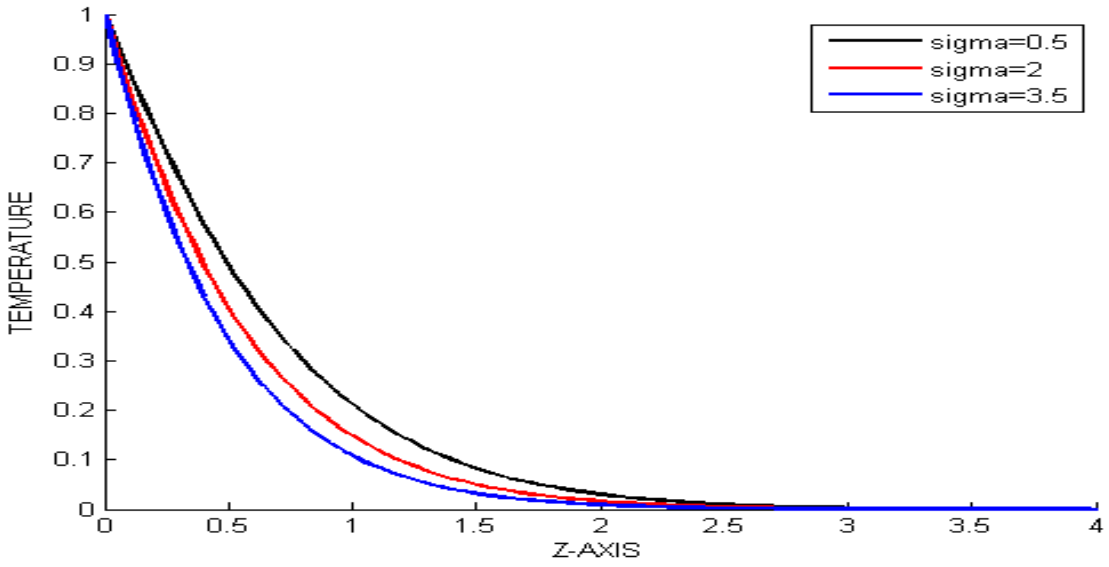

Figure 7: Variation of Temperature with heat source parameter σ

From figure 7, we note that, increasing heat source parameter $\sigma(sigma)$ decreases temperature profiles. This increases internal heat generation and because the plate is cooling, rate of energy transfer increases resulting to the decrease in temperature profiles.

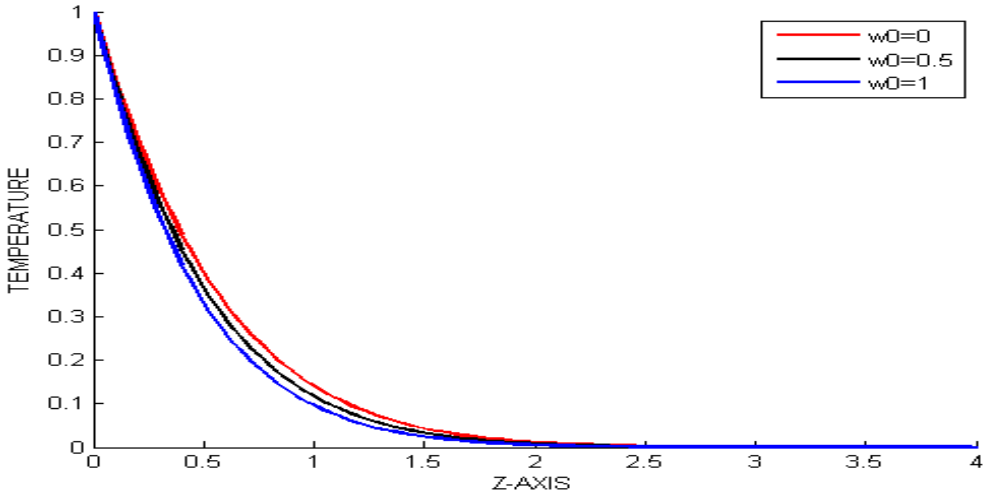

Figure 8: Variation of Temperature with suction velocity wo

From figure 8, we note that, decrease of suction velocity wo causes increase in temperature

profiles.

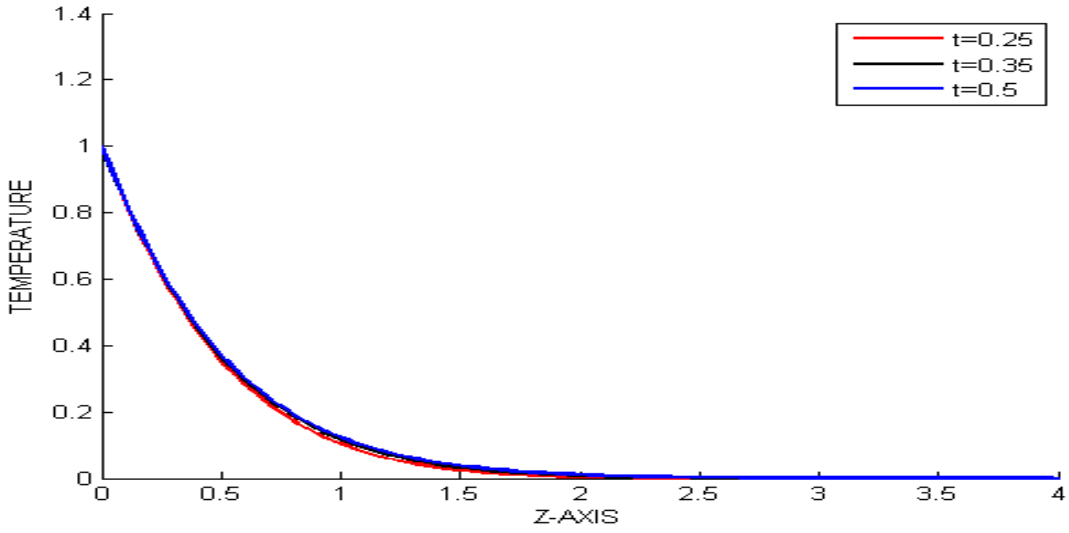

Figure 9: Variation of Temperature with time

From figure 9, we observe that, increases in time t has negligible increase in temperature profiles. This is because as the flow gets to the free stream where the velocity is high, the rate of energy transfer is increased and hence increases in temperature. The angle of inclination ϕ, Ion-Slip n, Hall parameter m and mass diffusion parameter Sc, have no effect on the temperature profiles.

From figure 10 below, we note that primary velocity profiles increase with increase in angle of inclination ϕ; this is because increasing the angle of inclination causes a decrease in the magnetic strength which accelerates the fluid motion by increasing the velocity profiles. Away from the plate it decreases primary velocity to a point after which it remains constantly distributed.

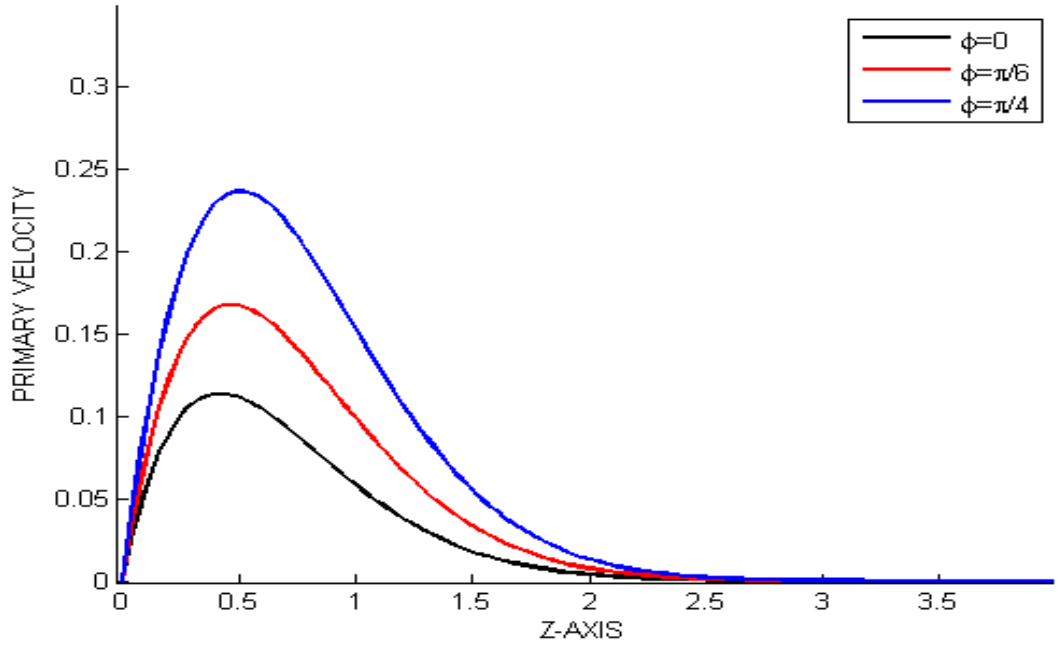

Figure 10: Variation of Primary velocity with angle of inclination ϕ

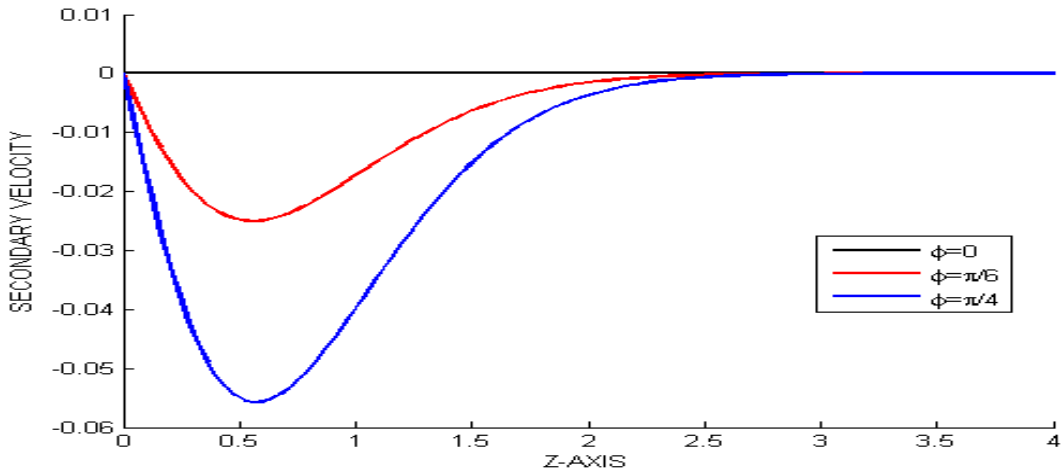

Figure 11: Variation of Secondary velocity with angle of inclination ϕ

From figure 11, we note that an increase in the angle of inclination ϕ causes a decrease in secondary velocity near the plate but away from the plate it minimally increases secondary velocity to a point after which in the main stream the secondary velocity remains constantly distributed.

This is because increasing the angle of magnetic field inclination ϕ causes an increase in the magnetic strength which retards the fluid motion affecting the velocity by reduction.

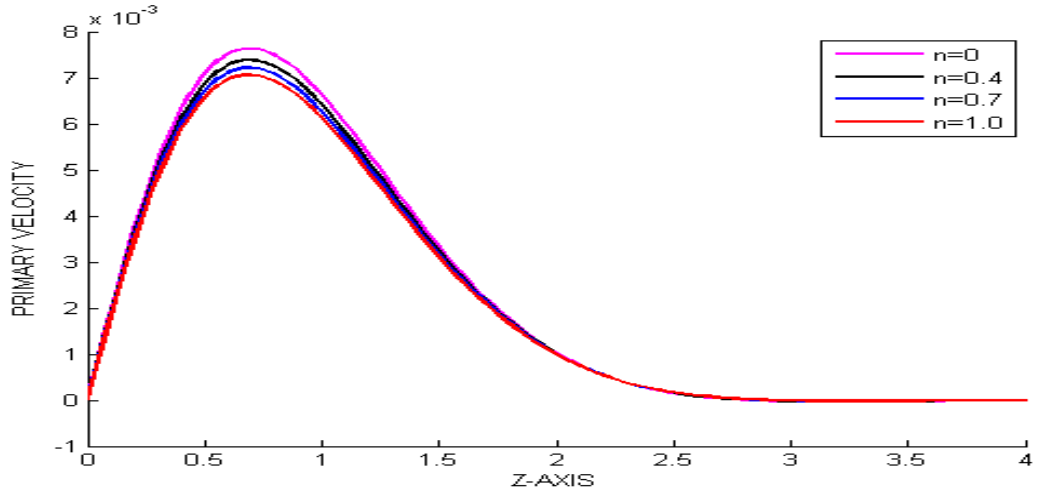

Figure 12: Variation of Primary velocity with Ion-Slip n

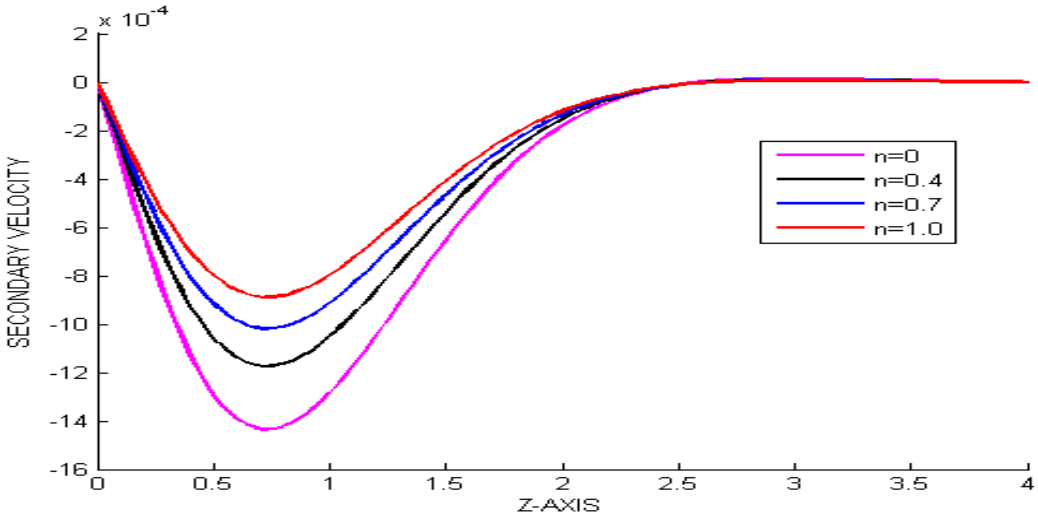

Figure 13: Variation of Secondary velocity with Ion-Slip n

From figures 12 and 13, it's observable that increasing Ion-Slip Parameter n has negligible primary velocity profiles increase while significantly increases secondary velocity profiles at the plate surface to a maximum, after which remain constantly distributed in the main stream. This is

because, increase in Ion-Slip currents cause the force in the direction of the fluid flow to increase and accelerate secondary velocity profiles to higher values in the flow field. Since the magnitude of primary velocity profile is very small, there is a very small increase in primary velocity profile with the change in the Ion-Slip currents.

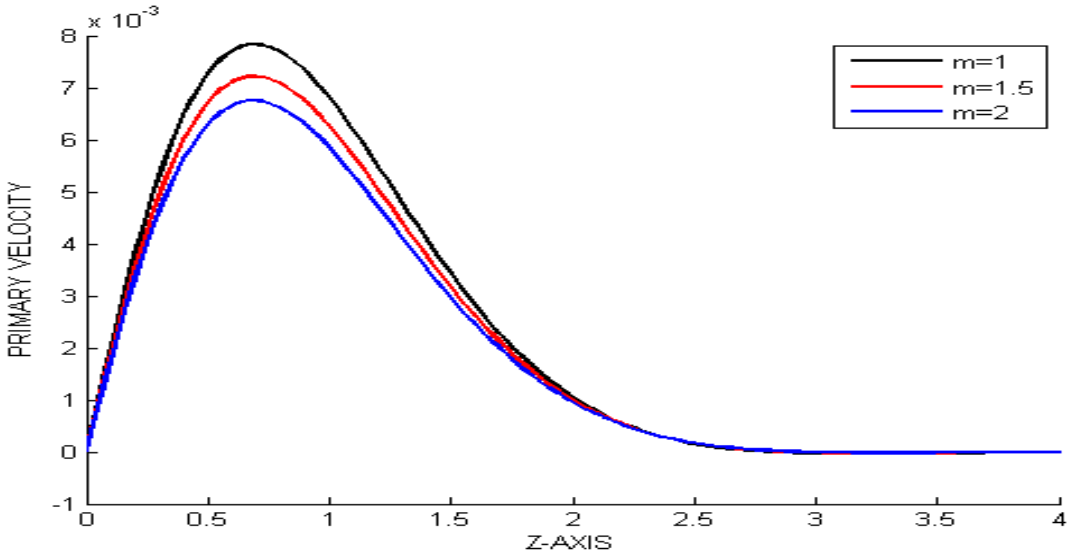

Figure 14:Variation of Primary velocity with Hall parameter m

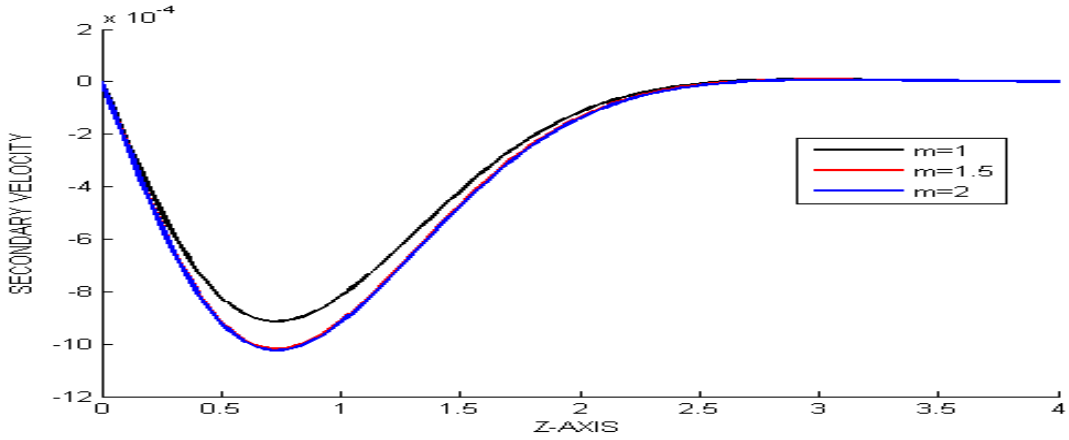

Figure 15:Variation of Secondary velocity with Hall parameter m

From figure 14 and 15, we note that an increase in Hall current parameter m causes a decrease in both primary and secondary velocity profiles, because, effective conductivity increases with an

increase in Hall current parameter m ,which increases magnetic damping force hence a decrease in both velocities since the plate is cooling.

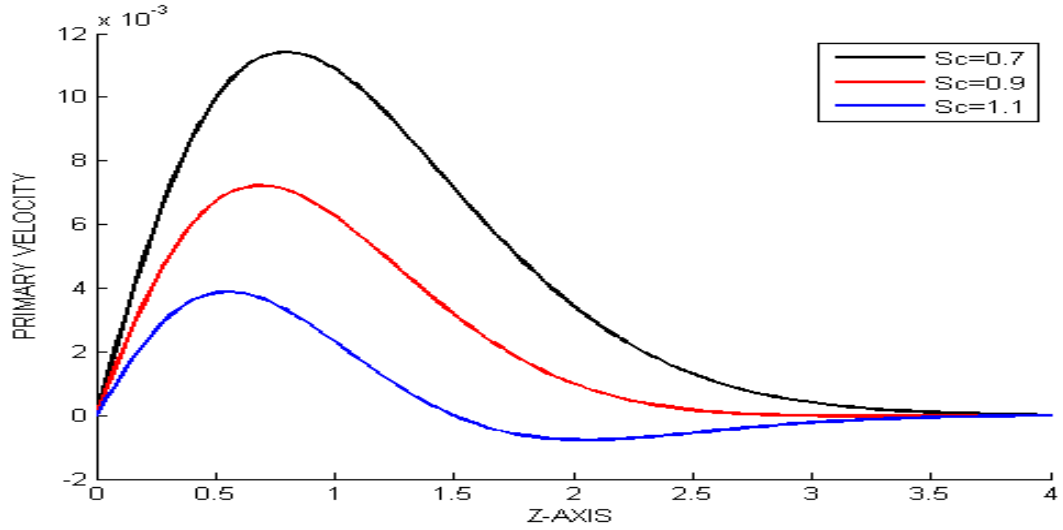

Figure 16: Variation of Primary velocity with Schmidt number Sc

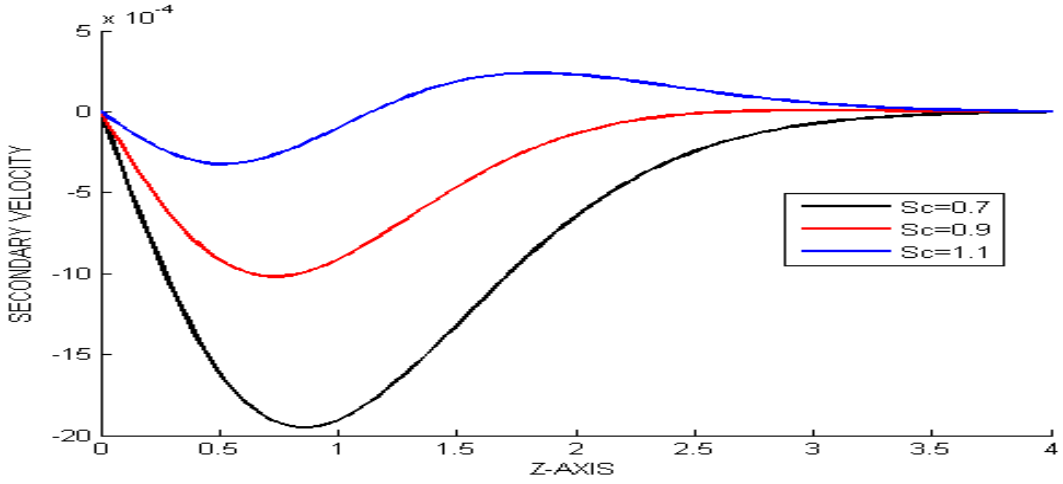

Figure 17: Variation of Secondary velocity with Schmidt number Sc

From figure 16 and 17, it's observable that increasing mass diffusion parameter Sc decreases primary velocity profiles due to the fact that increase in mass diffusion parameter decreases molecular (mass) diffusivity in fluids resulting to a decrease in primary velocity profiles but an

increase in secondary velocity profiles near the plate leaving the velocity profiles constantly distributed far away from the plate (in the main stream).

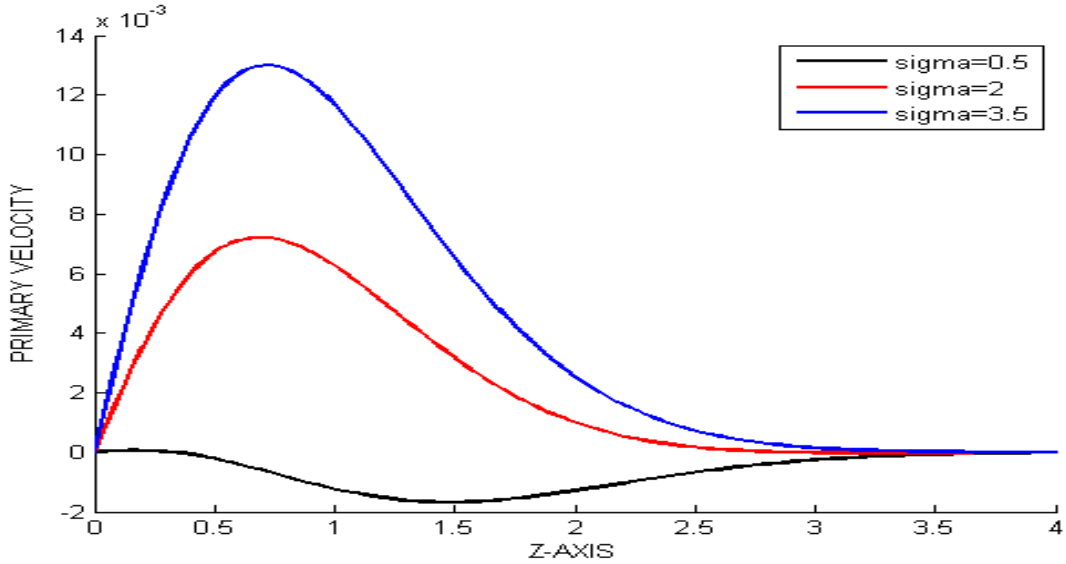

Figure 18: Variation of Primary velocity with heat source parameter σ

From figure 18, the result shows that an increase in heat source parameter $\sigma(sigma)$ increases primary velocity profiles to a maximum near the plate and constantly distributed in the main stream due to the increase in internal heat generation. Since the plate is cooling, the rate of energy transfer between fluid particles reduce leading to increase in fluid's velocity profiles.

From figure 19 below, we note that, increase in heat source parameter σ decreases secondary velocity profiles to a minimum near the plate, thereafter, maintains constant distribution to the free stream (far away from the plate). This is due to an increase in the internal heat generation, and because the plate is cooling, energy transfer rate between the fluid particles increases leading to a decrease in the fluids' velocity.

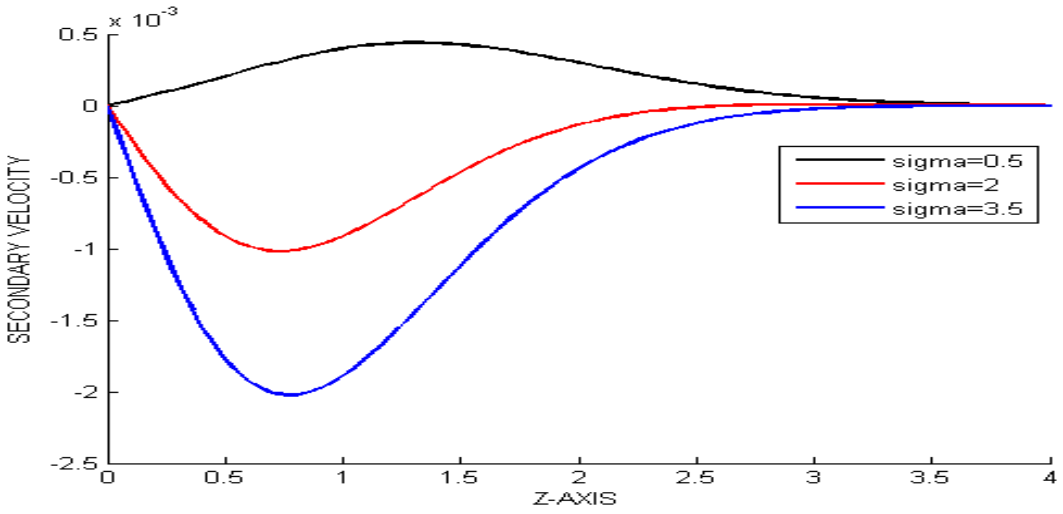

Figure 19: Variation of Secondary velocity with heat source parameter σ

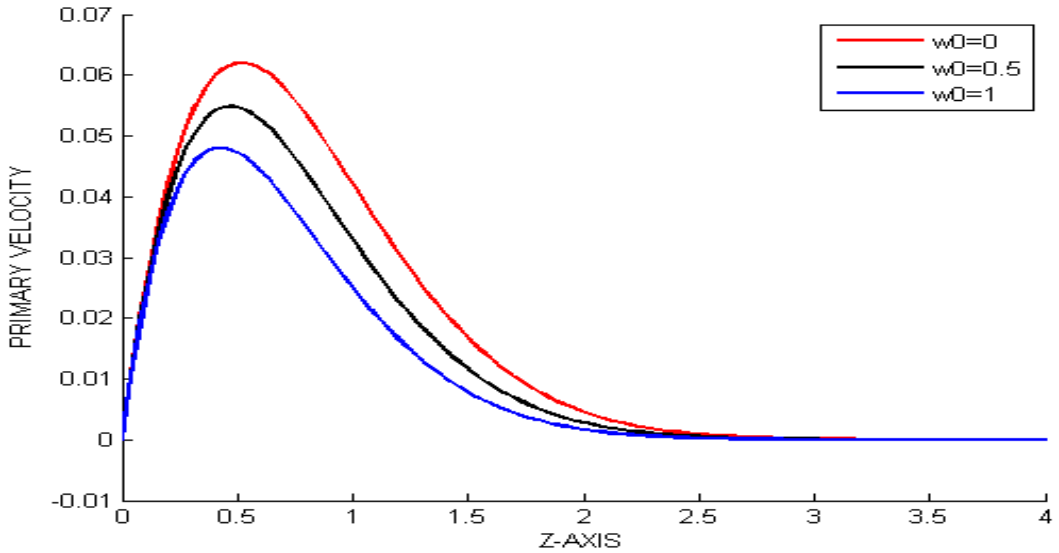

Figure 20: Variation of Primary velocity with suction velocity

From figure 20,we observe that, decreasing suction velocity *wo* gradually increases primary velocity profiles near the plate to a maximum point after which the primary velocity profiles assume the same value in the free stream.

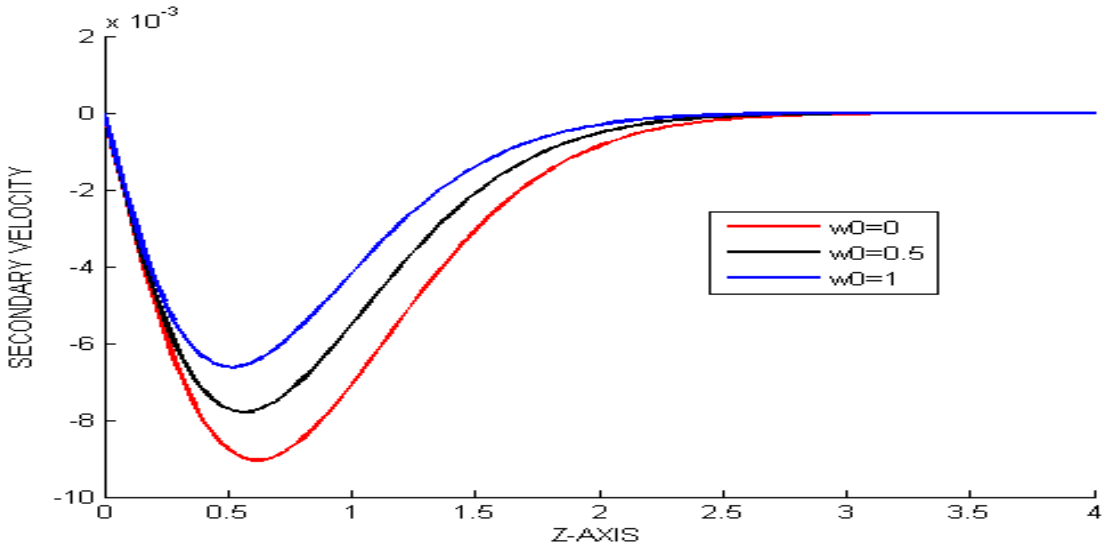

Figure 21: Variation of Secondary velocity with suction velocity wo

From figure 21, we observe that, removal of suction velocity *wo* gradually decreases secondary velocity profiles near the plate to a minimum after which velocity profiles begin to increase steadily to a constantly value of zero distribution in the free stream.

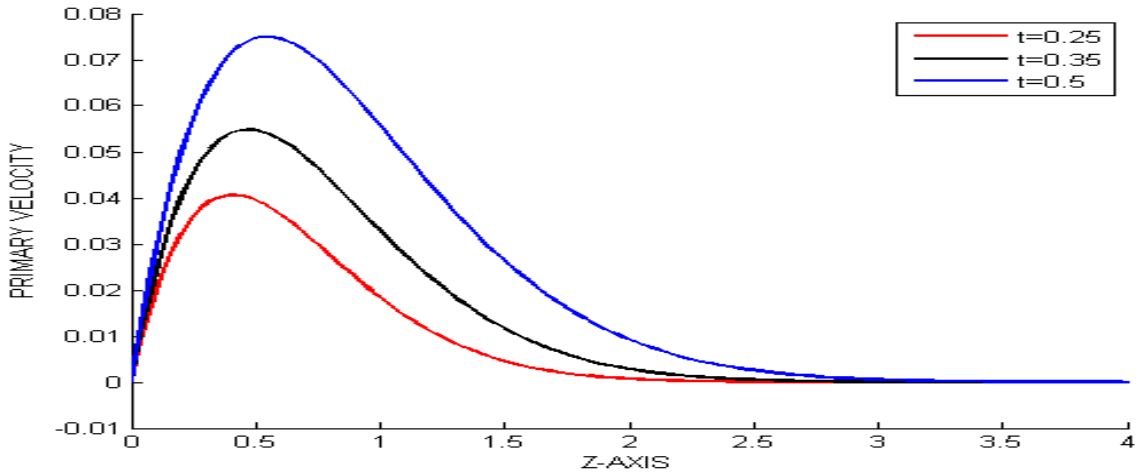

Figure 22: Variation of Primary velocity with time

From figure 22, we observe that, increasing time t, increases primary velocity profiles to a maximum point close to the plate,then begins to decrease steadily to zero. Reason being that,with

time the flow gets to the free stream where the fluid velocity profiles remain constantly valued at zero in the main stream.

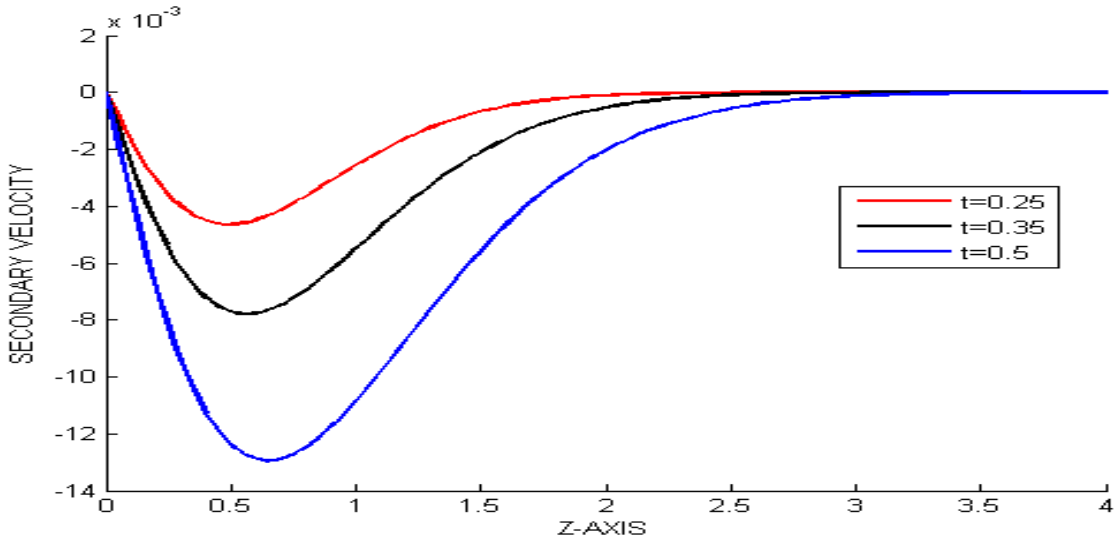

Figure 23: Variation of Secondary velocity with time t

From figure 23, observe that, increasing time t decreases secondary velocity profiles to a minimum near the plate then begins to increase uniformly to zero in the main stream. The flow gets to the free stream with time,where the secondary velocity diminishes and therefore, a decrease in velocity profiles.

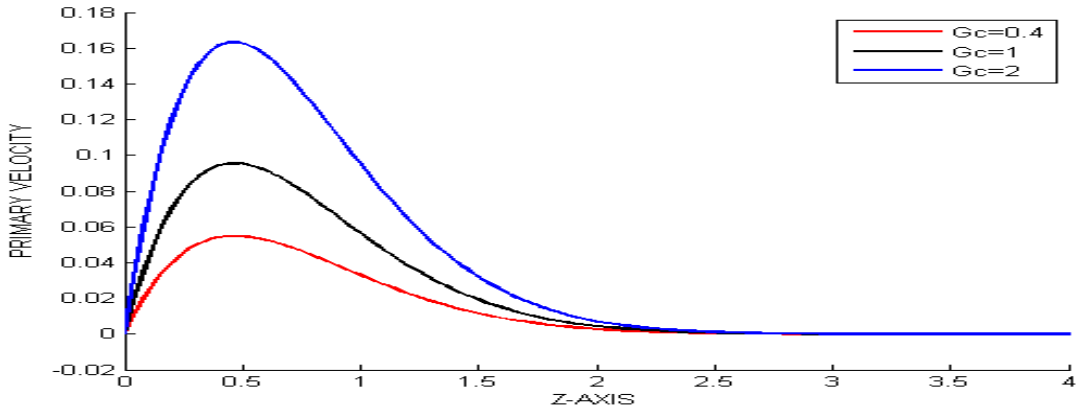

Figure 24: Variation of Primary velocity with Modified Grashof Gc

From figure 24, we observe that increasing modified Grashof number Gc gradually increases Primary velocity profiles near plate surface to a maximum after which the profiles begin to decrease gradually to a point in the free stream where the distribution remain constant and parallel to the z axis.

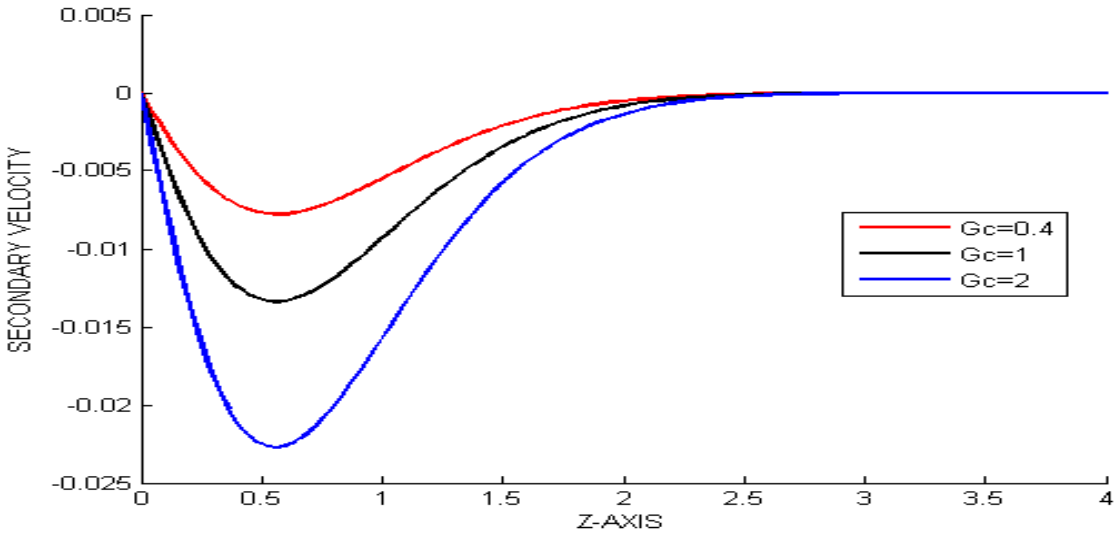

Figure 25: Variation of Secondary velocity with Modified Grashof *Gc*

From figure 25,we observe that, increases in modified Grashof parameter Gc has gradual secondary velocity profile decreasing near the vertical plate to a minimum after which the profiles begin to increase gradually to a point in the free stream where the distribution remain constant and parallel to the z axis.

Table 1:Rate of mass transfer Sh values, $M^2 = 5.0$, $Pr = 0.71$, $Gr = +0.4$

wo	**Sc**	**Time**	*phi*(ϕ)	**Sh**
0	1.1	0.25	$\pi/6$	2.1109
0.5	1.1	0.25	$\pi/6$	2.3356
1	1.1	0.25	$\pi/6$	2.5862
0.5	0.7	0.25	$\pi/6$	2.202
0.5	0.9	0.25	$\pi/6$	2.2672
0.5	1.1	0.25	$\pi/6$	2.3356
0.5	1.1	0.25	$\pi/6$	2.3958
0.5	1.1	0.35	$\pi/6$	2.3356
0.5	1.1	0.5	$\pi/6$	2.295
0.5	1.1	0.25	0	2.4002
0.5	1.1	0.25	$\pi/6$	2.4002
0.5	1.1	0.25	$\pi/4$	2.4002

From Table 1, we observe that;

i.) Increase in suction velocity *wo* increases Mass transfer *Sh* rate. The velocity of fluid increases with the removal of suction since the flow towards the plate will be decreased, increasing the rate of mass transfer *Sh*.

ii.) Increasing mass diffusion Sc increases *Sh* rate due to the increase in diffusion.

iii.) Increase in time *t* decreases the rate of mass transfer *Sh* because, with time the flow advances to the free stream where the velocity of fluid particles is high and hence reduction in the rate of mass transfer *Sh*.

iv.) The angle of inclination doesn't affect the rate of mass transfer *Sh*.

Table 2:Values of skin friction, τ_x *and* τ_y *for* $\Pr = 0.71, M^2 = 5.0, Gr = +0.4$

n	*wo*	m	Gc	Sc	Sigma	Phi	Time	τ_x	τ_y
0	0.5	1.5	0.4	1.1	2	$\pi/6$	0.35	-0.1732	0.02
0.5	0.5	1.5	0.4	1.1	2	$\pi/6$	0.35	-0.1689	0.0155
1	0.5	1.5	0.4	1.1	2	$\pi/6$	0.35	-0.1652	0.0123
0.7	0	1.5	0.4	1.1	2	$\pi/6$	0.35	-0.1674	0.0141
0.7	0.5	1.5	0.4	1.1	2	$\pi/6$	0.35	-0.1673	0.0141
0.7	1	1.5	0.4	1.1	2	$\pi/6$	0.35	-0.1653	0.0138
0.7	0.5	1	0.4	1.1	2	$\pi/6$	0.35	-0.176	0.0127
0.7	0.5	1.5	0.4	1.1	2	$\pi/6$	0.35	-0.1676	0.0141
0.7	0.5	2	0.4	1.1	2	$\pi/6$	0.35	-0.1609	0.0141
0.7	0.5	1.5	0.4	1.1	2	$\pi/6$	0.35	-0.1673	0.0141
0.7	0.5	1.5	1	1.1	2	$\pi/6$	0.35	-0.2932	0.0244
0.7	0.5	1.5	2	1.1	2	$\pi/6$	0.35	-0.503	0.0417
0.7	0.5	1.5	0.4	0.7	2	$\pi/6$	0.35	-0.1763	0.0155
0.7	0.5	1.5	0.4	0.9	2	$\pi/6$	0.35	-0.1715	0.0147
0.7	0.5	1.5	0.4	1.1	2	$\pi/6$	0.35	-0.1673	0.0141
0.7	0.5	1.5	0.4	1.1	0.5	$\pi/6$	0.35	-0.174	0.0749
0.7	0.5	1.5	0.4	1.1	2	$\pi/6$	0.35	-0.1673	0.0141
0.7	0.5	1.5	0.4	1.1	3.5	$\pi/6$	0.35	-0.1619	0.0135
0.7	0.5	1.5	0.4	1.1	2	0	0.35	-0.3737	0
0.7	0.5	1.5	0.4	1.1	2	$\pi/6$	0.35	-0.4350	0.0303
0.7	0.5	1.5	0.4	1.1	2	$\pi/4$	0.35	-0.4935	0.0609
0.7	0.5	1.5	0.4	1.1	2	$\pi/6$	0.25	-0.1457	0.0097
0.7	0.5	1.5	0.4	1.1	2	$\pi/6$	0.35	-0.1673	0.0141
0.7	0.5	1.5	0.4	1.1	2	$\pi/6$	0.5	-0.1942	0.0204

Table 2 shows that;

i.) Increasing Modified Grashof number Gc, decreases the skin friction τ_x (due to primary velocity) but increases Secondary velocity skin friction τ_y .

ii.) An increase in diffusion parameter Sc increases τ_x but reduces τ_y .

iii.) Increasing heat source parameter σ minimally increases primary velocity skin friction τ_x but slightly decreases secondary velocity skin friction τ_y. This is due to the effect of the heat source parameter on the velocity which decreases the primary but increases the secondary velocity.

iv.) The removal of suction velocity wo decreases primary velocity skin friction τ_x but minimally increases the secondary velocity skin friction τ_y.

v.) Increase in the angle of magnetic field inclination ϕ decreases the primary velocity skin friction τ_x but increases the secondary velocity skin friction τ_y.

vi.) An increase in Ion-Slip current n has little increases in the primary velocity skin friction τ_x but little decreases in the secondary velocity skin friction τ_y.

vii.) Increasing Hall current parameter m increases both skin frictions τ_x *and* τ_y because in the presence of ion-slip n,increasing Hall parameter m decreases the velocity which in turn increases the shear resistance.

viii.) Increase in time t decreases τ_x but increases τ_y. This is due to increasing primary velocity in the free stream which decreases shear stress due to primary velocity τ_x while the secondary velocity is decreased resulting to increasing shear stress τ_y.

Table 3:Values of convective heat transfer Nu rate, Pr = 0.71, M^2= 5.0, Gr = + 0.4

n	*wo*	*m*	*Gc*	*Sc*	Sigma σ	Phi ϕ	Time *t*	Nu
0	0.5	1.5	0.4	1.1	2	$\pi/6$	0.35	2.5488
0.5	0.5	1.5	0.4	1.1	2	$\pi/6$	0.35	2.5488
1	0.5	1.5	0.4	1.1	2	$\pi/6$	0.35	2.5488
0.7	0	1.5	0.4	1.1	2	$\pi/6$	0.35	2.4073
0.7	0.5	1.5	0.4	1.1	2	$\pi/6$	0.35	2.5488
0.7	1	1.5	0.4	1.1	2	$\pi/6$	0.35	2.7002
0.7	0.5	1	0.4	1.1	2	$\pi/6$	0.35	2.5488
0.7	0.5	1.5	0.4	1.1	2	$\pi/6$	0.35	2.5488
0.7	0.5	2	0.4	1.1	2	$\pi/6$	0.35	2.5488
0.7	0.5	1.5	0.4	1.1	2	$\pi/6$	0.35	2.5488
0.7	0.5	1.5	1	1.1	2	$\pi/6$	0.35	2.5488
0.7	0.5	1.5	2	1.1	2	$\pi/6$	0.35	2.5488
0.7	0.5	1.5	0.4	0.7	2	$\pi/6$	0.35	2.5487
0.7	0.5	1.5	0.4	0.9	2	$\pi/6$	0.35	2.5488
0.7	0.5	1.5	0.4	1.1	2	$\pi/6$	0.35	2.5488
0.7	0.5	1.5	0.4	1.1	0.5	$\pi/6$	0.35	2.2977
0.7	0.5	1.5	0.4	1.1	2	$\pi/6$	0.35	2.5488
0.7	0.5	1.5	0.4	1.1	3.5	$\pi/6$	0.35	2.769
0.7	0.5	1.5	0.4	1.1	2	0	0.35	2.5599
0.7	0.5	1.5	0.4	1.1	2	$\pi/6$	0.35	2.5573
0.7	0.5	1.5	0.4	1.1	2	$\pi/4$	0.35	2.5541
0.7	0.5	1.5	0.4	1.1	2	$\pi/6$	0.25	2.5636
0.7	0.5	1.5	0.4	1.1	2	$\pi/6$	0.35	2.5488
0.7	0.5	1.5	0.4	1.1	2	$\pi/6$	0.5	2.5425

From this table, it is observable that;

i.) Increasing *Sc* (mass diffusion) increases rate of heat transfer *Nu* due to decreased diffusion in the flow region.

ii.) Increasing angle of inclination ϕ decreases heat transfer *Nu* rate. This is because increasing the angle of magnetic field inclination (ϕ) produces a type of resistive force which opposes the flow.

It contributes to the thickening of the thermal boundary layer which in turn reduces the rate of heat transfer (Nu).

iii.) Modified Grashof (Gc), Hall parameter (m) and Ion-Slip parameter (n) have no effect on Nu in the flow field.

iv.) Decreasing the heat source parameter σ or increasing time t contributes to a decrease in heat transfer Nu . This is because the velocity of fluid reduces in the free stream leading to the reduced rate of heat transfer.

v.) Removal of suction velocity wo decreases the rate of heat transfer Nu due to increased diffusion in the flow region.

5.1.2 Figures and tables for heating of the plate by convection currents

$$\Pr = 0.71, M^2 = 5.0, Gr = -0.4$$

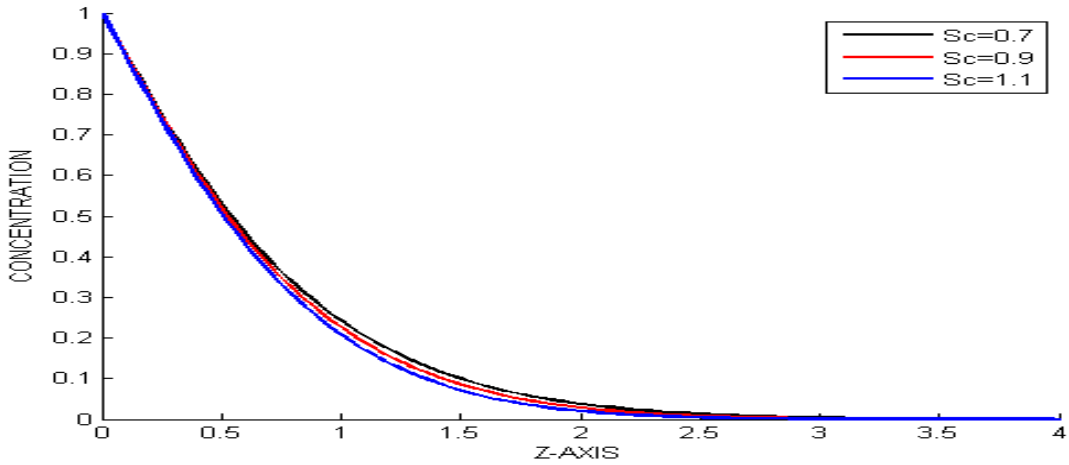

Figure 26: Variation of concentration with Schmidt number Sc

It is observable that increasing mass diffusion Sc decreases concentration profiles from $Sc = 1.1$ *to* $Sc = 0.7$ .This is because under a strong magnetic field, increasing values of Sc decreases

molecules diffusivity resulting to a decrease of concentration boundary layer, lowering concentration of species for large values of Sc .

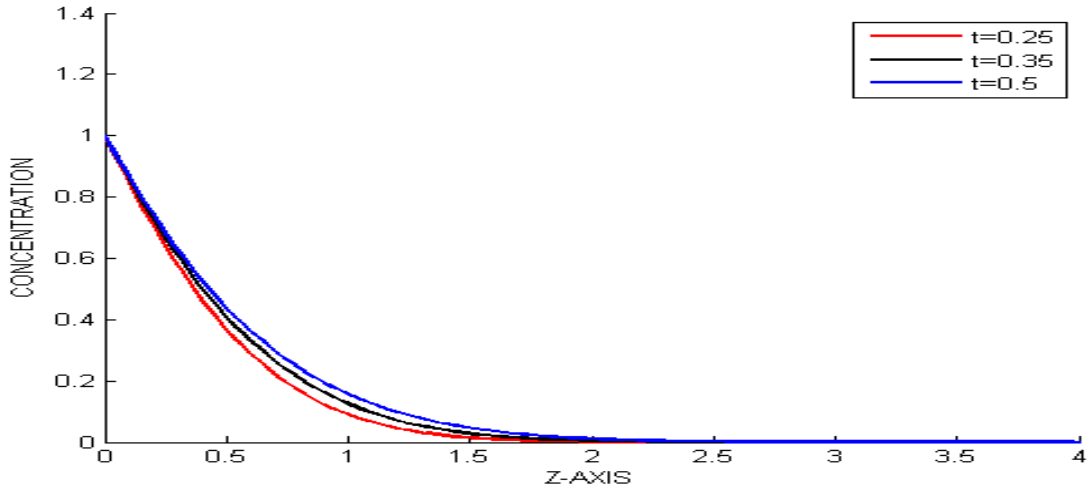

Figure 27: Variation of concentration with time t

From figure 27, we note that an increase in time increases the concentration profiles, due increases in concentration as the flow gets to the free stream with time.

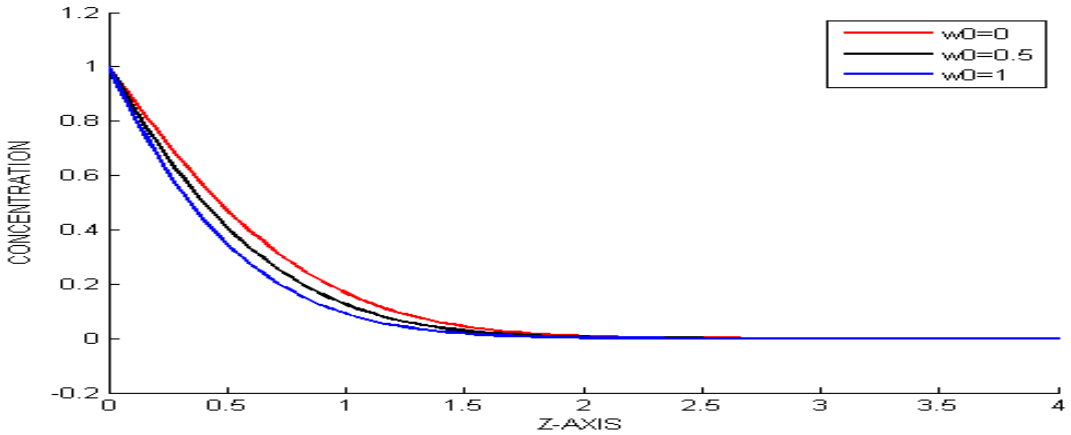

Figure 28: Variation of concentration with suction velocity wo

From figure 28, we observe that increasing suction decreases concentration profiles, due to the fact that growth of the boundary layers is reduced, decreasing the concentration profiles to zero in the

mainstream.

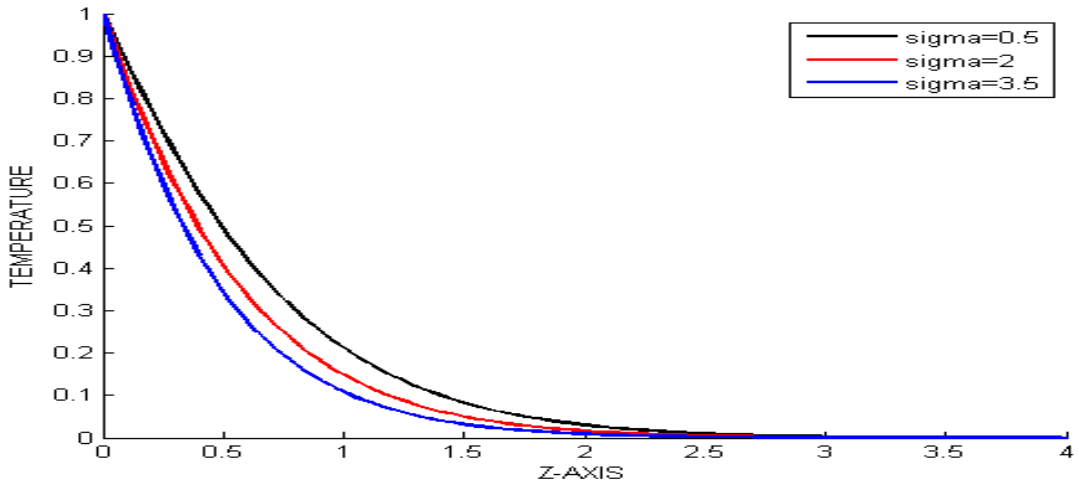

Figure 29: Variation of Temperature with heat source parameter σ

From figure 29, we observe that increase in heat source parameter σ ($sigma$) decreases temperature profiles from $\sigma = 0.5$ *to* $\sigma = 3.5$, because the internal heat generation is increase, but due to plate heating ($Gr = -0.4$), the rate of kinetic energy decreases, enhancing decrease in temperature profiles.

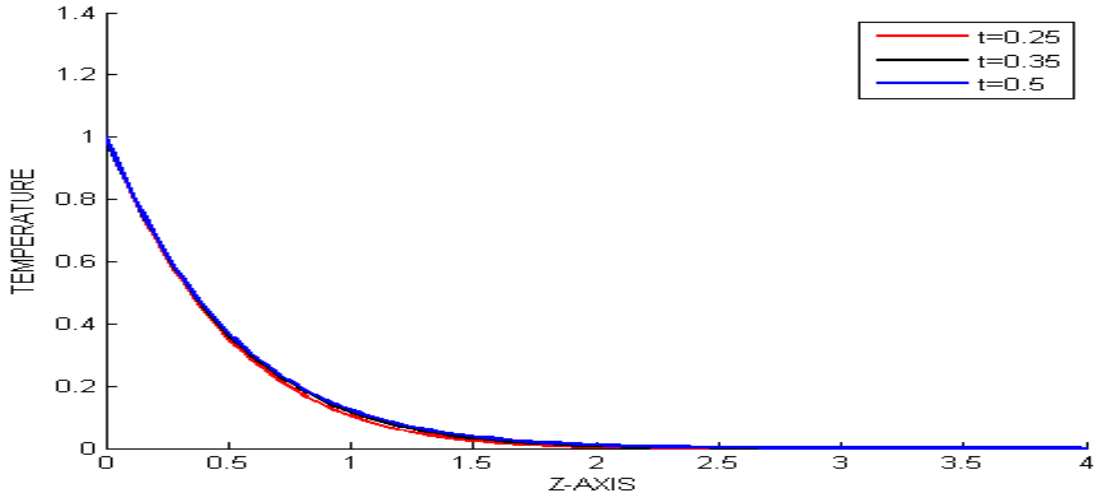

Figure 30: Variation of Temperature with time t

From figure 30, we observe that increases in time has insignificant increases in temperature profiles.

As flow gets to the mainstream, velocity increases accelerating the rate of energy transfer and since the plate is also heating the temperature will minimally increase (almost constant).

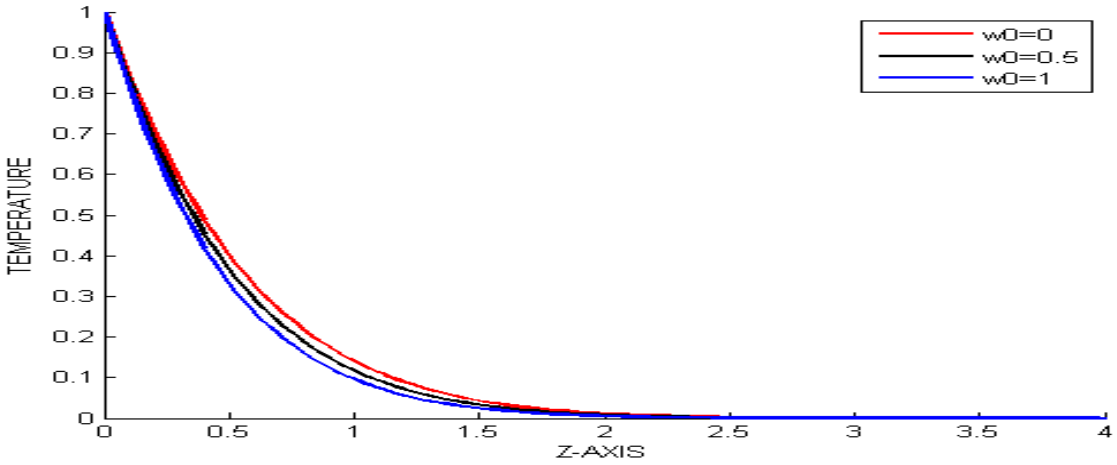

Figure 31: Variation of Temperature with Suction velocity wo

From figure 31, we note that an increase in suction velocity or angle of inclination causes a decrease in temperature.

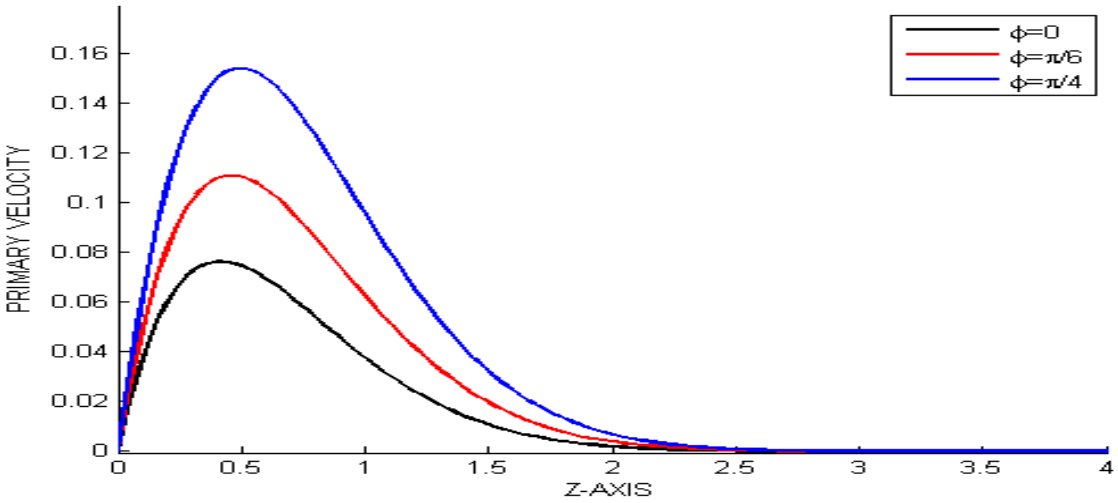

Figure 32: Variation of Primary velocity with angle of inclination ϕ

From figure 32, note that an increase in the angle of inclination ϕ corresponds to increasing primary

velocity profiles near the plate surface from $\phi = 0\pi$ *to* $\phi = \frac{\pi}{4}$, because, increasing the angle of inclination decreases the magnetic strength which accelerates the fluid motion by increasing the velocity profiles.

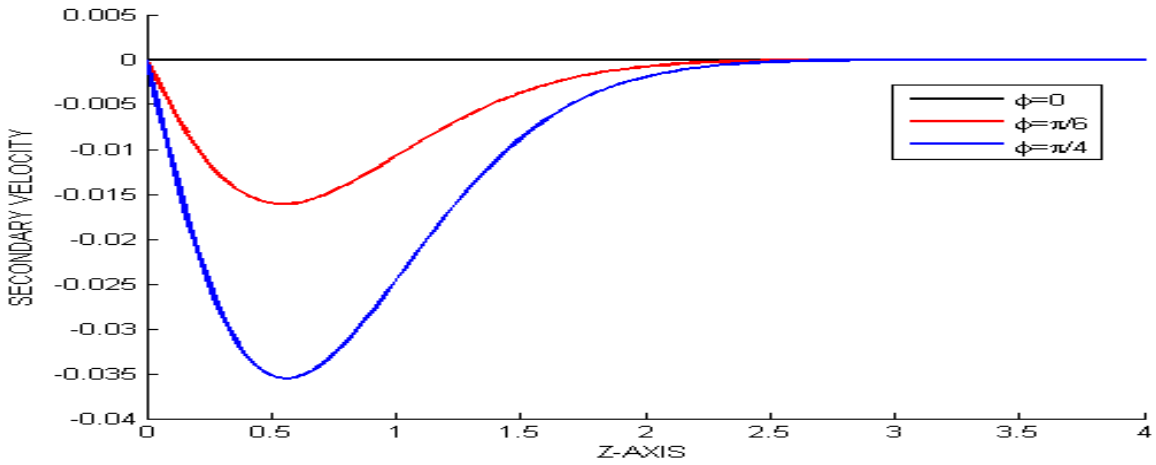

Figure 33: Variation of Secondary velocity with angle of inclination ϕ

From figure 33, note that increase in angle of inclination ϕ decreases Secondary velocity profiles from $\phi = \frac{\pi}{4}$ to $\phi = 0\pi$, increasing angle of Magnetic field inclination increases Magnetic strength which tends to retard fluid motion affecting the velocity by reduction.

From figures 34 and 35 below, we note that an increase in Hall parameter m leads to a decrease in both primary and secondary velocity profiles from $m = 2$ *to* $m = 1$near the plate. This is due to the fact that under the influence of a strong magnetic field, the effective conductivity increases with the increase in Hall parameter which increases the magnetic damping force and hence the decrease in velocity profiles.

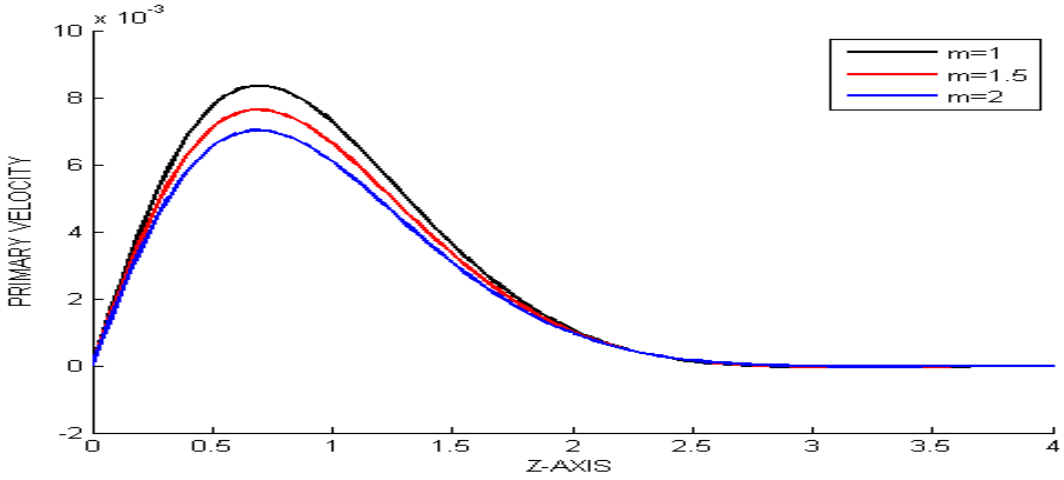

Figure 34: Variation of Primary velocity with Hall parameter m

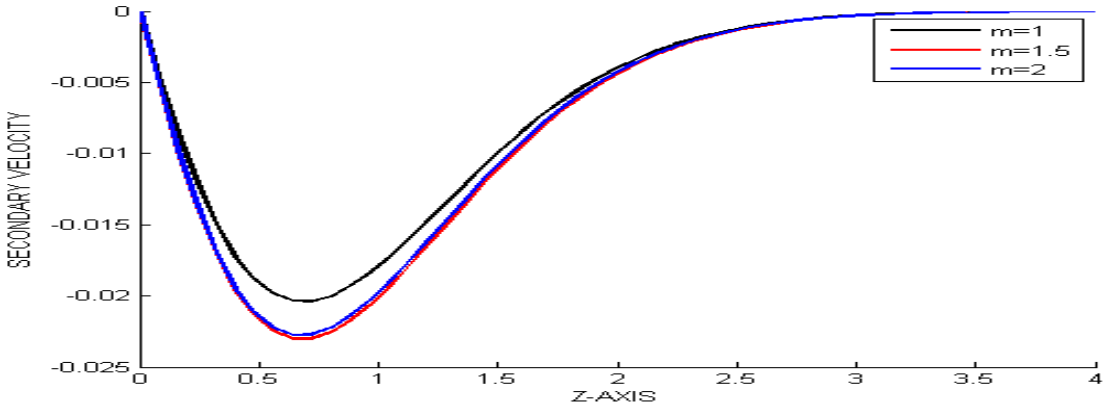

Figure 35: Variation of secondary velocity with Hall parameter m

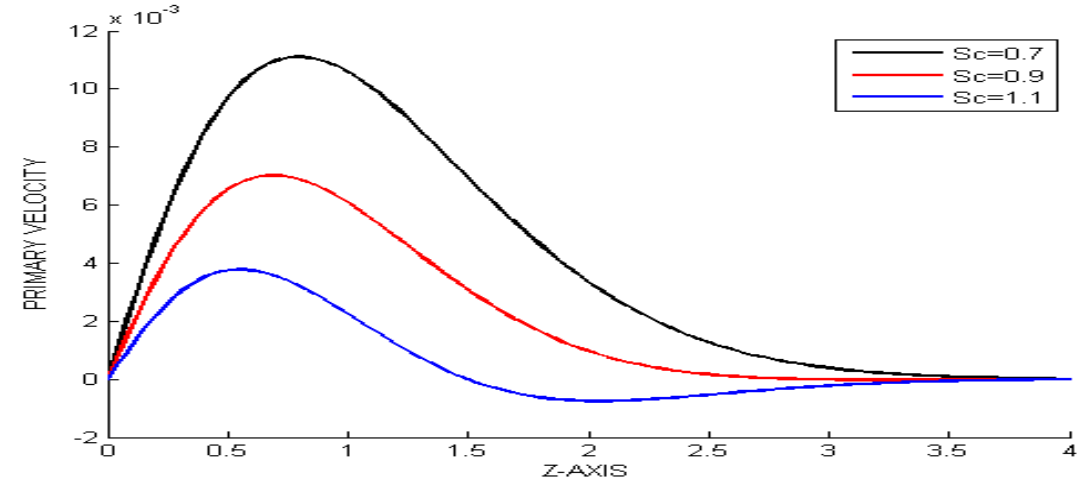

Figure 36: Variation of Primary velocity with Schmidt number Sc

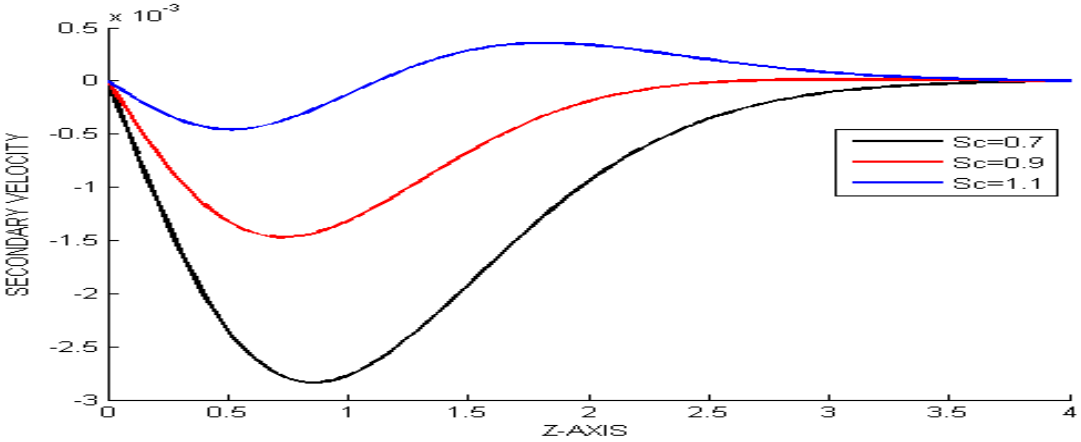

Figure 37: Variation of Secondary velocity with Schmidt number Sc

From figures 36 and 37, we observe that increasing diffusion of molecules Sc decreases Primary velocity profiles from $Sc = 1.1$ *to* $Sc = 0.7$, increase in Sc decreases molecular (mass) diffusivity in fluids flow under a strong magnetic field resulting to decreases in Primary velocity profiles, but increases in Secondary velocity profiles from $Sc = 0.7$ *to* $Sc = 1.1$

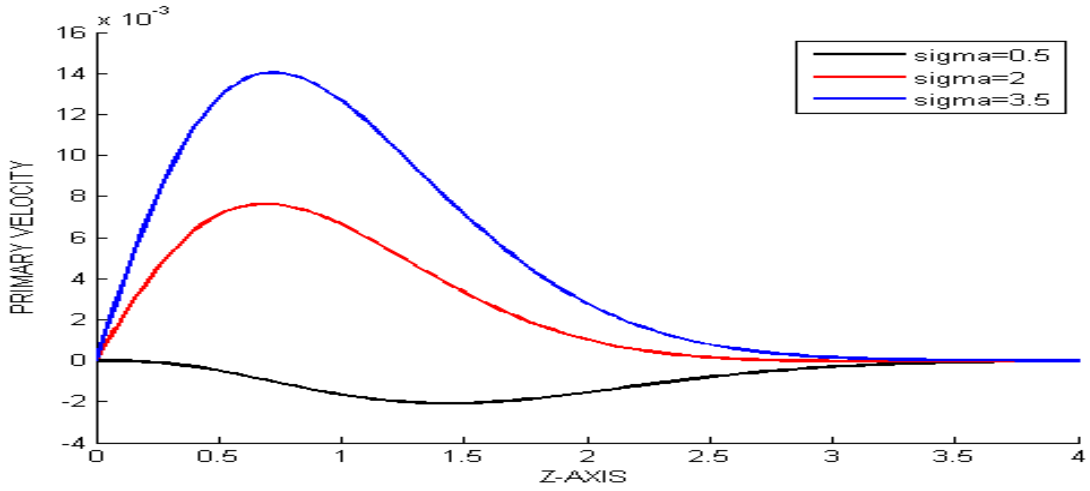

Figure 38: Variation of Primary velocity with heat source parameter σ

From figure 38, we observe that an increase in the heat source parameter $\sigma\,(sigma)$ leads to an increase in primary velocity profiles from $\sigma = 0.5$ *to* $\sigma = 3.5$. This is due to an increase in the internal heat generation and because the plate is heating, the rate of energy transfer at the plate is decreased enhancing an increase in the Primary velocity profile of the fluid.

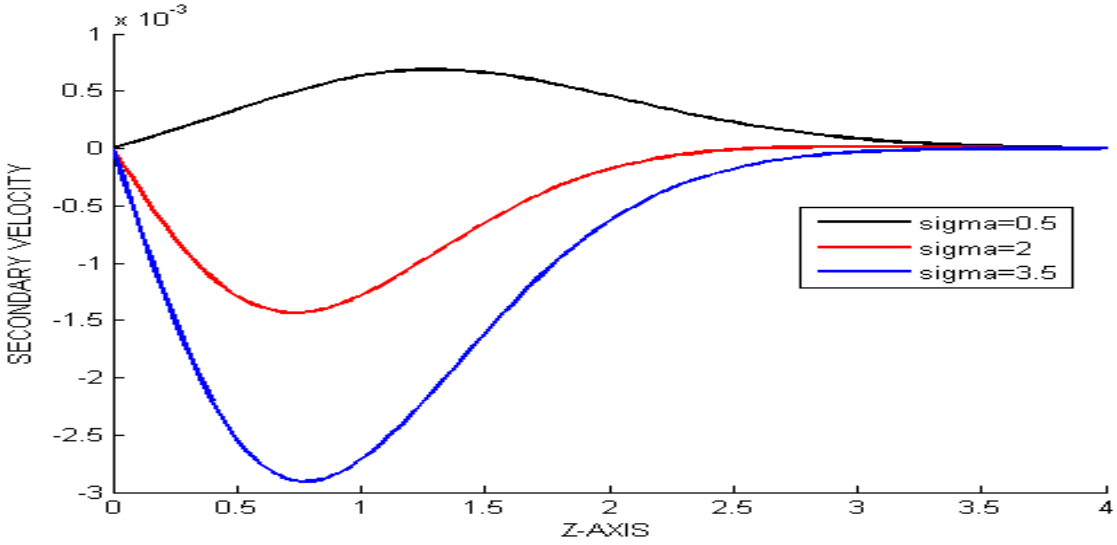

Figure 39: Variation of secondary velocity with heat source parameter σ

From figure 39, we observe that an increase in heat source parameter from $\sigma = 0.5$ *to* $\sigma = 3.5$ decreases Secondary velocity profiles. This is because the convective molecular heat generation is decreased and since the plate is heating, rate of energy transfers increases which then decreases Secondary velocity profiles.

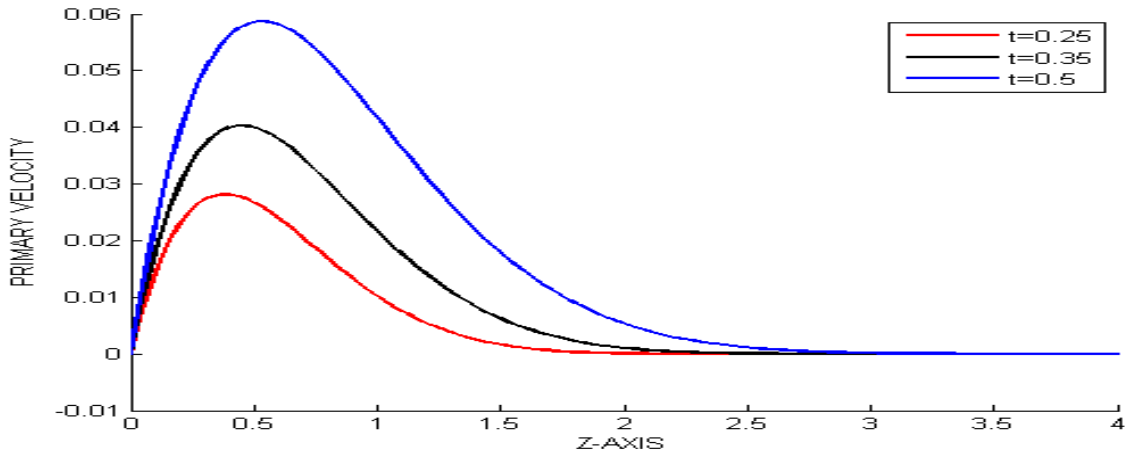

Figure 40: Variation of Primary velocity with time t

This graph (figure 40) displays that increasing time increases Primary velocity profiles gradually near the plate, reaches a maximum then begins to decrease gradually to the free stream. The flow gets to the mainstream with time, where velocity increases to a maximum then steadily decreases for some time before remaining uniformly distributed at zero to infinity.

From figure 41 below, we observe that, increase in time decelerates Secondary velocity profiles gradually near the plate, reaches a minimum before accelerating gradually away from the plate. After some time, the fluid particles spread to the mainstream where velocity decreases to a minimum before increasing gradually to a constant distribution infinitely.

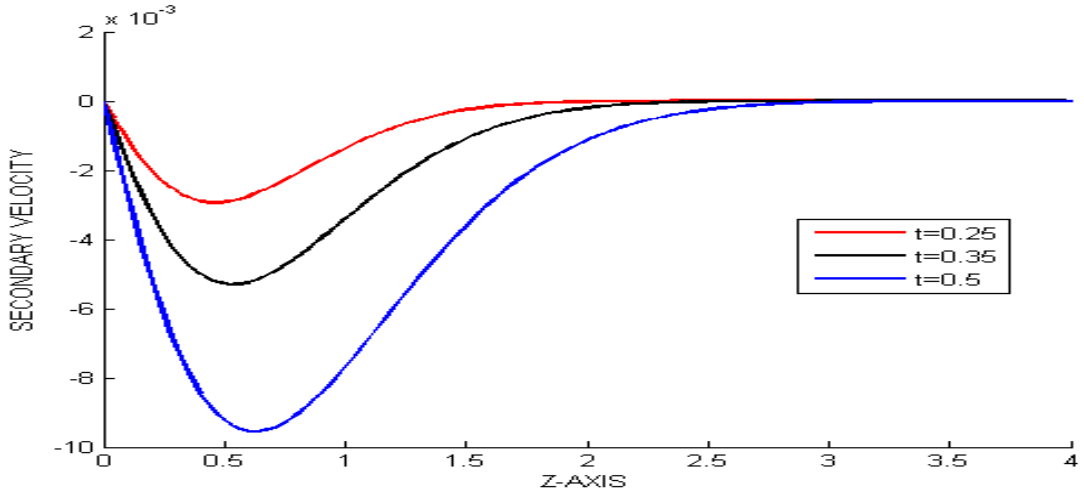

Figure 41:Variation of Secondary velocity with time t

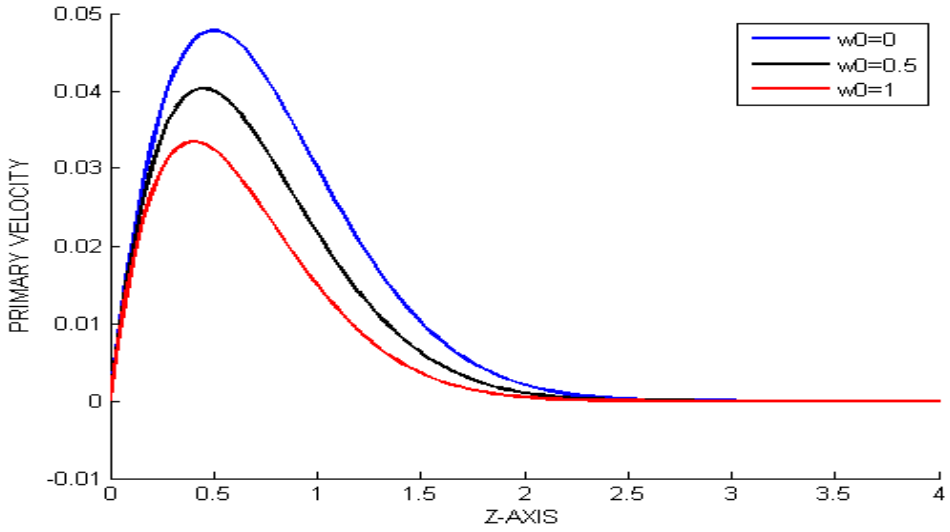

Figure 42: Variation of Primary velocity with Suction velocity wo

From figure 42, we observe that removal of suction *wo* increases Primary velocity profiles gradually close to the plate surface to a maximum, after which maintains constant spread to infinity far off in the free stream.

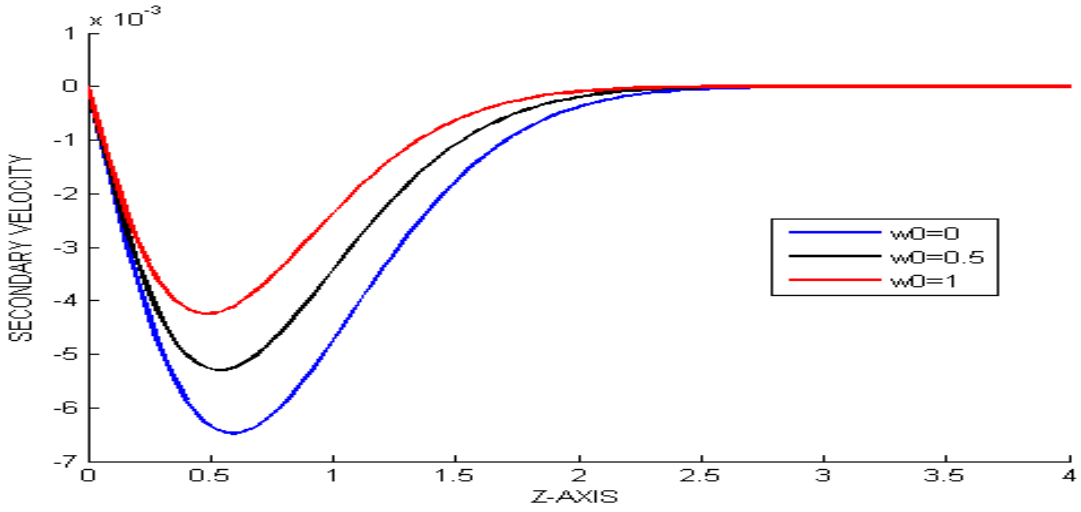

Figure 43: Variation of Secondary velocity with Suction velocity wo

From figure 43, we observe that removing suction velocity *wo* reduces Secondary velocity profiles from $wo = 1.0$ *to* $wo = 0$ gradually near the plate to a minimum then the profiles begin to decrease steadily to the main stream after which they remain constantly distributed to infinity.

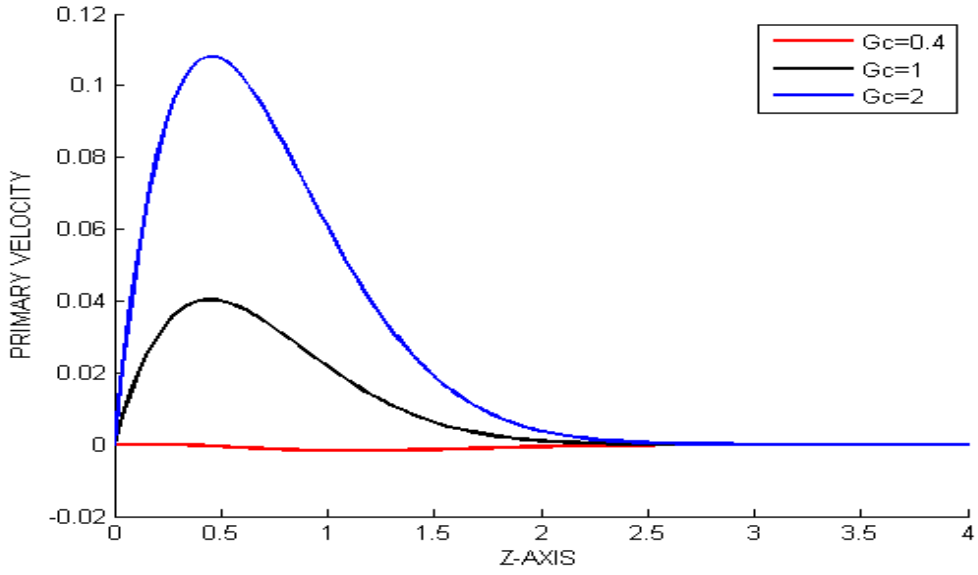

Figure 44: Variation of Primary velocity with Modified Grashof Gc

From figure 44, we observe that an increase in modified Grashof number *Gc* causes an increase

in primary velocity profiles but as the distance from the plate increases, primary velocity profiles exhibit a decrease and remain parallel to the z-axis far away from the plate.

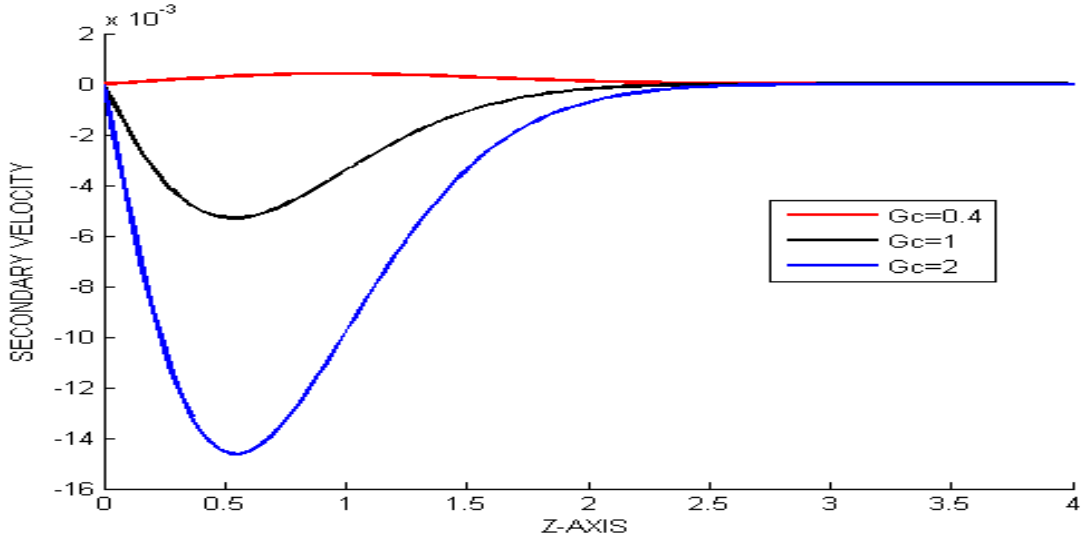

Figure 45: Variation of Secondary velocity with Modified Grashof Gc

From figure 45, we observe that an increase in modified Grashof number Gc causes a decrease in secondary velocity profiles but as the distance from the plate increase secondary velocity profiles exhibit an increase gradually and remain parallel to the z-axis far away from the plate.

From table 4 below, we observe that;

i.) Increasing magnetic field angle of inclination $\phi(phi)$ reduces τ_x, however, it increases τ_y

ii.) Increasing mass diffusion Sc slightly increases skin friction τ_x but decreases the skin friction τ_y . This is caused by the mass diffusion effect on the velocity by decreasing primary velocity resulting to increasing shear stress due to primary velocity τ_x but increases the secondary velocity leading to a decrease in shear stress due to the secondary velocity τ_y.

Table 4:Values of skin friction τ_x *and* τ_y *for* $\Pr = 0.71, M^2 = 5.0, Gr = -0.4$

n	wo	m	Gc	Sc	Sigma σ	Phi ϕ	Time t	τ_x	τ_y
0	0.5	1.5	0.4	1.1	2	$\pi/6$	0.4	-0.00021885	0.00047523
0.5	0.5	1.5	0.4	1.1	2	$\pi/6$	0.4	-0.00042832	-0.00035099
1	0.5	1.5	0.4	1.1	2	$\pi/6$	0.4	-0.0005871	-0.00026745
0.7	0	1.5	0.4	1.1	2	$\pi/6$	0.4	-0.0027	-0.00004362
0.7	0.5	1.5	0.4	1.1	2	$\pi/6$	0.4	-0.0004971	-0.0003137
0.7	1	1.5	0.4	1.1	2	$\pi/6$	0.4	0.0019	-0.00059513
0.7	0.5	1	0.4	1.1	2	$\pi/6$	0.4	-0.00017589	-0.00029941
0.7	0.5	1.5	0.4	1.1	2	$\pi/6$	0.4	-0.0004971	-0.0003137
0.7	0.5	2	0.4	1.1	2	$\pi/6$	0.4	-0.00071975	-0.0003009
0.7	0.5	1.5	0.4	1.1	2	$\pi/6$	0.4	-0.0004971	-0.0003137
0.7	0.5	1.5	1	1.1	2	$\pi/6$	0.4	-0.1264	0.01
0.7	0.5	1.5	2	1.1	2	$\pi/6$	0.4	-0.336	0.0272
0.7	0.5	1.5	0.4	0.7	2	$\pi/6$	0.4	-0.0095	0.0011
0.7	0.5	1.5	0.4	0.9	2	$\pi/6$	0.4	-0.0047	0.00033749
0.7	0.5	1.5	0.4	1.1	2	$\pi/6$	0.4	-0.0004971	-0.0003137
0.7	0.5	1.5	0.4	1.1	0.5	$\pi/6$	0.4	0.0062	-0.0011
0.7	0.5	1.5	0.4	1.1	2	$\pi/6$	0.4	-0.0004971	-0.0003137
0.7	0.5	1.5	0.4	1.1	3.5	$\pi/6$	0.4	-0.0059	0.00033006
0.7	0.5	1.5	0.4	1.1	2	0	0.4	-0.2482	0
0.7	0.5	1.5	0.4	1.1	2	$\pi/6$	0.4	-0.2873	0.00194
0.7	0.5	1.5	0.4	1.1	2	$\pi/4$	0.4	-0.3241	0.0389
0.7	0.5	1.5	0.4	1.1	2	$\pi/6$	0.3	0.014	-0.00041904
0.7	0.5	1.5	0.4	1.1	2	$\pi/6$	0.4	-0.0004971	-0.0003137
0.7	0.5	1.5	0.4	1.1	2	$\pi/6$	0.5	-0.0036	0.000081399

iii.) Increasing heat source parameter σ reduces the skin friction τ_x but slightly contributes to increases in skin friction τ_y. This is due to the effect of the heat source parameter σ on velocity by increasing the primary velocity but decreases the secondary velocity.

iv.) Increases in Hall current parameter m decreases skin friction τ_x while increases the skin friction τ_y. This is due to the reason that increasing Hall current parameter m decreases primary velocity causing an increase in the shear resistance, the opposite applies for the secondary velocity.

v.) The suction velocity removal wo decreases the skin friction τ_x but increases the skin friction τ_y. This is because removal of suction velocity wo increases fluid's primary velocity making τ_x to decrease while increasing the fluid's secondary velocity causing an increase in shear stress τ_y.

vi.) Increases in Time t leads to a decrease in the skin friction τ_x but minimally increases the skin friction τ_y. This is due to the heating of the plate which decreases primary velocity but increases secondary velocity enhancing a decrease in the shear stress due to primary velocity τ_x but increases shear stress due to the secondary velocity τ_y.

vii.) Increasing Gc (modified Grashof) decreases τ_x but increases τ_y. Heating the plate increases primary velocity but decreases the secondary velocity leading to the reduction of shear stress due to the primary velocity τ_x while increasing the shear stress due to the secondary velocity τ_y.

Table 5:Rate of convective heat transfer Nu *values, for* $, M^2 = 5.0,\ \Pr = 0.71,\ Gr = -0.4$

n	wo	m	Gc	Sc	Sigma (σ)	Phi (ϕ)	Time t	Nu
0	0.5	1.5	0.4	1.1	2	$\pi/6$	0.4	2.5488
0.5	0.5	1.5	0.4	1.1	2	$\pi/6$	0.4	2.5488
1	0.5	1.5	0.4	1.1	2	$\pi/6$	0.4	2.5488
0.7	0	1.5	0.4	1.1	2	$\pi/6$	0.4	2.4073
0.7	0.5	1.5	0.4	1.1	2	$\pi/6$	0.4	2.5488
0.7	1	1.5	0.4	1.1	2	$\pi/6$	0.4	2.7002
0.7	0.5	1	0.4	1.1	2	$\pi/6$	0.4	2.5488
0.7	0.5	1.5	0.4	1.1	2	$\pi/6$	0.4	2.5488
0.7	0.5	2	0.4	1.1	2	$\pi/6$	0.4	2.5488
0.7	0.5	1.5	0.4	1.1	2	$\pi/6$	0.4	2.5488
0.7	0.5	1.5	1	1.1	2	$\pi/6$	0.4	2.548
0.7	0.5	1.5	2	1.1	2	$\pi/6$	0.4	2.5433
0.7	0.5	1.5	0.4	0.7	2	$\pi/6$	0.4	2.5487
0.7	0.5	1.5	0.4	0.9	2	$\pi/6$	0.4	2.5488
0.7	0.5	1.5	0.4	1.1	2	$\pi/6$	0.4	2.5488
0.7	0.5	1.5	0.4	1.1	0.5	$\pi/6$	0.4	2.2977
0.7	0.5	1.5	0.4	1.1	2	$\pi/6$	0.4	2.5488
0.7	0.5	1.5	0.4	1.1	3.5	$\pi/6$	0.4	2.769
0.7	0.5	1.5	0.4	1.1	2	0	0.4	2.5627
0.7	0.5	1.5	0.4	1.1	2	$\pi/6$	0.4	2.5617
0.7	0.5	1.5	0.4	1.1	2	$\pi/4$	0.4	2.5604
0.7	0.5	1.5	0.4	1.1	2	$\pi/6$	0.3	2.5636
0.7	0.5	1.5	0.4	1.1	2	$\pi/6$	0.4	2.5488
0.7	0.5	1.5	0.4	1.1	2	$\pi/6$	0.5	2.5425

From table 5, we observe that;

i.) Increases in the modified Grashof number Gc corresponds to a decreasing rate of heat transfer Nu , this is because Gc has a decelerating effect on the flow velocity due to enhancement in Buoyancy force. This effect decreases the temperature and concentration gradients on the surface leading to a decrease in heat transfer Nu .

ii.) Increasing the angle of inclination ϕ (phi)slightly decreases Nu , this is because the angle of magnetic field inclination produces a resistive force which varies in opposing the flow with its size. This contributes to the thickening of the thermal and mass boundary layer when the angle is increased which reduces the rate of heat transfer in turn.

iii.) An increase in the mass diffusion parameter Sc increases rate of heat transfer Nu . This is because the fluid particles' molecular diffusion is decreased leading to an increase in the rate of heat transfer.

iv.) An increase in the heat source parameter σ (sigma)causes an increase in the Nusselt number Nu due to the increase in the fluid velocity and hence increasing the rate of heat transfer.

v.) Increasing Time reduces Nusselt number Nu ,this is because at the main stream, fluid velocity is decreased with time, causing the rate of heat transfer to decrease.

vi.) Changes in the Hall current m and Ion-Slip parameter n have no effect on the Nusselt number Nu .

CHAPTER SIX

CONCLUSIONS AND RECOMMENDATIONS

The conclusions and recommendations in this chapter are based on the results in chapter five. Research papers published in some journals from this work have also been cited.

6.1 Conclusions

The aim of this study is to analyze effects of Hall current m, ion-slip currents n, time t, modified Grashof Gc, mass diffusion Sc, heat source σ and magnetic field angle of inclination ϕ parameters to the concentration, temperature and velocity profiles on unsteady, free convection incompressible conducting fluid flowing over a strong magnetic field inclined at angle ϕ to a semi-infinite vertical porous plate with Hall and ion-slip currents restricted to a turbulent boundary layer. It's noted that free convection fluid flows consist of the boundary layer region on which concentration, temperature and velocities gradients prevail, and the free stream region where concentration, temperature and velocities are constants. The non-linear equations describing the flow's solution require an efficient numerical finite difference method to be developed as in chapter four. The method used in solving these equations are stable and convergent since a chosen time increment had no significant difference when compared with a similar time increment. Suitable Initial and boundary conditions were set for the problem. Newton interpolation was developed for computing values of skin friction, rate of heat and mass transfers at the plate.

This research maintained Prandtl Number ($\Pr$) and Magnetic Parameter (M^2) constant at the values of 0.71 and 5.0 signifying correspondence to the air and strong Magnetic field respectively. The two cases we considered in analyzing the results are;

a.) Grashof Number, $Gr > 0\ (+0.4)$ corresponding to convective cooling of the plate.

This case implies that the temperature of the plate is higher than that of the adjacent fluid particles in the free stream region leading to the transfer of heat from the plate to the fluid. From the results in chapter five, we make the following conclusions;

i.) Increase in mass diffusion parameter decreases the concentration profiles.

ii.) Removal of suction velocity and increase in time, increases the concentration profiles.

iii.) Increases in Hall parameter, mass diffusion and angle of inclination have no effect on temperature profiles.

iv.) Increases in heat source parameter decreases temperature profiles

v.) Increases in time and removal of suction velocity increases temperature profiles.

vi.) Increases in time, mass diffusion parameter, angle of inclination and Modified Grashof number increases primary velocity profiles.

vii.) Increasing Hall parameter, mass diffusion parameter and ion-slip current parameter decrease primary velocity profiles.

viii.) Increases in angle of inclination, heat source parameter, time, modified Grashof parameter and removal of suction velocity contribute to increases in the Primary velocity profiles.

ix.) Increases in ion-slip parameter and mass diffusion parameters enhances increase in the Secondary velocity profiles.

x.) Increases on Hall parameter, angle of inclination, time, heat source, modified Grashof number parameters and removal of suction velocity, decrease the Secondary velocity profiles.

b.) Grashof Number, $Gr < 0 (-0.4)$ corresponding to convective heating of plate.

This implies that the fluid temperature in the free stream is higher than plate's. The transfer of heat energy emanates from the fluid through the adjacent particles to the plate, a situation called convective plate heating. From the results in chapter five, we make the following conclusions;

i.) Increases in time and removal of suction velocity increase concentration and temperature profiles.

ii.) Increase in mass diffusion parameter decreases concentration profiles. Other parameters have no effect in the concentration profiles.

iii.) Increases in heat source parameter decrease temperature profiles.

iv.) Increase in time, modified Grashof number, angle of inclination, heat source parameters and removal of suction velocity, increase primary velocity profiles but lead to a decrease in secondary profiles.

v.) Increasing Hall parameter and mass diffusion parameters cause a decrease in primary velocity profile but an increase in secondary velocity profiles.

vi.) ion-slip current parameter has no effect in both primary and secondary profiles.

In both cases of convection heating and cooling of the plate the constant regions in most of the figures is attributed to the fact that away from the plate (in the main stream) there is no concentration, temperature and velocity gradients.

We further conclude that introduction of Hall and ion-slip currents to the strong magnetic field formed a thin boundary layer close to the stationary plate. The thickness of these boundary layers increases with an increase in either Hall parameter m or ion-slip parameter n. Moreover, it is noted that the shear stresses increase due to the primary and secondary

flows at the stationary plate with increase in Hall current parameter for a fixed value of M^2. Shear stress due to primary velocity (τ_x) decreases while Secondary velocity shear stresses τ_y increase with increases in Ion-Slip current number n.

Increases in modified Grashof number increases velocity profiles on the plate surface, while the free stream velocity profiles decrease in presence of mass transfer and plate's cooling or heating convective currents. It was observed that an increase in the angle of inclination ϕ ,modified Grashof, Hall parameter and time contribute to a decrease in skin friction (τ_x) due to primary velocity profiles but increases the skin friction (τ_y) due to secondary velocity profiles for both $Gr > 0$ and $Gr < 0$. Increases in Ion-Slip currents n , mass diffusion and heat source parameters increase τ_x but lead to decrease in τ_y for both $Gr > 0$ and $Gr < 0$. Removal of suction velocity decreases skin friction (τ_x) due to primary velocity profiles but increases skin friction (τ_y) due to secondary velocity profiles, for $Gr > 0$ while it increases τ_x and decreases τ_y for $Gr < 0$. Moreover, increase in the angle of inclination, time and suction velocity removal contributed to decrease in convective heat transfer rate, while increase in mass diffusion parameter and Heat source parameter increases the rate of convective heat transfer. The rate of convective mass transfer increased by increasing mass diffusion parameter and removal of suction velocity in both cases for $Gr > 0$ and $Gr < 0$. Generally, values of heat transfer Nu and mass transfer rates for both $Gr > 0$ and $Gr < 0$ proved approximately equal, indicating, plate's cooling or heating by convective currents don't affect rate of heat and mass transfers on the plate surface. We noted that if heat is supplied to the plate at a constant rate, then the flow field is affected. Due to the strong

magnetic field, the presence of the Hall current affected the flow significantly.

In the presence of hall current, cooling of the plate by free convection current increases the thermal boundary layer.

The future trend for the application of MHD is towards a strong magnetic field so that the influence of electromagnetic forces may be noticeable. Equally a good trend is towards a low density of the gas such as in space flights and in nuclear fusion reactions. Whatever the case may be, nothing explains the use of MHD better than power generation. MHD power generation is a new process that is receiving global attention because of much greater efficiency. Everybody is aware of the well-known fact that to convert heat energy into electrical energy several intermediate transformations are required. Each of these steps means a loss of energy. This certainly limits the overall efficiency, reliability and the compactness of the conversion process. Consequently, methods for direct conversion of energy by MHD generators are more efficient. If the degree of ionization of the gas is large and the density is low, gas dynamic forces will affect the current density, the temperature of electrons may not be the same as the temperature of ions and neutral particles. Thus without going further into detailed calculations it is recommended to modify (improve) equations of MHD using multifluid theory to show some interesting new results which can't be obtained by the classical theory. If the density of the gas is too low, it is better to use Kinetic theory, as the continuum approach will not be a good approximation to the actual conditions. Thus one should expect new results occurring in the rare field ionized gases. Again if the temperature is very large and the density is very small, the thermal radiation will be of the same order of magnitude as the heat convection. Under these circumstances it is recommended to consider thermal radiation effects simultaneously with those of heat convection and heat conduction. There are still a

number of problems in the field of MHD where the effects of Hall currents or ion slip or both, transverse or oblique, have not been studied. The fluid can further be seeded suitably to enhance the effects of Hall and ion slip. In the field of heat and mass transfer phenomena, flow through a porous medium, heat transfer through visco-elastic fluids and channel flow with continuous electrodes are areas still to be considered for future work. Another important area in the field of MHD to be determined is the transport properties of slightly ionized gases (particularly the air). Anyway these guidelines are not exhaustive but simply directions for future research work. All that we need to say is thorough investigation of MHD flow under the influence of Hall or ion slip effect systematically.

In the power industry, some methods of electric power generation include one where electrical energy get extracted directly from the moving conducting fluid. This category of flow encounters numerous applications in designing of MHD Generators, pumps and flow meters. Such flow devices are encountered accompanied by internally dissipated heat through viscous heating, joule heating or generated by electric currents in the walls. Our take to the designers of such devices is that they should take into consideration the effects of the parameters discussed in this research work.

It is hoped that the results will be useful for applications including nuclear engineering especially in designing more efficient cooling system of nuclear reactors and that they can also be used for comparison with other problems dealing with Hall current and ion-slip parameter which might be more complicated. It is also hoped that the results can serve as a compliment to other studies.

6.2 Recommendations

In this work we considered unsteady MHD free convection incompressible fluid flow in a turbulent boundary layer, past a semi-infinite vertical porous plate in a strong magnetic field at an angle ϕ to the plate with Hall and Ion –Slip currents effects. Fluid flow is restricted to turbulent boundary layer. We recommend extension of this research work by considering:

i. Compressible fluid
ii. Variable suction/injection
iii. Variable viscosity and thermal conductivity effects
iv. Viscous and Ohmic dissipations
v. Fluid flow between two moving plates (coutte flow)
vi. Effect of viscous dissipative heat (Eckert Number) to this MHD flow problem
vii. Effect of a rotating system to the flow problem.

REFERENCES

Abhay, K. J., Ajay, J. and Gupta V.G. (2016). Convective effects on MHD flow and heat transfer between vertical plates moving in opposite direction and partially filled with a porous medium." *Journal of Applied Mathematics and Physics*" **4**; 341-358.

Alim, M.S., Chaudhury, M.Z.U. and Alim, M.A. (2016). MHD Boundary Layer Flow of Heat and Mass Transfer over a Stretching Sheet in a Rotating System with Hall Current. "*Journal of Scientific Research*" **8**; 119-128.

Anderson, D. A., Tunnehill, J. C. and Pletcher, R. H. (1984). Computational Fluid Mechanic and Heat Transfer, Hemisphere, John Wiley and Sons Inc.

Benard, K. and Moreau, R. (2008). Magnetohydrodynamic Turbulence at low magnetic Reynolds." *Annual Review of fluid mechanics*" **40**; 25-45.

Boffetta, G., DeLillo, M. A. and Vozella, L. (2012). The ultimate state of thermal convection in Rayleigh- Taylor turbulence. "*Physical D: Nonlinear phenomenon*," **241;** 137-140.

BoLu, L. and Ziaonzhang, (2013). Three Dimensional MHD simulation of the electromagnetic flow meter for laminar and turbulent flows. "*International Journal of Fluid flow*," **33**; 239-243.

Boussinesq's, J., William, L. (1877). The 1877 Bousinesq's Conjecture: Turbulent Fluctuations Theory, Vol. 1. McGraw-Hill, New York.

Boussineq's, J. (1903). Theory Analytique de la Chaleur, Gauthier-Villars, Vol.2. Kluwer academic publishers, Netherlands.

Chamkha, J.A. (2004). "Unsteady MHD convective heat and mass transfer past a semi-infinite vertical permeable moving plate with heat absorption." *International Journal of Engineering and Science,"* **42**; 217-230.

Cebeci, T. and Smith, A.M.O. (1974). Analysis of Boundary Layers, Applied Mathematics and Mechanics, Vol.15, Academic Press, New York.

Chaundhary, R. and Shin, A. (2011). Direct Numerical simulation of transverse and span wise magnetic field effects on turbulent flow a 2:1 aspect ratio. "*International Journal MHD Turbulent fluid flow,"* **27**, 1123-1142.

Chien, K.Y. (1982). Prediction in Channel and Boundary-Layer Flows with a Low-Reynold's number Turbulence Model, AIAAJ. **20**; 33-38.

Cowling, T.G. (1957), "*Magnetohydrodynamics,"* Interscience, New York, pp. 101.

Crank, J. and Nicolson, P.A., (1947). Practical Method for Numerical Evaluation of Solutions of Partial Differential Equations of the Heat Conduction Type, proc. Cambridge Phil. Soc., **43**; 50.

Currie, I.G., (1974). Fundamental of Fluids, McGraw-Hill Inc.

Dol, H.S., and Hanjalic K. (2001). Computational study of turbulent natural convection in aside heated near – cubic enclosure at a high Rayleigh number. "*International Journal of Heat and Mass Transfer,"* **44**; 2323 - 2344.

Emmah, M., Kinyanjui,M. and Kwanza, J.(2012). Hydromagnetic Turbulent flow past a semi-infinite vertical plate subjected to heat flux with radiation absorption. "*International Knowledge Sharing platform journal,"* **2**; 15 - 25.

Frisch, U. (1995). Turbulence, "*Plasma and Fluid Turbulence*," Cambridge University Press.

Faraday, M. (1839). Experimental researches in electricity, Richard and John Edward Taylor.

Hatton, Y., Toshihiro, T., Ysutaka, N. and Nabukazo, T. (2006). Turbulence characteristics of natural convection boundary layer in air along a vertical plate heated at high temperatures. "*International Journal of heat and fluid flow*," **27**; 445-455.

Hatsopolous, G.N. and Keenan, J.H., (1965). Principles of General Thermodynamics, John Wiley and Sons Inc.

Hawa, S., Paras, R. and Ashok, K. (2014). An investigation of Turbulent unsteady MHD free convective heat and mass transfer flow past a vertical porous plate with suction." *International Journal of Applied Mathematics and Mechanics (IJAMM),*" **7**(20); 38-58.

Hinze, O., (1974). Turbulence, McGraw-Hill, New York.

Job,O.M, Kinyanjui, M. and Sigey, J. (2018). Magnetohydrodynamics turbulent fluid flow past an infinite vertical porous plate in a rotating system. "*International Journal of Applied Mathematics and Mechanics*," **8**(28); 1-10.

Kenjeres, J., Gunarjo, S., and Hanjalic, K. (2004). Contribution to elliptic relaxation modeling of turbulent natural and mixed convection. "*International Symposium. Advanced*." **26**; 569-586

Kennedy, J. M. K. and Dickson, K. K. (2017). Hydromagnetic Turbulent Flow Between Parallel Plates. "Science Journal of Applied Mathematics and Statistics," **5**; 31-40.

Kinyanjui, M., Emmah, M. and Kwanza, J. (2012). Hydromagnetic turbulent flow of a rotating system past a semi- infinite vertical plate with hall current. "*International Journal of Heat and Mass transfer,"* **79**; 97-119.

Kinyanjui, M. and Uppal, S.M. (1998). MHD stokes problem for a vertical infinite plate in a dissipative rotating fluid with hall current. "Journal of Magneto hydrodynamics and plasma Research," **8**; 15-30.

Kitagawa, A. and Murai, Y. (2013). Natural convection heat transfers from a vertical heated plate in water with micro bubble injection." *Chemical Engineering Science*," **99**; 215-224.

Maswai, R.C., Kinyanjui, M.N. and Kwanza, J.K. (2015). MHD Turbulent flow in presence of inclined magnetic field past a rotating semi-infinite plate. "*International Journal of Engineering Science and Innovative Technology,"* **4**; 344-360.

Mohammad, O. and Nicholas, G. (2012). Turbulence characteristics and vertical structures in combined convection boundary layers along a heated vertical flat plate." *International Journal of Heat and Mass Transfer,"* **55**; 3995-4002.

Mohamed, O. and Nicolas, G. (2006). Numerical Analysis of turbulent buoyant flows in enclosures: influence of grid and boundary conditions.

Moreau, R. (1990). Magnetohydrodynamics, Kluwer academic publishers. Netherlands pp. 56-65.

Nakaharai, H. and Yokomine, J. (2007). Influence of a transverse magnetic field on the local and average heat transfer of an electrically conducting fluid." *International Journal of Heat and Mass transfer,"* **32**; 23-28.

Pai, S. I. (1962). Magnetohydrodynamics and plasma dynamics, Wien Springer-Verlag, pp.420-450.

Prandtl, L., Angew, Z. (1925). Simple Phenomenological Theory of Turbulent Shear Flows,

Math. Mech. **5**; 136-139.

Rajput, U.S. and Neetu, K. (2016). MHD Flow Past a Vertical plate with Variable Temperature and Mass Diffusion in the presence of Hall Current. *"International Journal of Applied Sience and Engineering,"* **14**; 115-123.

Reynolds, O. (1886). Theory and application of Turbulent Shear Flows, Ann. Rev. Fluid Mech. **177**; 157-234.

Reynolds, W.C., (1976). Computation of Turbulent Flows, Ann. Rev. Fluid Mech. **8**; 183-208.

Rodi, W. (1980). Turbulent Models and Their Applications in Hydraulics, A state of the Art Review, International Associations for Hydraulic Research, Delft, the Netherlands.

Rodriquez-Sevillano (2012). On the onset of turbulence in natural convection on inclined plates. *"Experimental Thermal and fluid Science*," **35**; 68-72.

Sanvicentre, E., Giroux- Julien, S., Menezo, C. and Bouia, H. (2013). Transitional natural convection flow and heat transfer in an open channel. "*International Journal of Thermal Sciences,"* **99**; 215-224.

Satale, S., Kunug, T., Takase, K. and Ose, Y. (2006). Direct numerical simulation of turbulent flow under a uniform magnetic field for large-scale structures at high Reynolds number. "*Physical Fluids"* **18**; 125-106.

Shin- ichi, S., Chikamasa, C., Kazuyuki, M. and Kunugi, T. (2010). Direct Numerical Simulation of unstable stratified turbulent flow under a magnetic field. "*International Journal of Heat and fluid flow,"* **85**; 1326-1330.

Situma, H., Sigey, J.K., Okello, J.A., Okwoyo, J.M. and Theuri, D. (2015). Effect of Hall current and Rotation on MHD free convection flow past a vertical infinite plate under a variable transverse Magnetic field. "*The Standard International Journals,"* **3;** 59-65.

Soundalgekar, V.M., Bhat, J.P., and Mohiuddin, M. (1979). Finite difference analysis of free convection effects on stokes problem for a vertical plate in a dissipative fluid with constant heat flux. "*International Journal of Engineering and Science*," **17**; 1283-1288.

Xenos, M., Trirtzilaki, E. and Kafoussiass, N. (2009). Optimizing separation of compressible boundary-layer flow over a wedge with heat and mass transfer. *"International Journal of Heat and Mass transfer,"* **52**; 488-496.

Yamamoto, Y. (2008). DNS and k-ε model simulation of MHD turbulent channel flow with heat transfer," *International Journal of heat and mass transfer,*" **28**; 1-13.

Yoshinobu, Y. and Tomoaki, T. (2011). Heat transfer degradation in high Prandtl number fluid. "*International Journal of Heat and fluid flow,"* **22**; 67-83.

Zikanov O. and Thess A. (2004). Direct Numerical Simulation as a tool for understanding MHD liquid metal turbulence. "*Journal of Applied Mathematical Modelling*," **28**; 1-13.

Zoynal, M., Abedin, M., Toshihiro, T. and Jinho, L. (2012). Turbulence characteristics and vertical structures in combined- convection boundary layers along a heated vertical flat plate. "*International Journal of heat and mass transfer,*" **55**; 3995-4000.

APPENDIX I

THESIS ANALYSIS PROGRAM CODE

Computational fluid dynamics codes

As already discussed earlier, MHD has numerous applications like electromagnetic flow meters, MHD ejectors, MHD submarines, MHD accelerators, MHD lubrication, MHD thin air foils and nuclear fusion reactions etc. Despite the complexity of Physics involved electromagnetic pumping, electromagnetic stirring, electromagnetic valves, electromagnetic casting and even electromagnetic propulsion are becoming more and more popular these days.

Other important applications include coronal plasma flows in the configuration of plasma sheet formation in the active region of the sun or in the magnetic tail region and perhaps the most important application of such problems being focused at is the power generation by MHD generators. Because of these engineering applications, many engineers and aerodynamicists jointly with the astrophysicists and geophysicists study extensively the dynamics of electrically conducting fluids. Even though we do not discuss the practical applications of the MHD flow, the thesis should be undoubtly useful in developing the theory of these applications. It must be pointed out that the work done in this thesis is purely theoretical and not experimental. Then MHD generator transforms the internal energy of the fluid (a conducting liquid or a gas) in the same way as a turbogenerator does. In the MHD generator the fluid (normally the gas) itself is a conductor and the motion of the conductor through the magnetic field gives rise to an e.m.f. in accordance with Faraday's law of electromagnetic induction. The current in the MHD generator is carried by the electrodes and a very large amount of power can be produced by MHD generators. By varying the concentration of the field as well as the strength and the direction of the applied magnetic field, one can easily verify the conclusions drawn from e interpretation of the graphical solutions of the

differential equations in the thesis. There is considerable foreign activity in MHD energy conversion especially in Japan, Germany, England, France and Russia. A number of international meetings take place annually in the United States on the Engineering aspects of MHD. It is interesting to note that there exists a hidden analogy between magnetohydrodynamics (MHD) and conventional computational fluid dynamics (CFD) equations. This shows the generalization of any conventional CFD code so that the effects of MHD can be accounted for. This generalization is actually made for the FLUENT CFD Code and such generalized FLUENT CODE can easily be adjusted to any MHD environment. Equations in MHD have the same form as in the conventional CFD except the additional term $J \times B$ (Lorentz Force) and $J \cdot E$ (electrical heating). Hence, conventional CFD solvers can at once compute the equations in MHD problems by simply adding these terms as source terms. In fact, this is one of the best and the most modem way to study the validity of the results of numerical computations. Many institutions have developed extensive expertise in this very specialized field of CFD. In Europe, for example, we can mention MADYLAM in France, the Department of Engineering at Cambridge University in the UK., the Department of Mathematics at Ecole Polytechnique Federale de Lausanne in Switzerland and also the Institute of Physics at Riga University, Latvia. In that United States, the Department of Materials Science at California's Berkeley University, the Department of Aerospace Engineering at Pennsylvania University and MIT's Department of materials Engineering all work in this field. All of them have developed special purpose in house CFD codes to compute and study MHD flows. As if the challenge of solving the Navier - Stokes equations with high Reynolds number, dealing with turbulence, free surface flows etc. not only enough but also solving MHD driven flows involves the solution of Maxwell's equations. Furthermore, in majority of the cases the Navier - Stokes equations and the Maxwell's equations are tightly coupled thereby making the

problem even more non - linear in nature. In fact, Dr. M. Dupuis, in one of his recent publications (modelling of MHD flows) explained clearly that CFD codes have become commercial to solve MHHD flows equations and it is very possible to use, in combination, a commercial code to solve Maxwell's equations and a code for solving Navier - Stokes equations to do so. Over such possible combination is ANSYS and FIDAP finite element codes. Hence, computerization of modelling of magnetohydrodynamics (MHD) flow problem equations is no longer a difficult task but has become a common commercial style of the day. In this case we have used the Matlab code as below.

```
function NgesaProblem()
clear all;clc;
t0=0;tend=0.5;nt=801;
dt=(tend-t0)/(nt-1);
x0=0;xend=2;nx=41;
dx=(xend-x0)/(nx-1);
z0=0;zend=4;nz=51;
 dz=(zend-z0)/(nz-1);
 z=z0:dz:zend;
 x=x0:dx:xend;
 u=zeros(nx,nz,nt);v=zeros(nx,nz,nt);T=zeros(nx,nz,nt);C=zeros(nx,nz,nt);
 %%
 %PARAMETER SPECIFICATIONS%%%%%%%
 w0=0.5;M=5;m=1.5;K=0.45;Gr=-0.4;Gc=0.4;Sc=0.9;phi=0.5;sig=2;Pr=0.71;Ec=0.5;
 %%
```

```
color='r';
%INITIAL CONDITIONS%%%%%%%%%%%%
u(:,:,1)=0;v(:,:,1)=0;T(:,:,1)=0;C(:,:,1)=0;
%BOUNDARY CONDITIONS%%%%%%%%%%%%
u(:,1,:)=0;v(:,1,:)=0;T(:,1,:)=1;C(:,1,:)=1;%for z=0
u(:,nz,:)=0;v(:,nz,:)=0;T(:,nz,:)=0;C(:,nz,:)=0;%for z tends to infinity
u(1,:,:)=0;v(1,:,:)=0;T(1,:,:)=0;C(1,:,:)=0;%for x=0
u(:,nz,:)=0;v(:,nz,:)=0;T(:,nz,:)=0;C(:,nz,:)=0;%for x tends to infinity
%%
Up1=zeros(nx,nz,nt);Up2=zeros(nx,nz,nt);Up3=zeros(nx,nz,nt);
Vp1=zeros(nx,nz,nt);Vp2=zeros(nx,nz,nt);Vp3=zeros(nx,nz,nt);
Tp1=zeros(nx,nz,nt);Tp2=zeros(nx,nz,nt);Tp3=zeros(nx,nz,nt);
Cp1=zeros(nx,nz,nt);Cp2=zeros(nx,nz,nt);
for n=1:nt
for i=2:nx-1
for k=2:nz-1
[Up1(i,k,n),Up2(i,k,n),Up3(i,k,n)]=priVelo(u(i,k,n),u(i+1,k,n),u(i-1,k,n),w0,u(i,k+1,n),u(i,k-
1,n),dx,dz,Gr,Gc,T(i,k,n),C(i,k,n),K,x(i),M,m,v(i,k,n),phi);
[Vp1(i,k,n),Vp2(i,k,n),Vp3(i,k,n)]=secVelo(v(i,k,n),v(i+1,k,n),v(i-1,k,n),u(i,k,n),u(i+1,k,n),u(i-
1,k,n),w0,v(i,k+1,n),v(i,k-1,n),dx,dz,K,x(i),M,m,phi);
[Tp1(i,k,n),Tp2(i,k,n),Tp3(i,k,n)]=Temp(u(i,k,n),T(i+1,k,n),T(i,k,n),T(i-1,k,n),T(i,k+1,n),T(i,k-
1,n),sig,Pr,v(i+1,k,n),v(i-1,k,n),w0,v(i,k+1,n),v(i,k-1,n),...
dx,dz,u(i+1,k,n),u(i-1,k,n),Ec,u(i,k+1,n),u(i,k-1,n));
```

```
[Cp1(i,k,n),Cp2(i,k,n)]=Conc(u(i,k,n),C(i+1,k,n),C(i,k,n),C(i-1,k,n),C(i,k+1,n),C(i,k-
1,n),w0,dx,dz,Sc);
u(i,k,n+1)=u(i,k,n)+dt*(Up1(i,k,n)+Up2(i,k,n)+Up3(i,k,n));
v(i,k,n+1)=v(i,k,n)+dt*(Vp1(i,k,n)+Vp2(i,k,n)+Vp3(i,k,n));
T(i,k,n+1)=T(i,k,n)+dt*(Tp1(i,k,n)+Tp2(i,k,n)+Tp3(i,k,n));
C(i,k,n+1)=C(i,k,n)+dt*(Cp1(i,k,n)+Cp2(i,k,n));
        end
       end
    end
figure(1)
subplot(2,2,1)
mesh(u(2:nx-1,2:nz-1,nt))
title('U-VELOCITY')
subplot(2,2,2)
mesh(v(2:nx-1,2:nz-1,nt))
title('V-VELOCITY')
subplot(2,2,3)
mesh(T(2:nx-1,2:nz-1,nt))
title('TEMPERATURE')
subplot(2,2,4)
mesh(C(2:nx-1,2:nz-1,nt))
title('CONCENTRATION')
figure(2)
```

```
hold on
%plot(z(1:nz),v(floor(nx/2),1:nz,nt),color,'linewidth',2)
Wv=v(floor(nx/2),1:nz,nt);sp5 = spapi(5,z(1:nz),Wv);
fnplt(sp5,2,color),set(gca,'Fontsize',10)
xlabel('Z-AXIS')
ylabel('SECONDARY VELOCITY')
hold off
figure(3)
hold on
%plot(z(1:nz),u(floor(nx/2),1:nz,nt),color,'linewidth',2)
Wu=u(floor(nx/2),1:nz,nt);sp5 = spapi(5,z(1:nz),Wu);
fnplt(sp5,2,color),set(gca,'Fontsize',10)
xlabel('Z-AXIS')
ylabel('PRIMARY VELOCITY')
hold off
figure(4)
hold on
%plot(z(1:nz),T(floor(nx/2),1:nz,nt),color,'linewidth',2)
Wt=T(floor(nx/2),1:nz,nt);sp5 = spapi(5,z(1:nz),Wt);
fnplt(sp5,2,color),set(gca,'Fontsize',10)
xlabel('Z-AXIS')
('TEMPERATURE')
hold off
```

```
figure(5)
hold on
%plot(z(1:nz),C(floor(nx/2),1:nz,nt),color,'linewidth',2)
Wc=C(floor(nx/2),1:nz,nt);sp5 = spapi(5,z(1:nz),Wc);
fnplt(sp5,2,color),set(gca,'Fontsize',10)
xlabel('Z-AXIS')
ylabel('CONCENTRATION')
hold off
function [up1,up2,up3]=priVelo(uc,uir,uil,w0,ukr,ukl,dx,dz,Gr,Gc,Tc,Cc,K,x,M,m,vc,phi)
 up1=-uc*(uir-uil)/(2*dx)+w0*(ukr-ukl)/(2*dz)+(ukr-2*uc+ukl)/(dz*dz);
 up2=(uir-2*uc+uil)/(dx*dx)+Gr*Tc+Gc*Cc+2*K*K*x*(((uir-uil)/(2*dx)).^2);
  up3=2*K*K*((x).^2)*(((uir-2*uc+uil)/(dx*dx)).^2).*(uir-uil)/(2*dx)-
(M*M*phi*phi*(m*phi*vc-uc))/(1+m*m*phi*phi);
    end
  function [vp1,vp2,vp3]=secVelo(vc,vir,vil,uc,uir,uil,w0,vkr,vkl,dx,dz,K,x,M,m,phi)
   vp1=-uc*(vir-vil)/(2*dx)+w0*(vkr-vkl)/(2*dz)+(vkr-2*vc+vkl)/(dz*dz);
   vp2=(vir-2*vc+vil)/(dx*dx)+2*K*K*x*(((vir-vil)/(2*dx)).^2);
   vp3=2*K*K*((x).^2)*(((vir-2*vc+vil)/(dx*dx))).*(vir-vil)/(2*dx)-
(M*M*phi*phi*(m*phi*uc+vc))/(1+m*m*phi*phi);
    end
    function
[Tp1,Tp2,Tp3]=Temp(uc,Tir,Tc,Til,Tkr,Tkl,sig,Pr,vir,vil,w0,vkr,vkl,dx,dz,uir,uil,Ec,ukr,ukl)
 Tp1=-uc*(Tir-Til)/(2*dx)+w0*(Tkr-Tkl)/(2*dz)+(1/Pr)*(Tkr-2*Tc+Tkl)/(dz*dz);
```

```
 Tp2=(1/Pr)*((Tir-2*Tc+Til)/(dx*dx))-(sig/Pr)*Tc;
 Tp3=Ec*((((uir-uil)/(2*dx)).^2)+(((vir-vil)/(2*dx)).^2)+(((ukr-ukl)/(2*dz)).^2)+(((vkr-
vkl)/(2*dz)).^2));
   end
 function [Cp1,Cp2]=Conc(uc,Cir,Cc,Cil,Ckr,Ckl,w0,dx,dz,Sc)
  Cp1=-uc*(Cir-Cil)/(2*dx)+w0*(Ckr-Ckl)/(2*dz);
   Cp2=(1/Sc)*((Cir-2*Cc+Cil)/(dx*dx)+(Ckr-2*Cc+Ckl)/(dz*dz));
   end
end
```

APPENDIX II

Research papers and Publications.

i.) Ngesa J.O, Kennedy, O.A., Jeconiah, O.A., and Mark, E.M.K. "Heat and Mass Transfer Past a Semi-Infinite Vertical Porous Plate in MHD free convective flow in Turbulent Boundary Layer." published in the *World Journal of Research and Review* on February 2018.

ii.) Ngesa J.O, Kennedy, O.A., Jeconiah, O.A., and Mark, E.M.K. "Dynamics of MHD Heat and Mass Transfer Past a Semi-Infinite Vertical Porous Plate in a Turbulent Boundary Layer." published in the *International Journal of Research in Information Technology* on December, 2017.

iii.) Ngesa, J.O., Sigey, K.J, and Okelo A. Jeconia." Magnetohydrodynamic (MHD) Free Convective Flow past an Infinite Vertical Porous Plate with Joule Heating" published in the *Journal of Applied Mathematics* on May 2013.